Development and Verification of Methods for the Rheological Characterization of Materials for the Process Industry

Utvikling og verifisering av metoder for reologisk karakterisering av materialer for prosessindustrien

Philosophiae Doctor (PhD) Thesis

Carlos Salas Bringas

Dept. of Mathematical Sciences and Technology
Norwegian University of Life Sciences

Ås 2011

Thesis number 2011:19
ISSN 1503-1667
ISBN 978-82-575-0983-5

AKNOWLEDGEMENTS

First I would like to thank to my wife for her support and love throughout the period of the studies. My kids, Marko and Luka were undoubtedly one of the biggest contributors of fuelling the energies that I needed to perform my studies.

My gratitude to my supervisors Dr. Odd-Ivar Lekang and Dr. Reidar Barfod Schüller for the support and excellent guidance.

I would like to specially thank Professor Reidar Barfod Schüller for his extraordinary guidance and discussions in all rheological matters, by far he guided me more actively than any other second supervisor one could have. His contribution to the thesis is priceless. I would also like to thank him for his friendship, good humor and mood lifting during the bad moments.

Another very special thank is to my first supervisor, Dr. Odd-Ivar Lekang for his continuous help and support in all situations. Particularly I would like to thank his attitude when my former supervisor, Dr. Willy Jeksrud passed away. Dr. Odd-Ivar Lekang even though was not involved in rheology at the beginning, he actively contributed to open all doors at the department bringing funding when needed. His friendship, good humor, strategic view and his important contribution to structure the thesis are especially acknowledged.

Other acknowledgements at the department are to Dr. Jan Kåre Bøe for his help when developing the idea for the first time of a screw rheometer. Also my thanks to Tore Ensby and Egil Stemsrud for their help in the different prototypes I have developed. When it comes to the prototype electronics, I would like to thank Tom Ringstad and Andreas Flø for their help. Dr. Ulrike Böcker and Dr. Tom Tetzlaff are acknowledged for the translation of the abstracts of paper II and III into German.

In addition, I would like to thank all the good time that I have spent during conference trips in the company of Dr. Elling-Olav Rukke and Dr. Reidar Barfod Schüller whom made the trips to the rheology conferences not only a working trip, but a trip of friendship and joy.

TABLE OF CONTENTS

INDEX OF FIGURES

INDEX OF TABLES

SUMMARY

Process control, product quality and process design are continuously demanding new sensors and devices that can assess the rheological behavior of fluid and solid products. The need for more methods comes because of three main reasons: (1) there is no single instrument able to perform all the types of rheological characterizations that are needed in the industries, (2) there is no instrument able to characterize all types of fluids and solids, and (3) the complex rheological behavior of many process materials depends upon time, shear, stress, temperature, pressure and process history that restricts the validity of results when for example retrieving information to the process. The aim of this work was to develop two rheological instruments made for different purposes and verify their working and measurement principle. The first instrument is a screw type process rheometer that can handle fluid and semi-solid materials. The second instrument is a die compaction rig that is able to characterize powders.

Paper I focuses on an experimental calibration procedure to allow the screw type rheometer to measure the apparent viscosity of fluids using torque as a measurement of an average shear stress and the rotational speed as a measurement of a mean shear rate. From a first prototype, it was possible to predict viscosity with maximum errors or residuals smaller than 25 Pa s over a range of viscosities (35-450 Pa s) using a Newtonian standard fluid. The use of a dry sliding bearing created a friction in the system that resulted in flow curves having an intercept different than zero when using a Newtonian standard fluid. This encouraged the creation of another calibration method in **Paper II** that considers an intercept different to zero by using the area below the curve. Measurements of downstream pressure were included in **Paper II** as an alternative to the torque measurements. The flow curve formed between downstream pressure and rotational speed resulted in a linear curve with intercept zero when using the Newtonian standard fluid. Time variations in pressure and torque were also studied since they could affect the measurements. The variations became more notorious (e.g. increased amplitude of torque and pressure oscillations) at higher resistances to flow produced by either an increased viscosity or to a lesser extent by reductions in die diameter (a downstream restriction). The distribution of errors in **Paper II** was calculated through the root mean square error of prediction (RMSEP). The calibration model based on the area below the curve presented the significantly smallest ($p < 0.005$) RMSEP of 2.2 Pa s. All other models were not significantly different; however they varied from ± 3.7 Pa s up to ± 12 Pa s.

The calibration methods presented in **Paper I** and **II** to predict an apparent viscosity were based on the ratio torque – speed or downstream pressure – speed that was not needed to convert torque or downstream pressure into a shear stress unit or speed to a shear rate unit. For this reason **Paper III** studied the use of a coaxial cylindrical analogue to represent the geometrically complex screw. A replicate of the screw type rheometer with some modification of the recirculation system was assembled in a Paar Physica UDS 200 rheometer to take advantage of the low friction provided by its air bearing. The aim was also to have an insight to how a screw type rheometer could perform viscoelastic measurements in oscillation. The flow curves using non-Newtonian fluids, both time independent and time dependent, were closer to the flow curves obtained with cone-plate, plate-plate and bob-cup than to the ones obtained from a standard Paar Physica impeller. The storage and loss modulus from the screw rheometer were of relatively similar magnitude to the ones obtained from plate-plate and bob-cup systems. The good results also make this replicate an attractive set-up for laboratory use.

Paper IV and **V** were done using a third prototype (2^{nd} measurement principle) which is a laboratory die pelleting or compressing rig that presses powders under pre-determined load and speed to form cylindrical compacts (or pellets) of different densities. **Paper IV** investigates the compression rheology of ground Scots pine (*Pinus sylvestris*) pre-handled with different storage times and drying temperatures. The physical strength of the pellets formed in the laboratory die pelleting rig was also investigated. Ground Scots presented a ductile compression and the pellets resulted to be plastic and ductile. The highest drying temperature and longest storage time, produced pellets with the highest strength values under diametrical compression test.

Paper V uses the laboratory die pelleting rig to compare the yield stress measured in a stress relaxation test and the normal stress at incipient flow of Scots pine with the energy consumption of an industrial pellet press. The results show that normal stresses at incipient flow and yield stresses are linked to the energy consumed by an industrial pellet press. Long storage time of the raw material produced higher normal stresses at incipient flow and higher yield stresses in the materials. Most probably this is the cause for the higher energy consumption in the industrial pellet press. Drying temperature did not change incipient flow and normal stresses significantly.

SAMMENDRAG

Det er et stadig behov for å utvikle nye metoder og nytt utstyr for å karakterisere de reologiske egenskaper til faste og flytende produkter med tanke på prosesskontroll, prosessoptimalisering og optimering av produktkvalitet. Det finnes ikke noe enkelt instrument som kan gjøre en fullstendig karakterisering som tilfredsstiller behovene fra alle typer industri. Det finnes ikke noe enkelt instrument som kan karakterisere alle typer fluider og faste stoffer, og for mange materialer endres de reologiske egenskapene som funksjon av tid, temperatur, skjær, stress, trykk og historikk, noe som gjør at innhenting av tidligere målte data kan forårsake feil. Målet med dette arbeidet var derfor å utvikle og verifisere nye instrumenter for karakterisering av reologiske egenskaper. To instrumenter ble utviklet, et skruetype reometer for karakterisering av flytende og halvfaste materialer og et som baserte seg på pressing av materiale gjennom en dyse beregnet for pulver (fast stoff). **Artikkel I** fokuserer på den eksperimentelle kalibreringsprosedyren for et skruetype reometer når det brukes til å måle den tilsynelatende viskositet i væsker ved hjelp av dreiemoment, som mål på en gjennomsnittlig skjærspenning, og rotasjonshastigheten, som et mål på en gjennomsnittlig skjærhastighet. Fra en første prototype var det mulig å forutsi viskositet med maksimal feil mindre enn 25 Pa s i viskositetsområdet 35-450 Pa s ved hjelp av en Newtonsk standard væske. Bruken av et tørt glidelager gav en friksjon i systemet som resulterte i at kurver (dreiemoment versus rotasjonshastighet) ikke passerte gjennom origo ved bruk av en standard Newtonsk væske. Dette oppmuntret til etablering av en annen kalibreringsmetode i **Artikkel II** som vurderer et skjæringspunkt forskjellig fra null ved hjelp av området under kurven. Målinger av nedstrøms trykk var inkludert i **Artikkel II** som et alternativ til dreiemoment målingene. Flytkurven dannet mellom nedstrøms trykk og rotasjonshastighet resulterte i en lineær kurve gjennom origo ved bruk av en standard Newtonsk væske. Tidsvariasjoner i trykk og moment ble også studert siden de kunne påvirke målingene. Variasjonene ble mer dominerende (f.eks. økt amplitude av moment og trykk svingninger) ved høyere strømningsmotstand forårsaket av enten en økt viskositet eller i mindre grad av reduksjoner i dyse diameter (en nedstrøms begrensning). Fordelingen av prediksjonsfeil i **Artikkel II** ble beregnet ved bruk av RMSEP (Root Mean Square Error of Prediction). Kalibreringsmodellen basert på arealet under kurven presenterte signifikant minste ($p < 0.005$) RMSEP på 2.2 Pa s. Alle andre modeller var ikke signifikant forskjellige, men de varierte fra ± 3.7 Pa s opp til ± 12 Pa s.

Kalibreringsmetodene som presenteres i **Artikkel I** og **II** til å forutsi en tilsynelatende viskositet var basert på forholdet dreiemoment - hastighet eller nedstrøms trykk - roterende hastighet slik at det ikke var nødvendig å konvertere dreiemoment eller nedstrøms trykk til en skjærspenning eller farten til en skjærhastighet. Av denne grunn studerte **Artikkel III** bruken av en koaksial sylindrisk analog til å representere den geometrisk komplekse skruen. En replika av skruetype reometeret, med noen endringer i resirkuleringssystemet, ble montert i et Paar Physica UDS 200 reometer for å dra nytte av den lave friksjonen i luftlageret til dette instrumentet. Målet var også å få en innsikt i hvordan et skruetype reometer kunne utføre viskoelastiske målinger i oscillasjon. Strømningskurvene for ikke-newtonske væsker, både tidsuavhengige og tidsavhengige, var nærmere strømningskurvene oppnådd med kon-plate, plate-plate og konsentriske sylindere enn de man fikk ved bruk av en standard Paar Physica impeller. Lagringsmodul og tapsmodul fra skruereometeret var av forholdsvis samme størrelsesorden som verdier hentet fra plate-plate og konsentriske sylinder systemer. De gode resultatene gjør også at dette er et attraktiv oppsett for laboratoriebruk.

Artikkel IV og **V** ble gjort ved hjelp av en tredje prototype (andre måleprinsipp) som består av en komprimerings rigg som presser pulver ut gjennom en dyse under forhåndsbestemt belastning og hastighet for å danne sylindriske komprimerte elementer (pellets) med forskjellige tettheter. **Artikkel IV** undersøker komprimeringsreologi av oppmalt furu (Pinus sylvestris) forbehandlet med ulik lagringstid og tørketemperaturer. Den fysiske styrken til pellet dannet med komprimeringsriggen ble også undersøkt. Oppmalt furu gav en seig komprimering og de produserte pelletene var plastiske og duktile. Den høyeste tørketemperatur og lengste lagringstid, produserte pellet med høyest styrke ved diametral kompresjonstesting.

Artikkel V bruker kompresjonsriggen med dyse pelletering for å sammenligne materialets flytspenning målt i en spennings relaksasjonstest og normalspenningen ved begynnende strømning av furu med energiforbruket til en industriell pelletpresse som arbeider med samme materiale. Resultatene viser at normalspenninger ved begynnende strømning og flytspenning er relatert til energien som forbrukes av en industriell pelletpresse. Lang lagringstid av råstoff produserte høyere normalspenninger ved begynnende strømning og høyere flytspenninger i materialet. Mest sannsynlig er dette årsaken til det høye energiforbruket i industrielle pelletpresser. Tørketemperaturen påvirket ikke initiell strømning og målte normalspenninger i særlig grad.

RESUMEN

Las actividades de control en los procesos industriales, calidad en los productos y diseño de procesos continuamente demandan nuevos sensores e instrumentos que puedan caracterizar reológicamente los productos sólidos y líquidos. La necesidad de nuevos instrumentos se origina por tres razones: (1) No existe instrumento alguno que pueda realizar todos los tipos de caracterizaciones reológicas que la industria requiere, (2) no existe instrumento alguno que pueda caracterizar todos los tipos existentes de sólidos y líquidos, y (3) el complejo comportamiento reológico de muchos materiales usados en la industria (no-Newtoniano) dependen del tiempo, esfuerzo cortante, temperatura, presión y el historial de su procesamiento (cambios no reversibles) lo que restringe la validez de las caracterizaciones reológicas cuando se desean usar en el proceso. El objetivo de esta tesis es el desarrollo de dos instrumentos hechos para diferentes propósitos y verificar su funcionamiento y principio. El primer instrumento es un tipo de reómetro de tornillo para ser utilizado con líquidos y materiales semisólidos. El segundo instrumento es un instrumento de compactación de materiales particulados que utiliza un dado.

El **primer artículo** se enfoca en el desarrollo de una calibración en base experimental para que el reómetro de tornillo pueda medir la viscosidad aparente de líquidos usando torque como medida del esfuerzo cortante promedio y de la velocidad de rotación del tornillo como medida del promedio de la velocidad cortante. Con el primer prototipo, fue posible medir viscosidad con errores máximos o residuos menores a 25 Pa s sobre un rango de viscosidades (35-450 Pa s) usando un fluido Newtoniano estándar. El uso de un tipo de cojinete de deslizamiento en seco creo fricción en el sistema, el cual resulto en curvas de fluido Newtoniano con un intercepto diferente de cero al graficar el esfuerzo cortante con la velocidad de corte. Esto conllevo a la creación de otro método de calibración que fue presentado en el **segundo artículo**, el cual considero un intercepto diferente a cero usando el área bajo la curva.

Medidas de presión a la salida del tornillo fueron incluidas en el **segundo artículo** como una alternativa a las mediciones provenientes del torque. La curva formada entre la presión a la salida del tornillo y la velocidad de rotación resulto en una línea recta con intercepto cero cuando se uso el fluido Newtoniano estándar. Las variaciones con el tiempo de la presión y torque fueron estudiadas porque podrían alterar las mediciones. Las variaciones se hicieron más notorias (incremento en la amplitud de torque y oscilación de la

presión) cuando se produjeron cambios en la resistencia del liquido a fluir debido a incrementos de la viscosidad o en menor grado a reducciones del diámetro de dado (restricción ubicada más abajo del tornillo). La distribución de errores en el **segundo artículo** fue calculada mediante el error cuadrático medio de predicción (RMSEP). El modelo de calibración basado en el área bajo la curva presento el menor RMSEP de 2.2 Pa s de una manera significativa ($p < 0.005$). Todos los otros modelos no fueron significativamente diferentes ($p < 0.005$), sin embargo ellos variaron entre ± 3.7 Pa s hasta ± 12 Pa s.

Los métodos de calibración presentados en el **primer** y **segundo artículo** predijeron una viscosidad aparente basada en la razón entre el torque y velocidad de rotación del tornillo, y también basada en la razón entre la presión a la salida del tornillo y la velocidad de rotación del tornillo. Estos métodos no necesitan convertir torque o la presión a la salida del tornillo en unidades de esfuerzo cortante y velocidad del corte. Por esta razón el **tercer artículo** estudia el uso de un análogo de cilindro coaxial para representar la compleja geometría del tornillo. Una réplica del reómetro de tornillo con algunas modificaciones en el sistema de recirculación fue ensamblada en un reómetro Paar Physica UDS 200 para tomar ventaja de la poca fricción generada por su sistema de rodamiento de cojín de aire. El objetivo fue descubrir si un reómetro de tornillo pude efectuar mediciones de viscoelasticidad al oscilar. Las curvas de flujo usando ambos tipos de fluidos no Newtonianos, dependientes del tiempo e independientes del mismo, resultaron ser más cercanas a las curvas de flujo obtenidas en los accesorios estándar de cono- placa, placa-placa y cilindro rotatorio que a las pruebas utilizando un accesorio estándar de Paar Physica de tipo mezclador-hélice. El modulo elástico y el modulo viscoso calculados con el tornillo resultaron ser de una magnitud similar a las encontradas con placa-placa y cilindro rotatorio. Los buenos resultados hacen también de esta replica una configuración muy atractiva para ser utilizada en reómetros de laboratorio.

El **cuarto** y **quinto artículo** fueron hechos utilizando el tercer prototipo (segundo principio de medición) el cual es un peletizador de laboratorio, el cual también podría llamarse compactador de particulados. Este instrumento permite seleccionar diferentes presiones y velocidades de compresión, el resultado son compactos cilíndricos (o pellets) que pueden tener diferentes densidades deseadas. El **cuarto artículo** desarrolla estudios reológicos de compresión en molidos de pino Scot (*Pinus sylvestris*) manipulados bajo dos maneras distintas, la primera fue usar molido almacenado por tres y once meses, y la segunda variación fue la temperatura de secado (75 y 450 °C). La dureza de los pellets creados en el

compactador de laboratorio fue también investigada. El molido de pino Scot resulto tener una compresibilidad de tipo dúctil y los pellets resultaron ser de características plásticas y dúctiles. Los pellets provenientes de los molidos almacenados por mayor tiempo y secados con la mayor temperatura resultaron tener la mayor dureza bajo las pruebas de compresión dimétrica.

El **quinto artículo** emplea el peletizador de laboratorio para comparar los esfuerzos de flujo incipiente de los cuatro grupos de molido mediante pruebas de esfuerzo y relajación. El mismo artículo también realiza pruebas para cuantificar el esfuerzo que produzca el flujo incipiente a una velocidad de compactación fija y preseleccionada. Estas propiedades reológicas se compararon con los valores de consumo de energía de una peletizadora industrial durante la producción de los mismos materiales. Los resultados mostraron que el esfuerzo normal necesario para iniciar la fluencia a una velocidad de compactación fija y el esfuerzo normal determinado mediante la prueba de esfuerzo y relajación están relacionados con la cantidad de consumo de energía demandado por la peletizadora industrial. Los materiales almacenados por once meses provocan la necesidad de aumentar los esfuerzos normales para producir flujo cuando se comparan con los materiales almacenados por solo tres meses. Estos resultados fueron obtenidos bajo las pruebas de velocidad de compactación fija y bajo las pruebas de esfuerzo y relajación. Lo más probable es que los cambios reológicos en los molidos de pino sean los causantes del mayor requerimiento de energía demandado por la peletizadora industrial. Por último, la temperatura de secado no cambio significativamente ($p > 0.005$) el esfuerzo de flujo incipiente y los esfuerzos normales.

LIST OF PAPERS

The following papers are included in this thesis. They will be referred to by their roman numerals.

I. Salas-Bringas C, Jeksrud WK, Schüller RB: A new on-line process rheometer for highly viscous food and animal feed materials, Journal of Food Engineering 79 (2007) 383-391.

II. Salas-Bringas C, Lekang OI, Schüller RB: Time variations and calibration of a screw type process rheometer, Applied Rheology 20 (2010) 34526-1 – 34526-11.

III. Salas-Bringas C, Lekang OI, Schüller RB: Analysis of a screw type process rheometer to determine viscoelastic and flow properties of non-Newtonian fluids, Applied Rheology (2011) Submitted.

IV. Salas-Bringas C, Filbakk T, Skjevrak G, Lekang OI, Høibø O, Schüller RB: Compression rheology and physical quality of wood pellets pre-handled with four different conditions, Annual Transactions of the Nordic Rheology Society 18 (2010) 87-94.

V. Salas-Bringas C, Filbakk T, Skjevrak G, Lekang OI, Høibø O, Schüller RB: Assessment of a new laboratory die pelleting rig attached to a texture analyzer to predict process-ability of wood pellets. Energy consumption and pellet strength, Annual Transactions of the Nordic Rheology Society 18 (2010) 77-85.

1 GENERAL INTRODUCTION

During the last decades, it has been an emerging development of sensors and equipment that can be used in process operations, the reasons are increasing competitiveness within the industries, with many of them moving from batch to continuous production [1]. Today's industries are also using larger quantities of raw materials which are produced in shorter time, as a result the consequences for errors or failures during production can decrease the throughputs of products and thus the profits [2]. Furthermore today's industry must assure product quality to compete in the market and to comply with regulations. Measurement techniques that contribute to improve product quality, reduce processing costs, reduce raw materials usage and waste, and control of processing operation are continuously sought [3]. The insight for the industries in the future is fully automated processing operations with minimum human intervention which will rely on sensors and on-line instrumentation [4]. However, laboratory test are likely to be needed in the future as well for selection and purchase decision of raw materials.

Within the sensors and instrumentation needed today by the industries are the rheological ones, the reason is because rheological measurements assess the physical behavior of fluids, semi-solids and solids which is in direct connection with product handling, process efficiency, process design and the physical quality of products [5-10].

The number of new rheological instruments is increasing because of three main reasons: (1) there is no single instrument able to perform all the types of rheological characterizations that are needed in the industries, (2) there is no single instrument able to characterize all types of fluids and solids, and (3) the complex rheological behavior of many process materials depends upon time, shear, stress, temperature, pressure and process history that restricts the validity of results when for example retrieving information to the process, so different types of instruments are sought.

The aim of this work was to develop and verify the measurement principle of two rheological instruments made for different purposes. The first instrument is a screw type process rheometer that can handle fluid and semi-solid materials, its measurements can be categorized in the shear rheology type. The second instrument is a die compaction rig that is able to characterize powders and semi-solid materials, its type of measurement can be classified as compression rheology type.

The first instrument, a screw type process rheometer resembles a single screw extruder in its design, the rheometer can be classified as an impeller type of rheometer. The rheometer can be modified to have different types of restrictions at the downstream of the screw to enable the controlled use of a pressure build up, and consequently can allow the study of fluids under different conditions. In literature, helical screw rheometers have been described as having several benefits like good temperature control since it is enclosed in a cup system, it allows the study of fluids under different pressure, a recirculation in the rheometer can allow the study of chemically reacting systems having a time dependent viscosity, helical screw rheometers present a good handling of settling particles and present great advantages as a process monitoring device since can drag fluids and semi-solids materials continuously and can accumulate low concentrations of fouling [10, 11],

All previous work regarding the use of different types of helical screw rheometers focused on viscosity and flow curves (discussed in section 4.2.3.1), however no information was found by the author of this thesis regarding the use of a helical screw rheometer to perform viscoelastic measurements.

Powder flowability and compressibility are other types of measurements required in industries (discussed in section 4.1and 4.3). Particularly, in this thesis the use of a new fixture for texture analyzers to supply the information needed for the processing operations in pelleting is analyzed. Pellet presses are manufacturing units used to compact powders. This type of equipment provide very low control when compared for example to extruders, so the characteristics of the raw materials determine directly the characteristics of the products. Also pellet presses can be classified as “processing black boxes” since the information in the transition from powder to pellet is almost nonexistent given that only power consumption can be obtained. Temperature measurements are not common and compressive pressure is not measured.

Since a good pelleting operation relies so much on the characteristics of the raw materials, the use of a pre-processing instrument that could tell the ability of a powder to be pelleted together with the physical characteristic of the pellet can provide the valuable information to decide whether the raw material needs some pre-treatment or not. It can also tell whether the raw material is spoiled or not, or in some cases tell if the raw material can be processed at all. Consequently, an instrument determining pellet-ability can help the purchase decision of raw materials.

The instrument developed in this thesis is a compressing rig that enables the pelletization of powders. Because the rheological behavior of compressible powders is more complex to deal with than that of incompressible solids (to achieve good pelleting), new and more sophisticated production planning and process control are required. This includes knowledge of how the mixture responds to applied stresses during compaction and pellet release, keeping in mind crack prevention [12]. Consequently a rheological characterization of the powder material can provide new insight to the future of the pelleting process and the manufacture of pellet presses.

2 OBJECTIVES OF THE STUDY

The main objectives of this thesis were to develop and evaluate two different instruments that can be used in the process industries. The first instrument is meant to be used for processing of fluids and semi-solids materials. The equipment can be used in laboratories (off-line) as well as mounted in a process to do continuous measurements (in-line or on-line). The second instrument is meant to be used to help the processing operations of powders like for example pelleting process (e.g. wood and animal feed). Consequently the overall aim of the thesis was comprised by the following sub-tasks elaborated in five different studies:

The main objective of **Paper I** was to develop and verify the working principle of a new type of screw rheometer. For this reasons it was aimed to develop an experimental calibration method that enables the measurements of an apparent viscosity based on the use of torque (as an indication of shear stress) and screw speed (as an indication of shear rate), other aims were to quantify the prediction errors and to indicate that the equipment allow studies between rheological parameters like viscosity with extrusion parameters like power consumption.

The objective of **Paper II** was to quantify the extent of pressure and torque changes during the operation of the screw type rheometer because secondary flows and oscillating flows can be produced due to the non-symmetric geometry of the screw which could affect the rheological measurements. Another aim was to create a different calibration method that can take into account the relatively high friction which could be present in a bearing system made to work in a harsh environment, as it can produce a flow curve with an intercept higher than zero using a Newtonian fluid. It was also aimed to study the use of the downstream pressure as a substitute to the torque measurements since torque can be affected by the friction in the bearing system.

The main goal of **Paper III** was to analyze the capability of the screw type rheometer to characterize the flow behavior of non-Newtonian fluids, both time dependent and time independent using a cylindrical analogue. Another important goal was to analyze the capability of the system to perform viscoelastic measurements (e.g. the storage and the loss modulus) which could provide an insight to how an on-line or in-line screw type rheometer could perform viscoelastic measurements.

The main aim of **Paper IV** was to develop and verify the use of the die pelleting rig to characterize the compression rheology of wood powders and to correlate the compression data with the physical strength of wood pellets. Another goal was to study the compressibility and pellet strength effects of four different pre-treatments on ground Pine Scots. A secondary goal was to supply with more information to **Paper V**.

Paper V aim to discover whether the rheological information provided by the die pelleting ring can be used to assess differences between four rheologically different materials regarding their ability to be pelleted or not. For this purpose two rheological parameters were compared: the normal stress at incipient flow and the yield stress with the energy consumed by an industrial pellet press. A secondary goal was to study the grinding effects given by the industrial pellet press which could produce discrepancies with the laboratory measurements.

3 OVERVIEW OF THE STUDY

An overview of the study is shown in Figure 1.

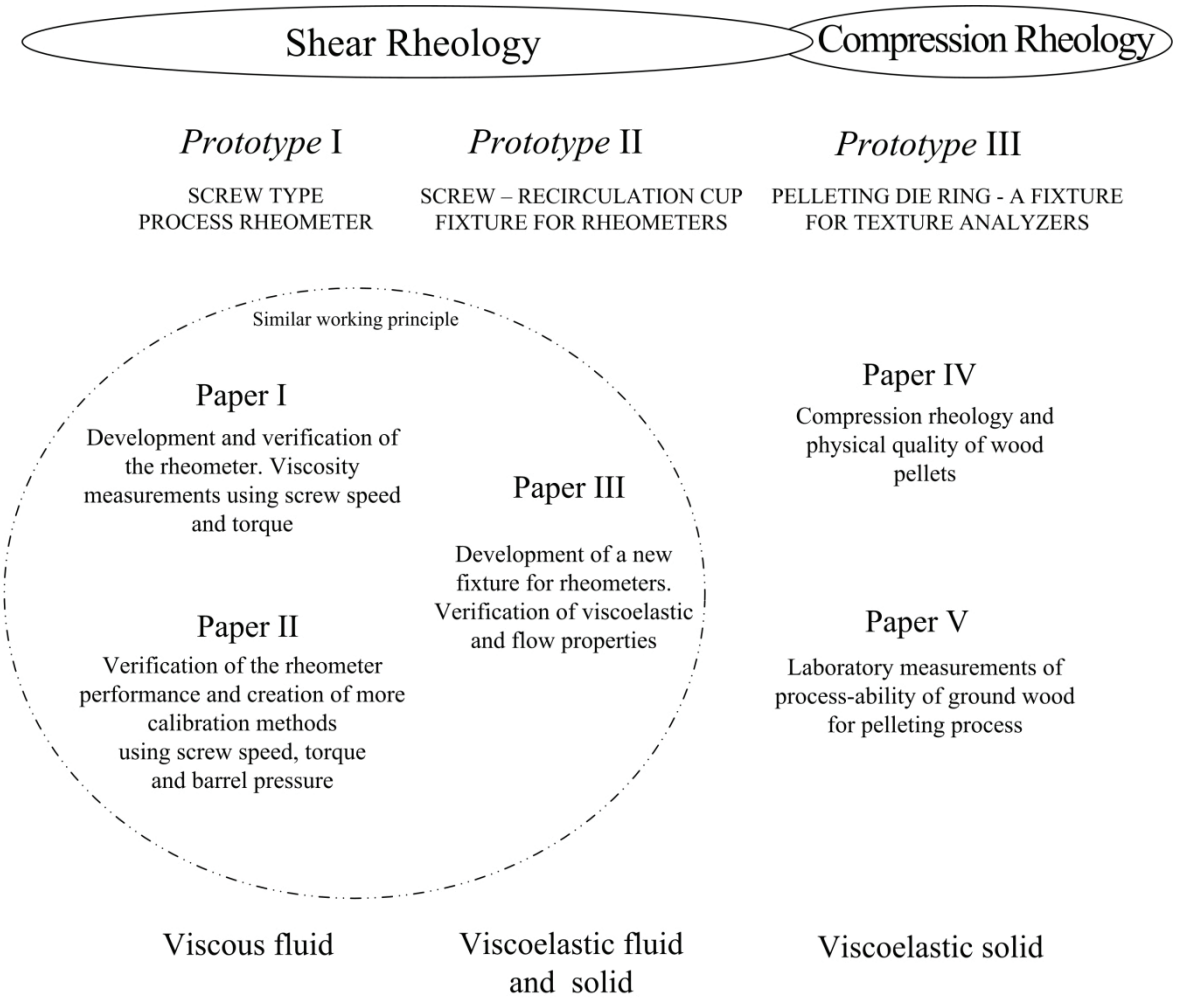

Figure 1: Sketch describing the prototypes used for the different articles and the type of fluids/materials used in the experiments

As can be seen in Figure 1, **Paper I**, **II** and **III** focus on the development and verification of a screw type rheometer. The development of the measurement principle for this rheometer has evolved throughout the different papers. **Paper I**, **II** and **III** provide different calibration methods that can be used for different situations. **Paper I** and **II** focus on viscosity measurements while **Paper III** also verifies the use of the system to perform viscoelastic measurements. As can be observed from Figure 1, the screw type rheometer was

used with viscous fluids, both Newtonian and non-Newtonian and with the solid phase of a viscoelastic material.

Paper IV and **V** were done using a different measurement principle consisting of a pressing mechanism with controlled stress (die pelleting rig). Both studies focus on the same type of materials, ground Scots pine. When pressed and heated, the ground wood becomes a viscoelastic solid. **Paper IV** and **V** were published simultaneously and the information from both is complementary. Specifically **Paper V** uses some of the rheological characterization made in **Paper IV** to complement its results.

4 GENERAL BACKGROUND

In this chapter, first a brief introduction is given to general rheology to later focus on the specific areas related to the contents of this thesis.

4.1 DESCRIPTION AND IMPORTANCE OF RHEOLOGY

Rheology is the science of the deformation and flow of matter [5, 10]. Rheology studies the manner in which materials respond to applied stresses or strain [5, 10]. A useful engineering definition of rheology is the description of materials using "constitutive equations" between the stress history and the strain history [13].

All materials have rheological properties and the area is relevant in many fields of study [10]:

Geology and mining [14, 15]

Concrete technology [17]

Soil mechanics [19, 20]

Plastics processing [22]

Polymers and composites [24, 25]

Tribology (study of lubrication, friction and wear) [10]

Paint flow and pigment [28]

Blood [30]

Wood pelleting [48-56]

Bioengineering [16]

Interfacial rheology [18]

Structural Materials [21]

Electrorheology [23]

Psycho-rheology [26]

Cosmetics and toiletries [27]

Pressure sensitive adhesion [29]

Food [5-10, 26, 31-41] and animal feed [8, 12, 42-47]

Below is listed some of the several situations where rheological data is needed:

- Process engineering calculations involving a wide range of equipment such as pipelines, pumps, extruders, mixers, coaters, heat exchangers, homogenizers, calendars, and on-line viscometers [9, 10]
- Plant design [2, 9]
- Determining ingredient functionality in food product development [5, 9, 10]

- Intermediate or final product quality control [9, 10]
- Food [9, 10] and animal feed [46] shelf life testing
- In general all process engineers handling and processing complex materials such as foams, slurries, emulsions, polymer melts, solutions, etc. [57]

Rheology assists the processor in several areas which are described by examples as follows [9]:

At plant design stage, pumps, pipes, heat exchangers, stirrers, etc. need to be selected. The behavior of liquid flow in a pipe is highly dependent on its rheological properties and thus, the specific pressures required for pumping at a given flow rate can be estimated. Now, if the pipe leads to a heat exchanger, the rheological properties may be changed by the heating effects, which in turn would lead to changes in the flow system. In the extreme case of a large, heat induced reduction in viscosity, the velocity flow might increase and give a product that has had a too short residence time in the system. More seriously the rheological changes may lead to a change in the flow (velocity) profile of the liquid in the system, to a change in the residence time distribution, and again to an under-processed product. However the example, not all heat induced changes lead to a reduction in viscosity. Starch gelation and similar processes can induce the opposite effects, slow liquid and increase the severity of the heating process.

There are many rheological problems in processing. Yield stress may lead to serious processing problems with significant economic relevance. For example, the coating of food products (e.g. chocolate enrobed confectionary to batter enrobed fish or meat products). All of them demand an enrobing material that exhibits yield stress. If this yield stress is too low, the weight of enrobing liquid adhering to the sides of the product will induce a stress higher than the yield stress, either on the vertical side of the product or on a plane parallel to this within the enrobing material, and will cause the material to flow off the product. Conversely, too high yield stress will lead to excessive thickness of enrobing material possibly attractive to the consumer of a chocolate bar, but with adverse economic consequences for the processor.

The dairy industry provides many examples of the use of rheological control techniques. While there are obvious textural related rheological attributes for both set and stirred yogurts, the ever increasing range of diary based spreads demands that the successful

product should have the correct viscoelastic properties of spreadability. Soft and cream cheeses also have liquid properties that must be kept within chosen ranges and which are highly dependent on the ongoing microbiological activity, proteolysis and syneresis within the product.

Rheological measurements are important for bread making. Dough rheology is important in bread making because of its influence in determining the texture of the bread crumb. Such has been the interest in dough rheology that a series of specialized instruments have been developed over the years to monitor these properties (e.g. farinograph and extensigraph).

Compression rheology is important as well as it helps a processor to answer the following questions: why is this batch presenting a manufacturing problem?, will this alternative source of material be ok?, will this powder be transported finely in the installed conveyors?, can powder flowability be improved by using a flow additive?, is this new powder suitable for the existing processing line?, how readily will this powder release entrained air?, will this powder dose satisfactorily?, etc.

4.2 FLUID AND VISCOELASTIC BEHAVIOR - MEASUREMENT PRINCIPLES

4.2.1 FLUID BEHAVIOR

Unlike solids, liquids cannot support their own weight, and are incapable of holding any shape. They must be contained in a vessel or surface depression. Otherwise, they will flow under the shear stresses caused by their own weight. Therefore, the way in which liquids deform to an applied stress is referred as flow (continuous deformation) [5].

Newtonian fluids have the same viscosity at low shear rates as at high shear rates (also referred to as linear fluids [58]). In contrast, non-Newtonian fluids do not have a constant viscosity with respect to shear rate (classified in Figure 2), they are referred to as non-linear fluids [58]. Their viscosity will depend on stress conditions (shear rate), and also often on time. The behavior of Non-Newtonian fluids is briefly described as follows:

Pseudoplastic or shear thinning (power law): their viscosity decreases with increased shear rate.

Dilatant or shear thickening (power law): their viscosity increases with increased shear rate.

Bingham plastic fluid: their viscosity is not dependent on shear rate and time like Newtonian fluids, but they have a yield stress.

Herschel-Bulkley fluids: these fluids have a yield stress and they have a behavior from shear thinning to shear thickening.

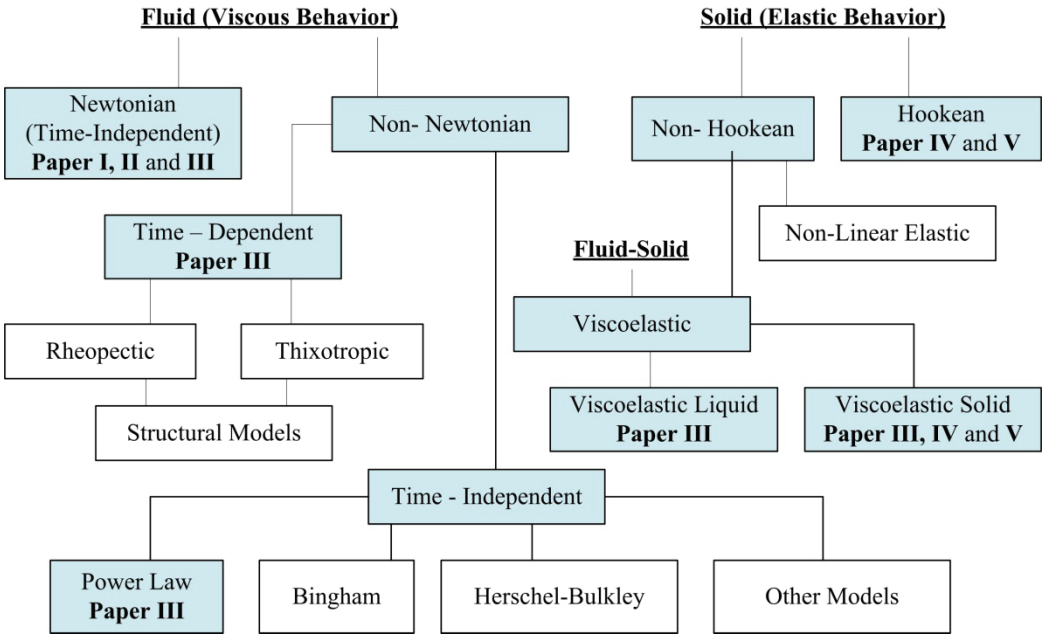

Figure 2. Simple classification of rheological behavior (modified from Steffe [10] to include the fluids or solids used for this thesis in the filled boxes).

4.2.2 SEMI-SOLID BEHAVIOR

The word viscoelastic means that the material simultaneously exhibits some of the elastic properties of an ideal solid and some of the flow properties of an ideal liquid [6]. These behaviors (classified in Figure 2) can be described as follows:

Viscous behavior: when a force is applied, the material begins to flow as soon as the deforming force is applied and it continues to flow as long as the force is applied. There is no recovery when the force is removed.

Elastic behavior: in the elastic solid behavior, there is an instantaneous deformation when a force is applied and when the force is removed, there is a complete recovery of the original shape.

Viscoelastic liquid behavior: there is an instantaneous deformation when the force is first applied, and then the material continues to deform so long as the force is pressing against it. When the force is removed there is some recovery of the original shape (elastic component) but not a full recovery (viscous component). The stress in viscoelastic liquids would decay to zero after the force applied against it is removed.

Viscoelastic solid behavior: these materials present the same behavior described for the viscoelastic liquids, except that the stress in viscoelastic solids would decay to an equilibrium stress higher than zero after the force applied against it is removed.

Plastic flow behavior: when a solid material keeps its deformation as a permanent set after taking away the shear stress, it is call plastic deformation. Liquids demonstrate plastic behavior when they do not begin to flow until a minimum shear stress is exceeded that allows them to yield and begin to flow. This initial stress that must be overcome before the liquid will yield to begin flow is called the yield stress. So, the yield stress is the minimum shear stress needed to get the material flowing, and it is a characteristic of plastic flow behavior. An example is steel which can be deformed if the shear stress from a hammer blow exceeds this value. Another example is butter, which look like a solid, but can be deformed, and keeps its deformation as a permanent set. When a solid body is loaded with a shear stress below its yield stress, in can be deformed elastically, but will not flow. Reasons for plasticity in liquids also stem from strong intermolecular interactions between the molecules within the molecular structure of the material. The stronger are these interactions, the higher the yield stress [5].

4.2.3 ROTATIONAL INSTRUMENTS

Fluids may be studied by subjecting them to continuous shearing at a constant rate [10]. The instruments that characterize the fluid behavior may be classified into two categories, rotational and tube type (see Figure 3). Costs vary tremendously from the inexpensive glass capillary viscometer to a very expensive rotational instruments capable of measuring dynamic properties and normal stress differences [10].

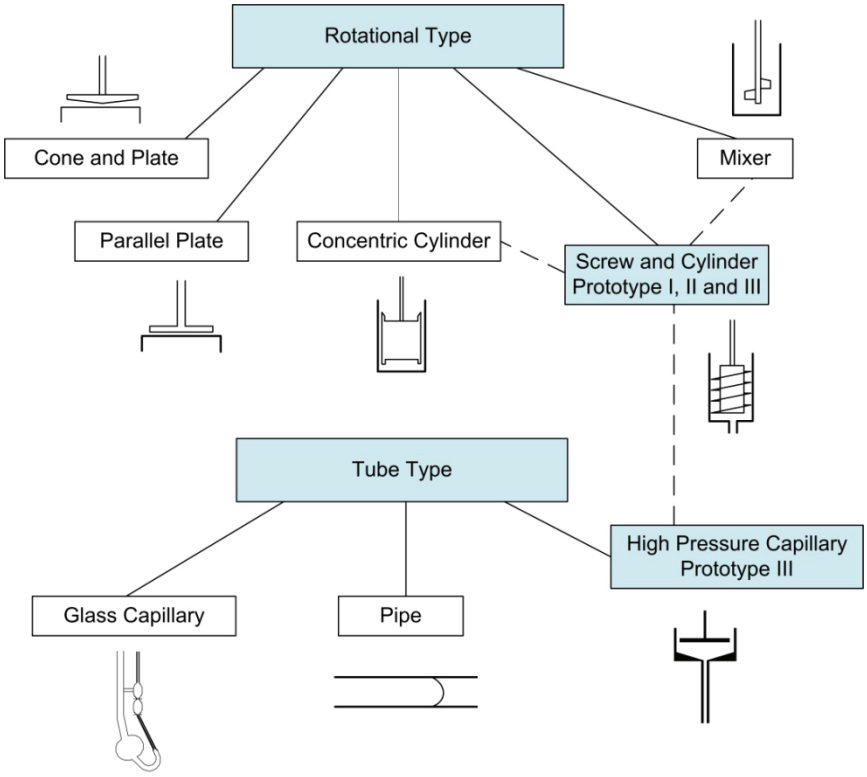

Figure 3. Common rheological instruments divided into two main categories: rotational and tube type. Dashed lines are used to indicate that the screw type rheometer present similarities with other methods. The figure was adapted from Steffe [10] to include the prototypes developed for this thesis.

Rotational instruments may be operated in the steady shear (constant angular velocity) or oscillatory (dynamic) mode.

4.2.3.1 SCREW TYPE RHEOMETERS

The development of screw rheometers is been described from 1984 by Kraynic et al. [59]. This type of rheometer which is shown in Figure 4, is been successfully used for tomato products [10, 60].

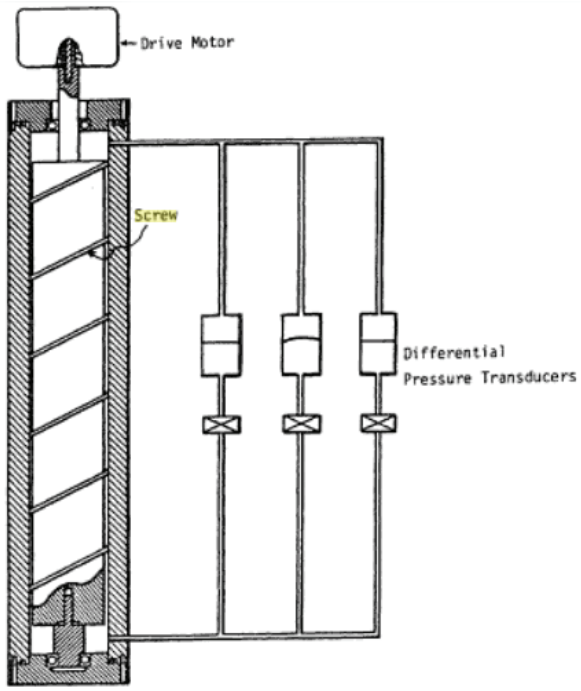

Figure 4: Helical screw rheometer presented by Kraynik et al [59].

The helical screw rheometer presented by Kraynik et al [59] is indicated as offering advantages at high temperatures and pressures, with chemically reacting systems having a time dependent viscosity, with settling suspensions, and as a process monitoring device [10, 61]. The instrument resembles a single screw extruder having minimal flight clearance and operating at close discharge. Two measurements are made, the angular velocity of the screw and the pressure difference between transducers located at two different axial positions in the wall of the barrel. As the screw turns and the flights pass under the pressure transducers, a periodic pressure is recorded. The average pressure difference along the barrel measured over cycles is related to an angular pressure gradient equation that considers the barrel length and radius, and the angle of the helical screw flights. Kraynik et al [59] and Tamura et al [41] showed that the angular pressure gradient could in turn be related to the parameters of specific constitutive relations that includes the power law, Ellis and Bingham models.

Another type of helical screw rheometer is the one developed by Shackelford [62] which is shown in Figure 5.

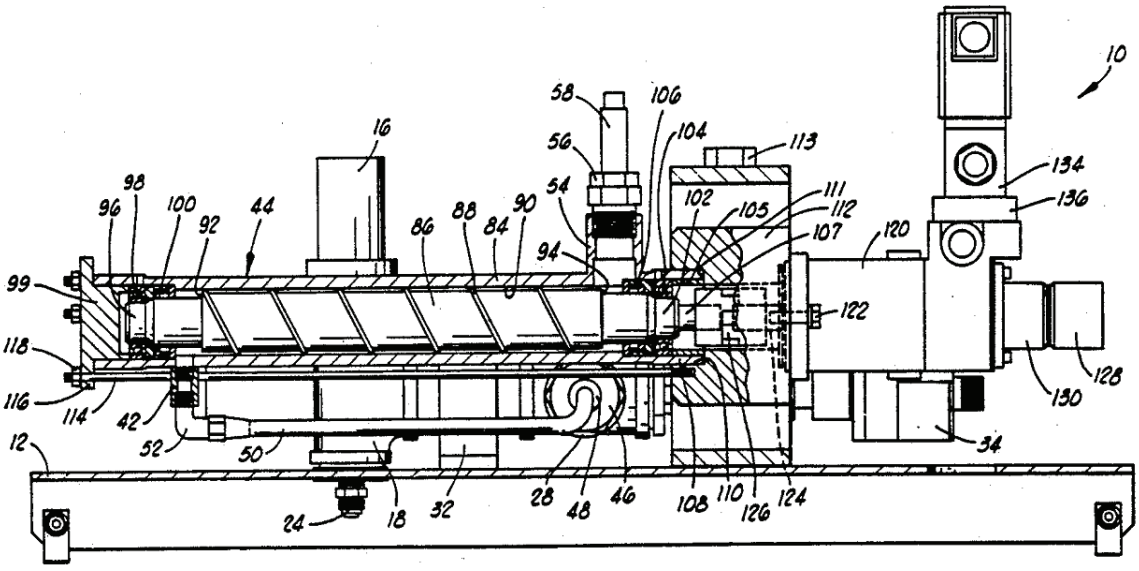

Figure 5: Helical screw rheometer developed by Shackelford [62].

A short description of how the rheometer presented in Figure 5 works is included in **Paper I** and is summarized as follows: a pressure transducer 58 is installed at the outlet of the rheometer 54 that has a horizontal leg connected to a solenoid valve (not shown in Figure 5) which is used to close the outlet downstream 54 from the pressure transducer 58. In a test, fluid flows into the rheometer 42. With the screw 86 stopped and the discharge 54 closed, a pressure transducer 58 measures a static pressure, and a computer resets this to a zero reference value. The screw 86 in the rheometer is then rotated at a constant speed with the discharge 54 closed, and the pressure transducer 58 measures dynamic pressure at the outlet 54. The test is repeated at different speeds. A computer then calculates, in response to the differential pressure and speeds, the shear rate and shear stress. Other main items are 12 a frame, 34 a temperature transmitter, 84 housing, 96 outboard end of screw, 98 and 104 bearing, 99 end cap, 102 drive end portion, 107 shaft portion, 120 hydraulic motor, 124 shaft with optical encoder to transmit speed signal and 134 hydraulic proportional valve to control speed. A more detailed description can be found in the patent [62].

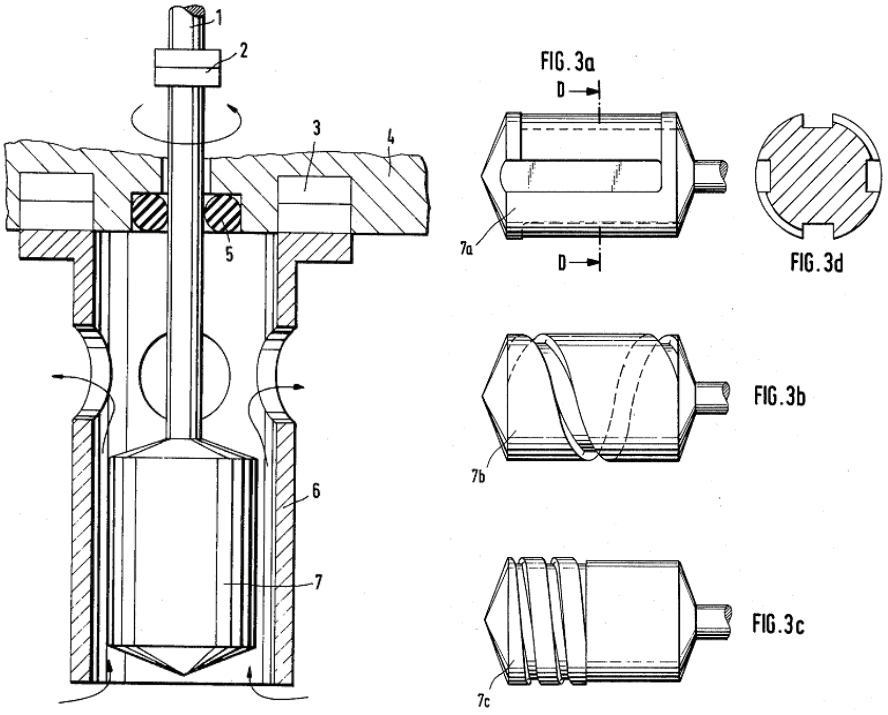

Figure 6: Rotary viscometer for continuous measurement of viscosity developed by Winter [63]. The arrows at the left sided drawing show the flow direction.

Another similar rheometer is developed by Winter [63] (Figure 6) and a short discussion and comparison with *Prototype* I and II is included in **Paper I** and **III**. To help understanding the working principle of the device developed by Winter [63], a description of the preferred embodiment and main components is indicated according to the numbers shown in Figure 6 where: 7 is a rotor, 6 housing, 1 shaft, 2 torque sensor, 5 seal, 7a a blind grooved torpedo type of probe, 7b shows a cut into the cylindrical portion of a helical duct to ensure axial transport and 7c shows a probe split into a delivery zone and a shearing zone. A more detailed description of the system can be found in the patent [63].

The patent from Winter [63] was probably granted due to design novelty (working principle) and not measuring principle due to the claims in the patent does not indicate how viscosity is calculated and consequently it is assumed that is taken analytically from a coaxial cylindrical analogue. An analytically calculated viscosity from a coaxial cylindrical analogue without including pressure can affect greatly the measurements as indicated in **Paper II** where it is shown that different pressures at the downstream generated through different restriction can produce different slopes between rotational speed and torque for the same

Newtonian fluid. This effect is likely to affect the measurement when using the probe 7b and 7c indicated in Figure 6.

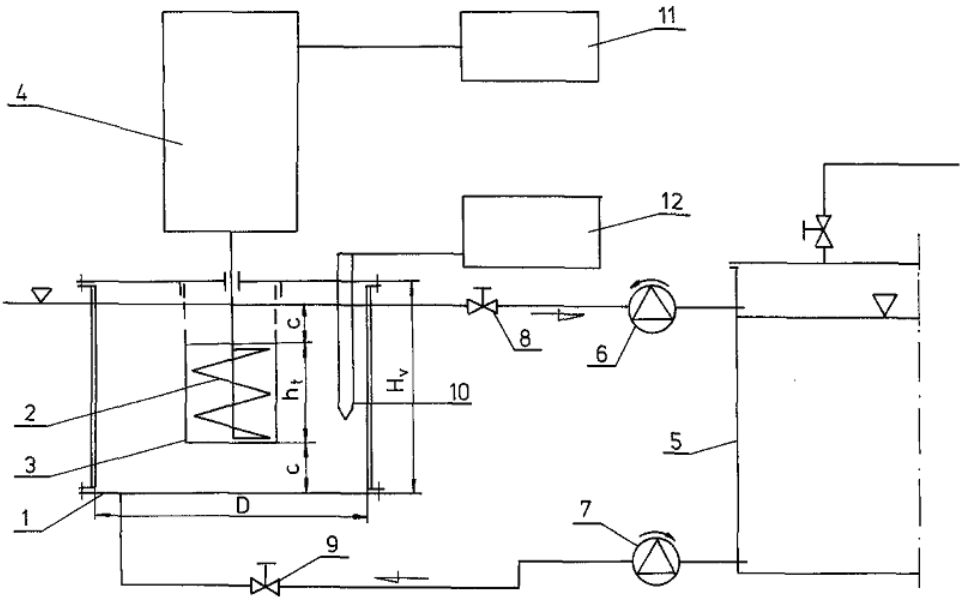

Figure 7: The helical screw impeller presented by Kemblowski et al [64].

A short description of how the rheometer presented in Figure 7 works is included in **Paper III** and a more detailed description can be found in the patent [64]. To help understanding the working principle of the measuring device developed by Kemblowski et al [64], a description of the preferred embodiment and main components is indicated here according to the numbers shown in Figure 7 where: 1 is a tank, 2 the helical screw impeller, 3 draught tube, 4 measuring head, 5 reservoir, 6 and 7 peristaltic pumps, 8 and 9 valves, 10 thermocouple, 11 torque recorder and 12 a temperature recorder.

The working and measuring principle of the rheometer used by Kemblowski et al [64] in 1988 resembles the system developed by Winter [63] in 1978. Consequently, both systems differ to the rheometrical system presented in this thesis (*Prototype* I and II) where the relation between torque and speed can change at different pressures for the same Newtonian viscosity and rotational speed generated by the use of restrictions with different sizes (studied in **Paper II**).

In the process for patenting, the author of this thesis successfully received a patent in Norway for the screw rheometer and system used in **Paper I** and **II**. However, the international patent application was dropped due to the high costs after encountering problems with the similarities of the rheometer developed by Shackelford [62], although the rheometer developed by the author of the thesis is more close to the rheometer developed by Winter [63]. Also the international patenting process was dropped because of a lack of interest from the rheometer maker companies.

The author of this thesis did not find any evidence in literature about using a screw type rheometer to perform viscoelastic measurements. **Paper III** proposes an insight for screw rheometers to perform oscillatory tests and to measure viscoelastic properties.

4.2.4 TUBE TYPE OF INSTRUMENTS

These instruments may be placed into three basic categories: glass capillaries, high pressure capillaries and pipe viscometers. All establish a pressure difference to create flow. The major difference between a capillary and a pipe viscometer is the diameter of the tube. Although there is no clearly defined size at which a tube should be called capillary or a pipe [5, 9]. Diameters in commercial capillary instruments typically range from 0.1 to 4 mm [5, 9] with a variation in entrance angles of 15 to 90 degrees [5]. Pipe viscometers are usually built "on-site" so sizes vary widely. Some may be as small as 7 mm in diameter but values between 12 – 32 mm are not uncommon in food applications. Length to diameter (L/D) values in tube viscometers range from 2 – 400, the smaller values are found in the capillary units but are seldom seen in pipe systems [10] .

4.3 POWDER BEHAVIOR, COMPACTION AND MEASUREMENT PRINCIPLES

A powder consists of a number of individual particles, the bulk property of a powder is not usually the simple summation of the physical properties of single particles. Also in most cases, each packing particle has unique physical properties such as size and shape [65].

The flow properties of bulk solids depend on many parameters like particle size distribution, particle shape, chemical composition, moisture and temperature [66]. It is not

possible to determine theoretically the flow behavior of bulk solids as a function of all of these parameters. Even if this were possible, the expense for the determination of all parameters of influence would be very high. Thus, it is necessary, and also simpler, to determine the flow properties in an appropriate testing device [66].

The phrase “good flow behavior” usually means that a bulk solid flows easily, i.e. it does not consolidate[1] much and flows out of a silo or a hopper due to the force of gravity alone and no flow promoting devices are required. Products are “poorly flowing” if they experience flow obstructions or consolidate during storage or transport [66].

With an easy-flowing, dry bulk solid with large, hard particles (e.g. wheat grains or glass beads), bulk density will increase very little. With a fine and/or moist bulk solid (e.g. flour, moist sand), one will observe a clear increase in bulk density.

Funnel flow from a small beaker or cup is a very simple method for checking the flow behavior or a powder. It consists of a beaker or cup with a funnel outlet at the bottom. The cup is filled with a powder sample to a designated level, and then the time required for the sample to drain out through the funnel at the bottom is measured. This drain time relates to shear rate and the fixed elevation head of the powder sample in the cup relates to the shear stress [5]. In the industry, no attempt is made to convert these measurements into rheological variables (shear stress or shear rate). The technician simply needs to confirm that the time measured to drain the sample agrees with the given specification of drain time for that product.

One disadvantage of this funnel flow cup method is that the sample level decreases in the cup while draining. This means the elevation head or hydrostatic pressure that is driving the flow rate is decreasing during the time of a test. Therefore, shear stress is not constant over the time of the experiment [5].

When a volume of powder is loaded (consolidation stress), the powder becomes compressed. The more the volume of the bulk solid is reduced at a given consolidation stress, the more compressible the bulk solid is. This is normally assessed in a compaction stress – density plot [66].

[1] Consolidation (powder): a process whereby a powder decreases in volume.

Compaction will proceed along different steps: the free flowing region where aggregates of particles move mutually to reduce the bulk volume, the compaction region where the aggregates are broken to yield a dense phase and the region where particles undergo plastic deformation [65]

The mechanism of densification during pressure agglomeration includes as a first step, a forced rearrangement of particles requiring little pressure followed by a steep pressure rise during which brittle particles break and malleable particles deform plastically as shown in Figure 8 [65, 67].

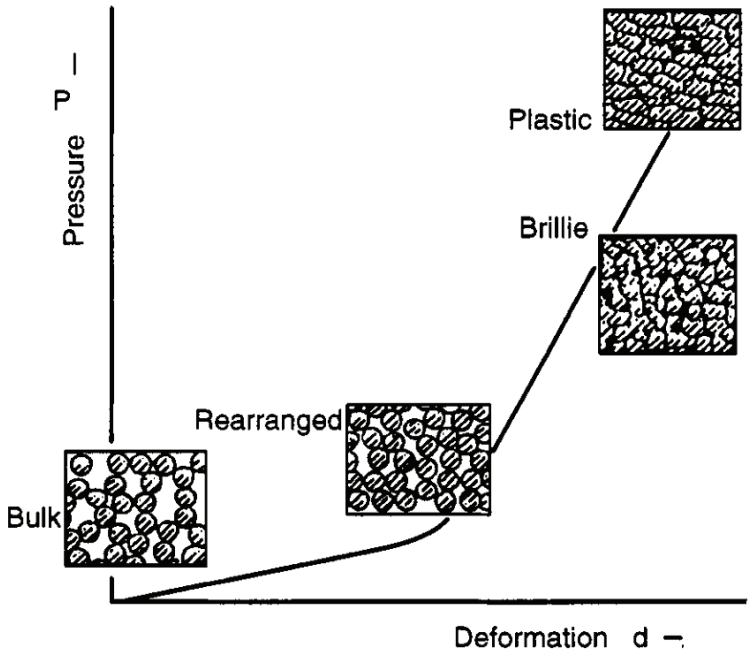

Figure 8. The mechanisms occurring during pressure agglomeration [65, 67].

At low pressure, rearrangement of the particles takes place, leading to a closer packing. At this stage, energy is dissipated mainly overcoming particle friction, and the magnitude of the effect depends on the coefficient of inter particle friction. In the case of fine powders, cohesive arches may collapse at this stage [65].

At higher pressures, elastic and plastic deformation of the particles may occur, causing particles to flow into void spaces and increasing the area of inter particle contact. Interlocking of particles may also occur. For materials of low thermal conductivity and low melting point, the heat generated at points of contact may be sufficient to rise the local

temperatures to a point where increased plastically and even melting facilitate particle deformation. With brittle materials, the stress applied at inter particle contacts may cause particle fracture followed by rearrangement of the fragment to give a reduced volume [65].

High pressure continues until the compact density approaches the true density of the material. Elastic compression of the particles and entrapped air will be present at all stages of the compaction process [65].

The mechanisms discussed may occur simultaneously. The relative importance of the various mechanisms and the order in which they occur depend on the properties of the particles and on the speed of pressing [65].

The aim of compaction is to bring small particles into sufficiently close contact so that forces acting between them are large enough to produce a product that has sufficient strength to withstand subsequent handling [65]. An increase in the bulk density can be observed with an increase in strength of the bulk solid specimen [66].

From an operational viewpoint there are several kinds of compaction. Piston press and hydrostatic pressing are static ways of compaction, whereas tapping, vibration, hammering, and explosion belong to impact compaction. Other types of compaction are also available such as roller pressing, vacuum pressing, multi axis compression, pellet presses, etc [65].

Die compaction of powders that develop strength on the compacts is the absolutely dominating forming technology for powdered materials. Areas of application are structural parts, hard metal and ceramic indexable inserts, pharmaceutical tablets, electrical contacts, filters, hard magnets, soft magnetic composites, friction materials [66], animal pelleted feed [12, 46, 68-72], wood pellets [50, 52, 53, 73, 74] and many others.

The progress in compaction of powders required further intensive development work, because the mechanical behavior of compressible powders is more complex to deal with than that of incompressible solids [75]. Die compaction is certainly the most representative test for studying powder densification phenomena or compressibility [76].

During the consolidation process, if the bulk solid is relieved of the consolidation stress and removed from its solid container and then further compressed, one will notice that with an increased compressive stress, the specimen will deform and finally break (fail) at a certain stress [66].

4.3.1 PELLETING MANUFACTURING PROCESS

To help to understand the pelleting process that was used in the experiments of **Paper V**, a short description is given. Pelleting can be regarded as a kneading, compressing and forming process where rheological transformations in the material take place [12]. Pellets are produced in a press where the confinement pressure depends on the length and diameter of the die [43]. The agglomeration and shaping are due to the pressure forcing the material through the die holes, as well as frictional forces. A high pelleting pressure will likely increase agglomeration by increasing the degree of densification, resulting in lower voids. Typically, the products from high pressure agglomeration feature high strength immediately after discharge from the equipment [12, 38, 66].

A representation of the pelleting die ring and pressing rollers of the pellet press used in **Paper V** is shown in Figure 9. The die ring rotates at constant speed and normally cannot be controlled, as for example the case of the Sprout matador M30 industrial pellet press used in **Paper V**. The two rollers press the material in the gap roller - die ring (X in Figure 9) and the material is forced to pass through the die holes where they are later cut by knives. During a pelleting process of animal feed and using a similar pellet press to the one used in **Paper V**, Salas-Bringas et al [72] utilizing infrared thermography showed that the material also increases its temperature due to the friction generated in the gap between the rollers and the die, mostly in the nip area [72]. Unfortunately, because of equipment design, the rheological properties of the material during pelleting are difficult to measure, and thus, to a large extent pelleting remains as black box [12].

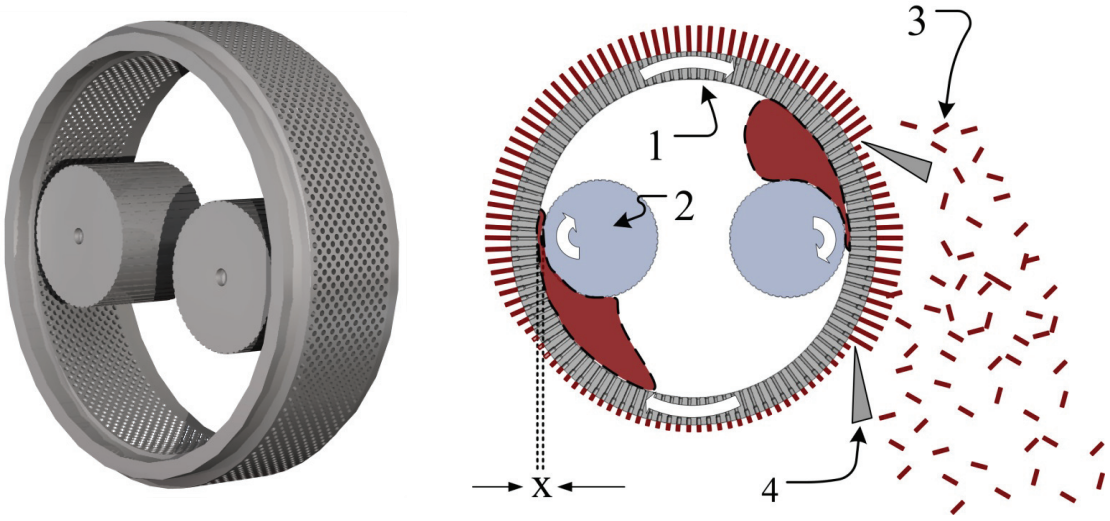

Figure 9: Pelleting die ring with two pressing rollers. At the right side of the figure items are indicated by numbers: 1 a rotating die ring, 2 rotating rollers, 3 cut pellets, 4 knives and X is the gap roller-die ring. The right side of the figure has been modified from Salas-Bringas et al [72]

As previously said, the rheological behavior of compressible powders is more complex to deal with than that of incompressible solids and thus, to achieve good pelleting, new and more sophisticated production planning and process control are required, that includes knowledge of how the mixture responds to applied stresses during compaction and pellet release, keeping in mind crack prevention [12]. Consequently a rheological characterization of the powder material can provide new insight to the future of the pelleting process and manufacture of pellet presses.

Computer modeling of powder die compaction has a reputation of being limited to density predictions on simple shapes and has been slow to perform, however, today modern PCs are fast and capable. Providing modeling input data with sufficient accuracy (e.g. rheological characterization), these software programs can deliver accurate quantitative information on stresses and press functions that previously could only be estimated [12, 75]. This can lead to the development of a more efficient process.

4.4 SOLID BEHAVIOR OF COMPACTS AND MEASUREMENT PRINCIPLES

When a solid body at rest on an immovable surface is loaded with a weight (in this case, a force acting downward), it will respond with a deformation that can be characterized by a reduction in its initial height dimension. Therefore, as stress increases on a sample, it will cause the responding strain to increase as well [5]. When a material exhibits a linear relationship between increased stress and strain, it is said to be an elastic behavior. Beyond this region at increased levels of stress, it is observed a nonlinear deformation when the solid begins to flow or yield. At the yield point, the strain is able to continue increasing with little or no increasing stress. If the stress was to be released at this point, the sample would keep its deformation as a permanent set (it was deformed by flowing and therefore a nonelastic or plastic deformation). At a certain point, the strain reaches a limit beyond which the sample can no longer sustain its original structure, and fracture or breakage occurs [5].

The yield stress of many solid materials like metals are listed in tables. However, the yield limit of a compacted bulk solid is dependent on its stress history, because the consolidation stress affects the bulk density and cohesive strength [66]. For example, in pharmaceutical tablets, the dominant process parameter that determines the tablet strength is the compression pressure [77].

The mechanisms of fracture of the solid components are different as it is indicated below [6]:

Type 1; Simple fracture is the separation of a body into two or more pieces in response to an imposed stress. In most cases the body breaks into two or more pieces, but sometimes the fracture may be partial when the fracture plane does completely cross the specimen.

Type 2: Brittle fracture in which there is little or no plastic deformation before fracture and a low energy absorption up to fracture. Nuts and good quality potato chips are a good example of brittle fracture, other examples are compacts of milk and buttermilk powders [78].

Type 3: Ductile fracture in which there is substantial plastic deformation with high energy absorption before fracture. Meat is an example of ductile failure [6]. Other examples are wood [55] and animal feed pellets [46].

The strength of lignocellulosic agglomerates is frequently tested using crashing, drop, abrasion tests, methods for the determination of impact, bending, cutting or shear strength.

All values obtained by these methods are strictly empirical and cannot be predicted by theory because it is not known which component of the applied stresses causes the agglomerate to fail. For the same reason, the experimental results from different methods cannot be compared with each other [67].

The strength of lignocellulosic agglomerates can be determined through the tensile strength which is defined by the tensile force divided by the cross section or, if the test body has no uniform shape, the area of the failure plane(s) of the agglomerate [67]. However and unfortunately, this is not possible in all cases as for example wood pellets produced through pellet presses because the equipment produces cylindrical pellets with undefined ends and they cannot be tested in compression as shown in Figure 22(A), thus the common way to test them (also used in **Paper IV**) is as shown in Figure 11. In addition to the undefined ends of the pellets, the pellets breaks in different and random failure planes so it is difficult to know the area of stress. Additionally, in wood pellets with low density, the volume might not be filled entirely, leaving voids of air that can affect the way the force is transmitted.

The way the stresses are transmitted in completely filled agglomerated materials is described as follows referring to Figure 10:

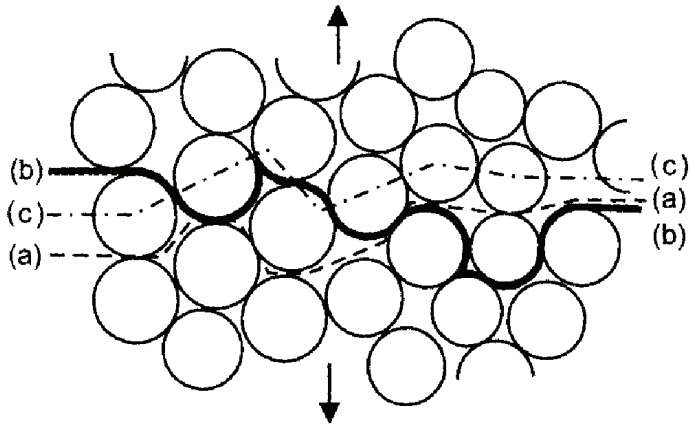

Figure 10. Two-dimensional schematic representation of the failure lines describing strength of agglomerates with a matrix binder [67]

where (a) represents the pore volume strength, that is the tensile strength component of the binder substance (e.g. lignin), (b) represents the particle boundary strength, that is the tensile strength component caused by adhesion between binder and particulate solids forming the agglomerate, and (c) representing the strength component of the particulate solids

forming the agglomerate. The lowest strength component determine the overall agglomerate strength [67].

Many biomaterials like solid foods or wood pellets maybe changed from a brittle to a ductile fracture or vice versa. Changing the temperature or moisture content can move a material from a glassy state to a rubbery state by moving it through the glass transition temperature range [6].

Determination of agglomerate strength in industry is pragmatic [67]. Although knowledge and understanding of the fundamentals of agglomeration, particularly the nature and effect of the binding mechanisms and how they can be influenced, become more and more important during the development and optimization of agglomeration processes. Agglomeration as a unit operation is still more an art than a science [67].

In the industry of agglomerates, the definition of strength and quality differs. Strength related requirements may differ whether it is an industrial bulk material or a consumer product. The industrial bulk material may break down to a certain extent during process, and as long as it remains free flowing and dust free it can still be useful to the process, while a consumer product must have perfect and pleasing appearance where even a minimal chipping or breakage into large chunks should be avoided [67]. Intermediate products such as wood pellets for combustion must have characteristics that are suitable for the intended use. For example, the wood pellets should be strong enough and abrasion resistant for storage and handling to avoid bridging. Flow problems in ducts or silos, dusting and segregation of components is avoided. Another case is animal feed pellets that are expected to be strong enough to avoid similar problems described for wood pellets, but at the same time should be weak enough to be broken down by the molars of a ruminant. For these reasons, “strength” means many different things in industry.

Three tests are well known to describe the rheology of compacts; the tensile test, the diametral compression test and the simple compression test. It will be described only the diametral compression test because as it was commented in this section, it is the most appropriate testing method for pellets with undefined ends.

The diametral compression test is used for comparing different materials and it is commonly used on pharmaceutical tablets [77], animal feed pellets [45, 46], wood pellets [55, 56] and it had been successfully used on food powders like buttermilk [78]. Tests are

carried out by applying two diametrically opposed forces on cylindrical specimens as shown in Figure 11.

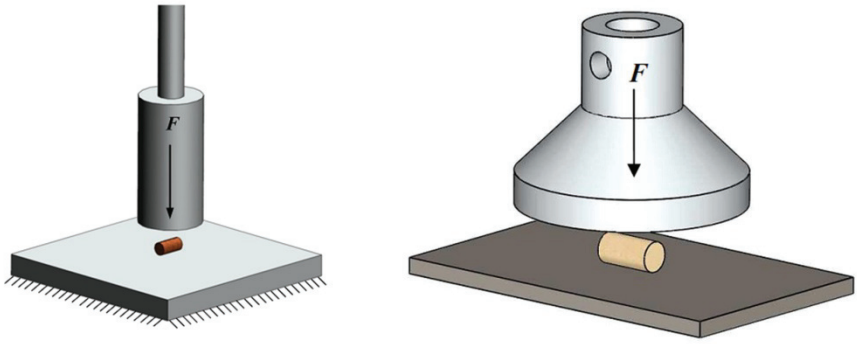

Figure 11. Different probes for diametral compression test of cylindrical specimens. The arrangement on the left was used by Salas-Bringas et al [46] and on the right by Salas-Bringas et al [55]. The later was used in **Paper IV**.

The location of the failure line depends on the density of the compact, more specifically on its cohesion. Failure analysis can be performed using several different tests. These tests require specimens compacted with a certain level of cohesion in order to handle and fix them to the testing machine [79].

If the behavior of the solid specimen is isotropic and linear elastic, a uniform tensile stress is developed along the loaded diameter as shown in Figure 12. However, if the compact is anisotropic, the tensile stress could be different from the one obtained from a true tensile test [79].

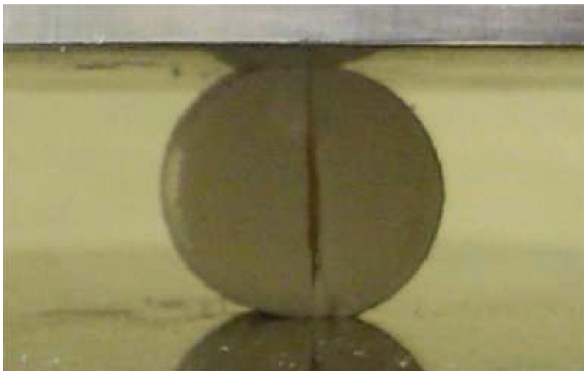

Figure 12. Tensile failure of a brittle buttermilk pellet during a diametral compression test (Salas-Bringas et al. [78]).

4.5 IMPORTANCE OF RHEOLOGICAL INSTRUMENTATION FOR PROCESS APPLICATIONS

Where are we going and why?

The increasing competitiveness has driven a conscious move from traditional factory quality assurance and process control to a rapid, real time response to ensure satisfying process efficiency, product quality and reduced waste of raw materials. This move requires a variety of on-line or in-line measurements. Real time measurements can be used for process adjustments by an operator or used in a control loop by an automated system. Real-time monitoring and process control are the primary justifications for using in-line rheometers and viscometers during production [1]. As mentioned earlier, the future of many processes is full automation which will demand a large number of sensors and process instrumentation.

Why is it difficult to relate off-line measurements to the process?

Many materials being primarily suspensions, emulsions, gels, foams, or frequently a combination of these structures, display a complex rheological behavior. This behavior encompasses time, shear, temperature, and pressure dependence, each of which severely restricts the validity of off-line rheological measurements to provide information pertinent to the processing conditions. An off-line analysis provides a retrospective snapshot of the sample rheology, which may not reflect the sample behavior a minute before or after the sampling time [1].

Although the process of off-line measurements is often limited by the material history and the type of process information sought, modern laboratory rheometry can provide access to a wide temperature and shear rate range, high pressure, dynamic low strain measurements, normal stress measurement, creep experiments and extensional rheology, therefore providing an in-depth characterization of a food system. For research and finished product analysis modern laboratory rheometers offer an important source of information. However, to obtain real time knowledge of fluid performance during processing, both in-line and on-line rheometry is extremely desirable [1].

5 MAIN RESULTS AND DICUSSIONS

5.1 DEVELOPMENT OF THE PROTOTYPES

The development of prototypes is a process which is normally not included in the scientific papers. However, it is briefly mentioned in the process done for this thesis as it demanded a large effort and time throughout the studies.

The prototyping process involved CAD design, simulations for stress analysis, construction of the prototype, sensor selection and installation, development of a control system and electrical wiring.

Generally speaking, design cycles are expensive and time-consuming due to prototyping and field testing. Due to time and cost constraints, most designers accept a solution that may not be optimum, at this point it should be stated that many products are always being optimized and the re-design is a regularly task without ending [80]. This can explain the reason for developing *prototype* II and the existence of an ongoing project to improve *prototype* III.

The CAD design was made using SolidWorks program (Dassault Systèmes, SolidWorks Corp.) which can perform stress analysis through the simulation package "SolidWorks Simulation". The following figures from this section show some of the steps in the development process of *prototype* I.

The design process in *prototype* I demanded the use of stress analysis to produce a safe equipment because it is a robust system made to work and generate relatively large pressures and torques.

The simulation shown in Figure 13 was made based on an assumption of an atmospheric static pressure at the top of the inner face of the barrel, and a maximum pressure of 4 MPa at the bottom of the barrel. The change in pressure was assumed to be linear. For the case of the screw shown in Figure 13, the pressure was assumed to be 4 MPa affecting the bottom face of the screw and the bottom face of the helical flights. The material of both components were construction steel S355.

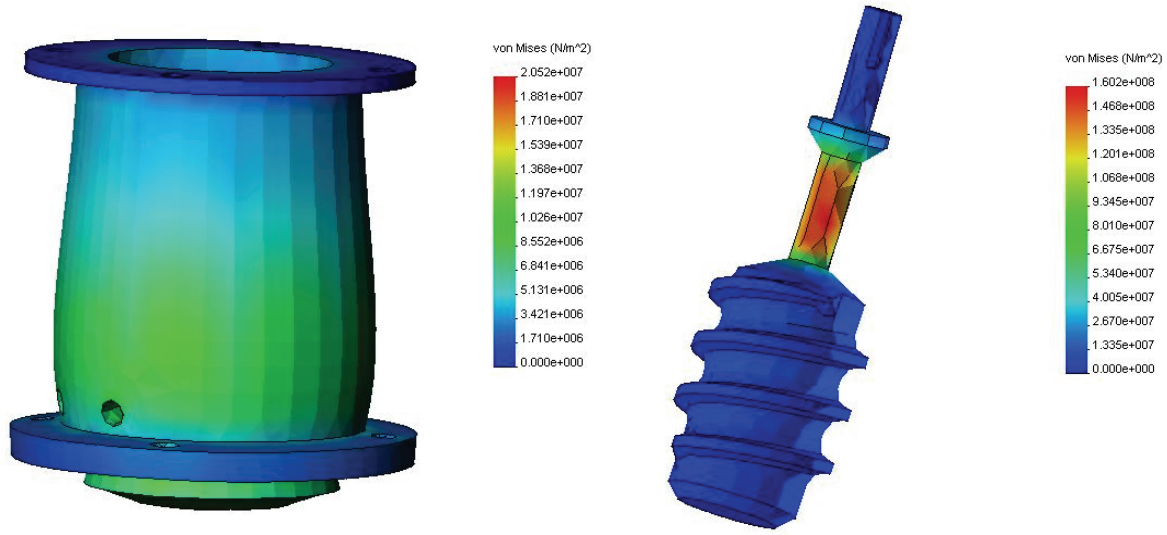

Figure 13: Von Misses stress analysis of the barrel and screw of *prototype* I. The deformation scale used in the drawing of the barrel is 3937.86 and 89.9583 for the drawing of the screw.

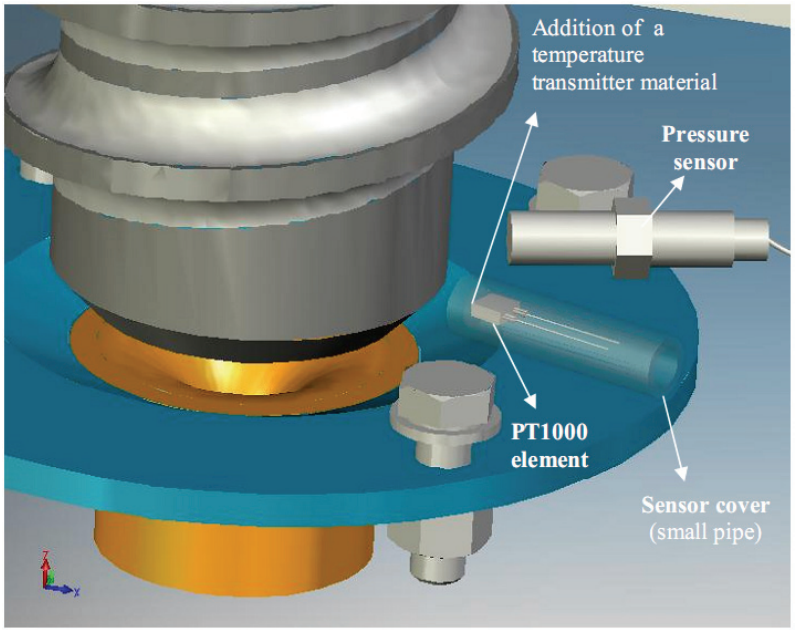

Figure 14: Location of pressure and temperature sensor. The temperature sensor was also designed by the author of this thesis.

The temperature sensor shown in Figure 14 was also designed by the author of this thesis which included the addition of thermo-conductive paste to improve the time response of the PT1000 element.

Figure 15: At the left the 3D model of *prototype* I and at the right the built *prototype* I (without recirculation path).

The 3D model was essential in the development process of all prototypes as it represents accurately the clearances and spaces in the assembly, it also provided help in developing the mechanisms and working principle.

Among the different activities for the author of this thesis was to make drawings of the wiring for the main electrical connections. Figure 16 shows the wiring of one of the two cabinets used for the connections.

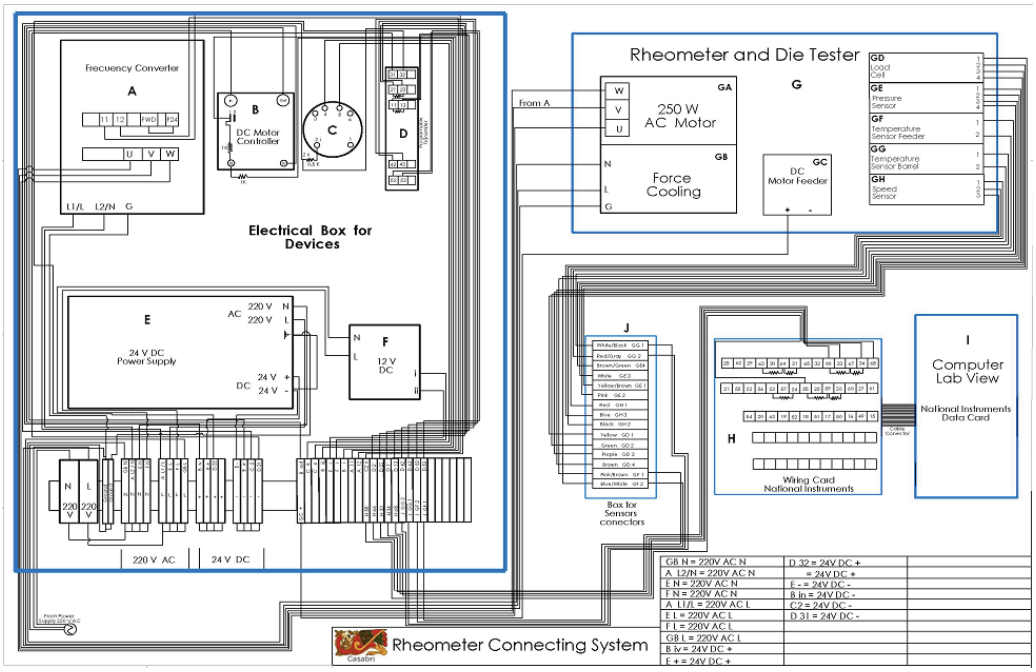

Figure 16: Drawing of the electrical wiring for cabinet 1 of *prototype* I.

It is important to mention that *prototype* I began to be design and built before the formal engagement to the PhD studies and it continuous during the PhD studies.

As it is commented in **Paper I** and **II**, *prototype* I was built using a relatively low cost bearing system which produced an intercept in the linear regression between torque and speed different to zero when using a Newtonian viscosity standard (N450000, Cannon Instruments Co., PA). This is one of the reasons that encouraged the author of this thesis to develop *prototype* II to be driven with lower friction by a Paar Physica UDS 200 rheometer. Consequently *prototype* II showed that a linear regression with intercept zero is obtained when using a Newtonian fluid in a screw type rheometer. This is what was expected when doing **Paper I** and that led to the new improved calibration methods in **Paper II**.

The other reason for making a replicate of the screw type rheometer in a Paar Physica UDS 200 rheometer was to take advantage of the controlling system which allows performing oscillatory tests for viscoelastic characterizations at different strains.

The screw of *prototype* II was designed to have a low moment of inertia which is desirable when performing oscillatory tests. A comparison with standard probes in **Paper III** shows that the screw has a lower moment of inertia than many of the Paar Physica probes (Z4 bob, CC27 bob, PP50 Plate and MK22 cone).

Prototype III started as a modification of a capillary rheometer developed by the author of the thesis during the PhD studies [36, 81]. The development process of *prototype* III also included similar steps to the ones shown for *prototype* I, CAD design, stress analysis and development of the electrical system.

It is important to mention that *prototype* II and III were much simpler in their construction than *prototype* I.

5.2 CALIBRATION METHODS AND RHEOLOGICAL CHARACTERIZATIONS

A summary of the different calibration methods is included in Table 1. The table shows the calibration methods used on each paper and the type of uses.

As it can be deduced from Table 1, different calibration methods were developed throughout different studies which indicate that this work has been a rather "evolutionary work". **Paper II** improved the calibration method used in **Paper I** and **Paper III** tries to solve the limitations of the methods used in **Paper I** and **II**. The improvement from **Paper I** to **Paper II** comes as a result of a limitation given by the bearing system in *prototype* I which did not produce a linear regression with intercept zero in the flow curve of a Newtonian fluid. Finally **Paper III** uses a new *prototype* (number II) to avoid the problems of the bearing system from *prototype* I and takes advantage of a better control system. As a result, it was possible to widen the range of applications in **Paper III** by including viscoelastic measurements. The measurement method used in **Paper IV** and **V** did not require a calibration due to the use of direct measurements. However, the mechanical design and measuring capabilities are currently under improvements in an ongoing project (discussed in section 7).

Table 1: Summary of types of calibration and uses

Paper	Calibration method and number		Used for
I, II	1	Slope between torque and speed	Apparent viscosity
II	2	Area below curve: torque versus speed	Viscosity: Newtonian*
II	3	Slope between downstream pressure and speed	Apparent viscosity
II	4	Area below flow curve: downstream pressure versus speed	Viscosity: Newtonian*
III	5	Coaxial cylindrical analogue: torque and speed	Viscosity and Viscoelasticity
III	6	Normal force versus speed based on cylindrical analogue	Viscosity for low viscoelastic materials
IV	-	Not required	Powders: compression rheology
V	-	Not required	Powders: studies of pellet-ability

* For non-Newtonian fluids it will compare different resistance to flow

Papers I and **II** describe how the rotational speed of the screw is proportional to the local shear rates, which are located at the different parts of the screw surface. It is also described that the torque from the screw (**Paper I** and **II**) and the pressure from the downstream of the screw (**Paper II**) are proportional to the shear stress. A first method describes how an average viscosity can be estimated using the slope formed between torque and the screw speed, indicated as calibration method 1 in Table 1, the method is used in **Paper I** and **II**).

A second method proved that is possible to use the area under the flow curve formed between torque and screw speed to predict viscosity, indicated as method 2 in Table 1 (used in **Paper II**). This method determines viscosity for Newtonian fluids. For non-Newtonian fluids, the areas can only be compared to indicate an overall resistance to flow (not viscosity units) which can allow relative comparisons among fluids as shown in Figure 17.

The third method according to Table 1 can predict an apparent viscosity by using the slope formed between the pressure at the downstream of the screw versus the screw speed (used in **Paper II**). Using a Newtonian fluid, the intercept of the linear regression in method 3 was zero and consequently it is not affected by the bearing system. Consequently this is a

good method to predict viscosity when using screw rheometers with low cost bearing systems.

The fourth method indicated in Table 1 can predict viscosity of Newtonian fluids through the area below the flow curve formed between downstream pressure and screw speed. For non-Newtonian fluids, the results can be used in the same way as described for method 2 (Table 1) which is shown in Figure 17.

To help to understand the type of indication of a fluid resistance to flow that can be obtained using the area below the curve (method 2 and 4 in Table 1), Figure 17 is included. A1 and A2 are the areas below the curve for the different fluids. In the *y*-axis, pressure and torque are indicated to show that any of these two variables can be used. The limitation of this method is that the apparent viscosity cannot be obtained, however an indication of a resistance to flow through the areas can be used to compare relative differences among fluids.

Paper III investigates the use of an experimental calibration procedure to estimate the mean shear stress from torque or from the normal force in the screw shaft, and the average shear rate from the rotational speed. This calibration uses a coaxial cylindrical analogue, Searle type to represent the complex geometry of the screw. In addition to the Newtonian fluid used in the calibration procedure, this time different non-Newtonian fluids were measured, and the flow curves were compared with the flow curves obtained using standard measuring systems like cone-plate, bob-cup and a standard Paar Physica stirrer. The use of a coaxial cylindrical analogue and the driven mechanism of the UDS 200 rheometer allowed the utilization of oscillatory tests to measure the viscoelastic data storage and loss modulus. The results indicate that is possible to determine the storage, loss modulus and the flow curves of non-Newtonian fluids, both time independent and time dependent fluids.

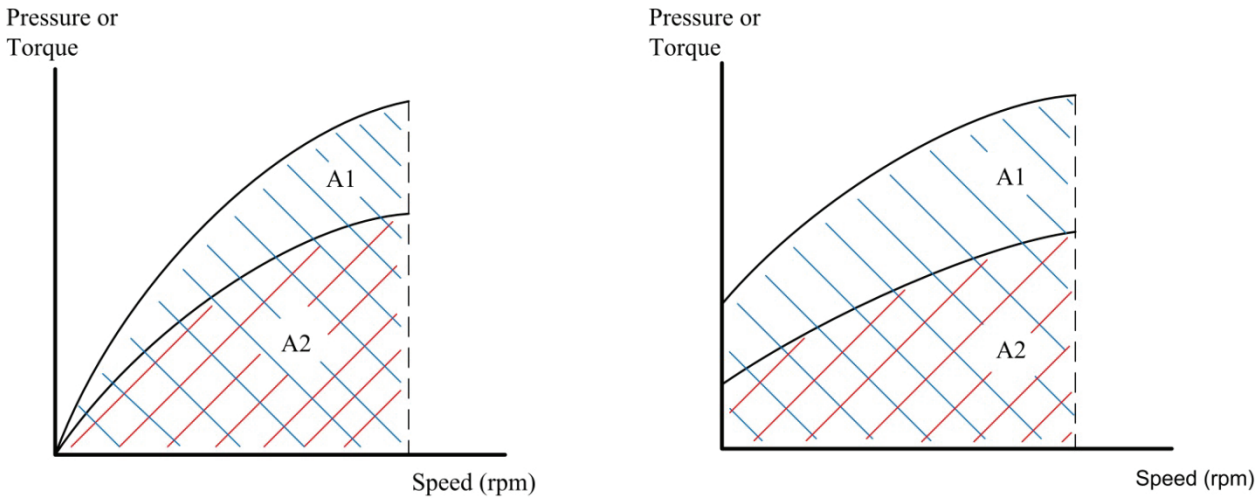

Figure 17: Areas below the curve to perform relative studies on non-Newtonian fluids. At the left two pseudoplastic fluids and at the right two pseudoplastic fluids with yield stress. The area A1 is represented with blue lines and A2 with red lines.

Method 5 in Table 1 must be used in rheometers having low friction in the bearing. This method proved to be the most advantaged because it also allows viscoelastic measurements in oscillatory tests and provides a mean shear stress and an average shear rate. Method 6 in Table 1 allows the determination of a mean shear stress through the normal force in the screw shaft which makes the measurement of screw rheometers even more flexible. The use of the normal force to perform viscoelastic measurements is not included in **Paper III**, however it would be of interest in future research to study whether it can be used or not.

Calibration is not required in *prototype* III. This prototype allowed to measure the relation between compressive stress and density of the pellets formed from the powders. **Paper IV** and **V** used ground Scots pine and the equipment was able to produce pellets at different densities.

Paper IV shows that the lowest density pellets were plastic in nature and had the lowest slope (normal load – strain) among all pellets densities. The clear straight line with the lowest slope at the beginning of the plot normal force – strain (200-600 kN) indicate a low stiffness. As the pellet density increased the yield began to present a maximum value showing the presence of a ductile failure. The general trend was that the higher the pellet density, the higher the stiffness of the pellets and the higher the yielding load.

5.3 ACCURACY AND PERFORMANCE OF THE METHODS

The accuracy of viscosity prediction in *prototype* I through the slope between torque and speed (calibration method 1 in Table 1) was assessed in **Paper I** and **II**. The accuracy estimation was based in the difference in viscosity of a standard Newtonian fluid (N450000, Cannon Instruments Co., PA) measured in cone-plate and in the screw rheometer. Different viscosities were used in the experiments by changing the temperature in the fluid.

Paper I showed that the maximum errors or residuals were ± 25 Pa s of magnitude over a viscosity range between 30 to 450 Pa s, while **Paper II** showed that most of the residuals were no larger than 7 to 9 Pa s in viscosity for two different dies (or restrictions). This estimation was made using the root mean square error of prediction (RMSEP) that is commonly used to give an indication of the majority of the expected errors when using a model again [82].

The difference between the calibration methods 1, 2 and 3 (ref. Table 1) based on the slope between torque and speed, area below the curve torque versus speed, and the slope between downstream pressure and speed were not significantly different ($p > 0.005$). However when using two dies (or restrictions), the predictions made through the area below the curve downstream pressure versus speed (method 4 in Table 1) were significantly smaller ($p < 0.005$) than the predictions obtained through method 1, 2 and 3 (ref. Table 1). Conversely, this was not the case observed for method 4 (ref. Table 1) using the smallest restriction where a large RMSEP of 12 Pa was determined. These results were plotted in Figure 6 **- Paper II**.

The time variations in torque and speed of *prototype* I were investigated in **Paper II**. Time variation of these parameters seems to be mainly caused by time dependent flows produced by the non-symmetric geometry of the screw. Increased amplitude of torque and pressure can become more notorious at higher resistances to flow which can be produced by either increased viscosity or to a lesser extent by reductions in die diameter. The influence of different running speeds does not seem to affect the variations in amplitude of torque and pressure.

The accuracy of *prototype* II (**Paper III**) was estimated by the difference between the viscosity of a Newtonian standard fluid (Brookfield 12 500 cP, Brookfield Engineering Laboratories, Inc.) measured at different temperatures in cone-plate and in *prototype* II. The maximum errors were found to be smaller than ± 1 Pa s which contrasts with the maximum

error of ± 25 Pa s found in *prototype* I. This is regarded to the better bearing and control system used by *prototype* II.

Paper I, **II** and **III** can be used as the preliminary background to construct a commercial on-line screw type process rheometer or a commercial screw-recirculation cup for laboratory rheometers.

Paper IV verifies the ability of *prototype* III to determine the compressibility of a powder material like ground Scots pine and also its capability to form compacts (i.e. pellets). The performance of *prototype* III to carry out compressibility tests was demonstrated in a plot of compaction stress (MPa) versus pellet density (kg m^{-3}). The compressibility of all wood samples showed to be a ductile type indicated by high correlations ($R^2 > 0.99$) in a power curve.

The strength of the wood pellets having different densities provided a good overview of the relations density – strength, however the correlations were relatively poor ($0.537 < R^2 < 0.692$) using at least 15 samples (*n*). The relatively poor correlations can be regarded as each one of the pellets probably had a different particle size distribution because it is difficult to make a series of pellets of 7 ml of pre-compressed volume having the same particle size distribution. This result contrast to another study carried out by Salas-Bringas et al [78] using the same *prototype* III to compress buttermilk powder having a narrow particle size distribution. The result showed a high correlation in a power law curve between pellet density and strength ($R^2 > 0.99$). This indicates that *prototype* III is well suited to perform this type of tests and that the poor correlations found for wood pellets are due to the characteristics of the compressed wood powder and not due to bad functioning of the equipment. It is of future interest to use *prototype* III to investigate how the particle size distribution can affect the strength of pellets.

Paper V also used the third prototype to verify its capability to indicate the process-ability of a material to be pelleted. The same Scots pine was also chosen for this article. The resistance to flow specified by the maximum normal stresses that initiate flow at a given pressing speed in the third prototype, correlated relatively well with the energy consumed by an industrial pellet press. A similar connection was found between the yield stress of the forming compact and the energy consumed by the industrial pellet press. One of the limitations from *prototype* III that were commented in **Paper V** was the 72 MPa of maximum compressive stress that did not manage to achieve the same density of the pellets produced by

the pellet press. However this problem can be easily solved by reducing the diameter of the compressive channel and rod. A 8 mm diameter rod could produce 100 MPa of compressive pressure which can produce a higher density wood pellet. The other solution is to assemble *prototype* III into a more powerful texture analyzer.

5.4 PROBLEMS, SOLUTIONS AND LIMITATIONS RELATED TO THE USE OF THE METHODS

In this chapter are commented some of the problems that can be found when performing rheological characterizations or during a manufacturing process. This section focus on how the different methods presented in this thesis could address these situations.

Table 2 gives an overview of some of the possible problems that might be encountered when performing rheological characterizations of fluids and how this can be faced with a screw type rheometer.

In the first instance (**Paper I**), the screw type rheometer was meant to be used for highly viscous food and animal feed materials since it can easily handle these type of materials, actually screw conveyors and extruders are part of the manufacturing process. Additionally, effects like viscous heating occurring in extruders can be studied with a screw type rheometer. However, **Paper II** started to consider the use of this equipment for the general use in the different manufacturing industries. This leaded a third study (**Paper III**) utilizing fluids and semi-solid fluids like suspensions, toothpaste and chocolate in its liquid and solid states.

Table 2: Problems, solutions and limitations related to the use of a screw type rheometer (*Prototype* I and II).

Problems	Solutions	Limitations
Relatively large particles in the fluid produce measurement problems in most standard probes[1].	Use of an impeller type of measuring system, like the screw type rheometer.	An average shear rate is used. The particles should not be larger than the screw channel.
Sedimenting fluids produce problems in most standard probes[1].	Use of an impeller type of measuring system. The screw type rheometer could decrease segregation by increasing mixing.	Care should be exercised: the screw should be run at rather high rotational speeds to avoid sedimentation and secondary flows can affect the measurements.
How to determine the viscosity of non-Newtonian fluids in the screw type rheometer.	Determination of an average apparent viscosity.	The range of a truth viscosity inside the rheometer is unknown due to complex flows and the geometry of the screw.
Different local shear rates in the screw type rheometer. How to produce a flow curve?	An average shear rate can be used through a coaxial cylindrical analogue.	The average shear rate cannot compete with the nearly constant shear rate that can be provided by cone-plate. However cone-plate cannot measure all fluids.
Viscous heating in the screw type rheometer.	The rheometer should be run at either lower speeds, use smaller restrictions at the downstream or to use low viscous fluids.	High rotational speeds with large restrictions can limit the reliability of results.

[1] Standard probes are cone-plate, bob-cup and plate-plate

Table 3 presents an overview of some of the possible problems that can be present in a pelleting process or problems that researchers can face. Table 3 describes how the problems can be approached with a laboratory pelleting equipment.

Table 3: Problems, solutions and limitations related to the research use of a laboratory die pelleting rig attached to a texture analyzer (*Prototype* III).

Problems	Solutions	Limitations
High costs and large amount of materials are needed to pellet industrially. Consequently research is limited.	The laboratory die pelleting rig can be used with small samples at a low cost.	It is necessary a texture analyzer or another type of dynamic equipment with force measurement and accurate speed control.
Industrial pellet presses cannot be well controlled. Consequently, research is limited.	The laboratory die pelleting rig can manufacture pellets at different compressive stresses and temperatures providing a better control and experimental design.	The ideal process parameters like compressive stress might not be possible to be replicated back in the industrial pellet press.
It is difficult for a pellet manufacturer to purchase the "best" pelleting die for production.	Since the laboratory die pelleting rig can use different dies, it is possible to feed back the information to the maker of the industrial pellet die to manufacture a customized pelleting die for specific raw materials, or to choose a die among the ones in stock.	The laboratory die pelleting rig cannot simulate the shear stresses occurring in the gap roller-die ring (shown in Figure 9).
Pellet presses are black boxes because the material is difficult to be characterized during pelleting. Only power is displayed in most pellet presses.	The laboratory die pelleting rig can characterize rheologically the material.	The particles making a single pellet (e.g. particle size) should represent the particles used in large quantities. A number of pellets made in the laboratory may be needed to obtain a representative result.

5.5 PRACTICAL APPLICATIONS OF THE MEASUREMENT METHODS

The screw type rheometer should represent an attractive equipment to perform measurements in the process industry because the apparatus is able to convey the samples while simultaneously measure viscosity, and can also perform viscoelastic measurements satisfactorily.

One of the possible forms to use the equipment to control a process is to rotate the screw at constant speed to measure viscosity in real time and after a period of time the screw should stop. As soon as the fluid is at rest, the screw can start oscillating to perform the viscoelastic characterization.

A drawing showing the possible process installations of a screw type rheometer has been included in **Paper II**, Figure 9.

A similar measuring system to *prototype* II can be a good alternative to the standard stirrers like the ST24 Paar Physica used in **Paper III** when performing measurements of sedimenting suspensions. Also it can provide an advantage over fluids or semi-solids that can easily slip. The better grip of the screw compared to a bob-cup was evidenced during experiments with cooled chocolate in Paper **III**. Measurements using suspensions having large particles were not performed in the thesis, however it is expected that the screw rheometer is more suitable for this type of fluids than bob-cup system. However, a larger recirculation channel should be considered.

A similar apparatus to *prototype* III can help to perform studies of compressibility of powders and the process-ability of pelleted products like wood and animal feed pellets.

In a pelleting plant, the purchaser can order small samples of raw materials before purchase and use *prototype* III to compare how the physical characteristics can affect the physical quality of the pellets. By comparing different samples of the same raw material from different suppliers, the purchaser is also able to classify the energy demands for pelleting to make an even better purchase decision.

6 CONCLUSIVE REMARKS OF PAPER I, II, III, IV AND V

In conclusion, the results from this thesis show the development and verification of three different measurements methods. The three methods focus on rheological measurements for the processing of fluids, semi-solids and solid materials.

The use of a screw concentrically assembled in a cup or barrel as a rheometer to perform rheological characterizations was assessed in **Papers I, II** and **III** (*prototype* I and II). It is believed that these studies generated the necessary background to produce such equipment commercially. The results from **Paper I, II** and **III** show that it is possible to predict viscosity and **Paper III** show that it is possible to measure viscoelasticity from this rheometer.

Paper I show that a screw type process rheometer can predict the viscosity of a fluid composition using torque and rotational speed. Torque can be used to represent an average shear stress and the screw speed to represent a mean shear rate. **Paper II** investigates the causes of the time variations in torque and speed (e.g. amplitude of the oscillation) that can be present in a screw type rheometer. The results show that the variations can be caused by time dependent flows produced by the non-symmetric geometry of the screw. **Paper II** also shows that the time variations can become more notorious at higher resistances to flow caused by either an increased viscosity or to a lesser extent by increasing the downstream restriction. **Paper II** presents additional calibration methods that can be used when using a process rheometer with relatively high friction bearing systems. One of the method can use the same information from torque, but using the area bellow the flow curve to deal with the friction in the bearing. Another method is to use a downstream pressure as an indication of shear stress in the system. This last method is ideal for bearings with high friction.

The calibration approach used in **Paper III** that uses a cylindrical analog to represent the complex geometry of the screw, seems to be the best of all calibration methods when using low friction bearings. This method allows to obtain directly an average shear stress and a mean shear rate. The results show that the method is appropriate to measure the flow characteristics of non-Newtonian fluids, both time independent and time dependent fluids. The flow curves using this method are closer to the measurements of cone-plate and bob-cup when compared to the ST24 Paar Physica stirrer. The screw measuring system with the analog cylinder allows satisfactory measurements of viscoelastic data of fluids, and it can be used to detect phase changes (fluid-solid). The results also show that it is appropriate to use

the normal force along the screw shaft to estimate an average shear stress. This has been confirmed by observing similar predictions of viscosity based on torque and normal force. However, it is important to mention that Weissenberg effects can affect the viscosity prediction when using the normal force. Therefore care must be considered when measuring viscosity in rotation on fluids with high elastic modulus. Yet this effect is not likely to affect the oscillatory tests.

The use of a laboratory die pelleting rig (*prototype* III) to perform compression rheology studies and to provide help in the manufacturing pelleting operations of wood pellets was demonstrated in **Paper IV** and **V**. **Paper IV** shows that the wood materials, ground Scots pine presented a ductile compression following a power curve. The manufactured pellets were plastic and ductile. The different treatments (pre-handling of the raw materials) did not affect the compressibility. However, the strength of the pellets was increased by drying and storing the raw materials in a pile for 11 months before they were made. Increased compaction stresses produced pellet with higher strength. The use of *prototype* III to provide information to the manufacturing pelleting operations seems to be appropriate. The most important assets from **Paper V** were to show that rheological properties like yield stress and the normal stresses at incipient flow are connected with the power consumption observed in an industrial pellet press. However, a laboratory operator must ensure that the 7 ml sample that is used to make a single pellet should represent a much larger amount of material processed in the manufacturing process, often a batch of raw material can be of the order of several tons. Also care should be exercised because the grinding effect of the industrial pellet press is not replicated in the laboratory die pelleting rig.

The future uses of *prototype* III can not only include wood pellets, but also to include the determination of pellet-ability of by products from other industries to form solid fuels. The determination of pellet-ability of raw materials or recipes for animal feed is interesting as well, this has turn in an on-going project for the author of this thesis.

7 POSSIBLE FUTURE IMPROVEMENTS AND PERSPECTIVES FOR PROTOTYPES I, II AND III

The prototypes developed for this thesis had the objective of verifying working and measurement principles. The following recommendations focus on the main issues to improve the working principle and not on how they can be built for a special industrial use (e.g. rheometer in a horizontal pipe) or for a special assembly.

7.1 PROTOTYPE I

The main concern regarding *prototype* I in **Paper I** and **II** was the friction in the bearing system. As briefly explained in **Paper I** and **II**, high thrust pressures increased the friction in the spherical plain thrust bearing (GX-17, SKF Inc., Gothenburg) assembled with the screw. This bearing has a sliding contact surface made of a combination steel/PTFE composite. Consequently the rheometer was not able to produce flow curves (rotational speed – torque) having intersect at the origin when using Newtonian fluids. The GX-17 bearing is shown in Figure 18 and Figure 19.

Depending on future applications and expected costs, it is possible to improve the bearing system using air or magnetic bearings. These types of bearings are specially needed to perform oscillatory tests during viscoelastic measurements. However depending the use and requirements (e.g. process control), also ball bearings might be sufficient for cases where only the viscosity of the processed fluid is required to be kept within not so strict margins. If costs for some industry makes unpractical the use of a satisfying bearing system, the rheometer should use downstream pressure instead of torque.

Possible arrangements of *prototype* I in a process were included in **Paper II** – Figure 9.

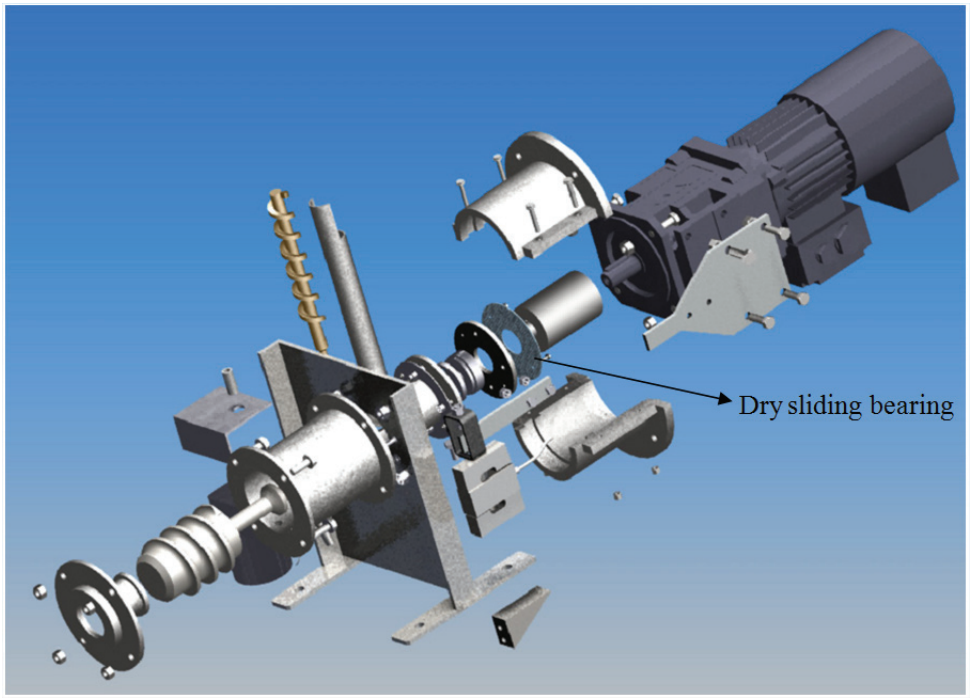

Figure 18. Exploded view of *prototype* I showing the bearing system.

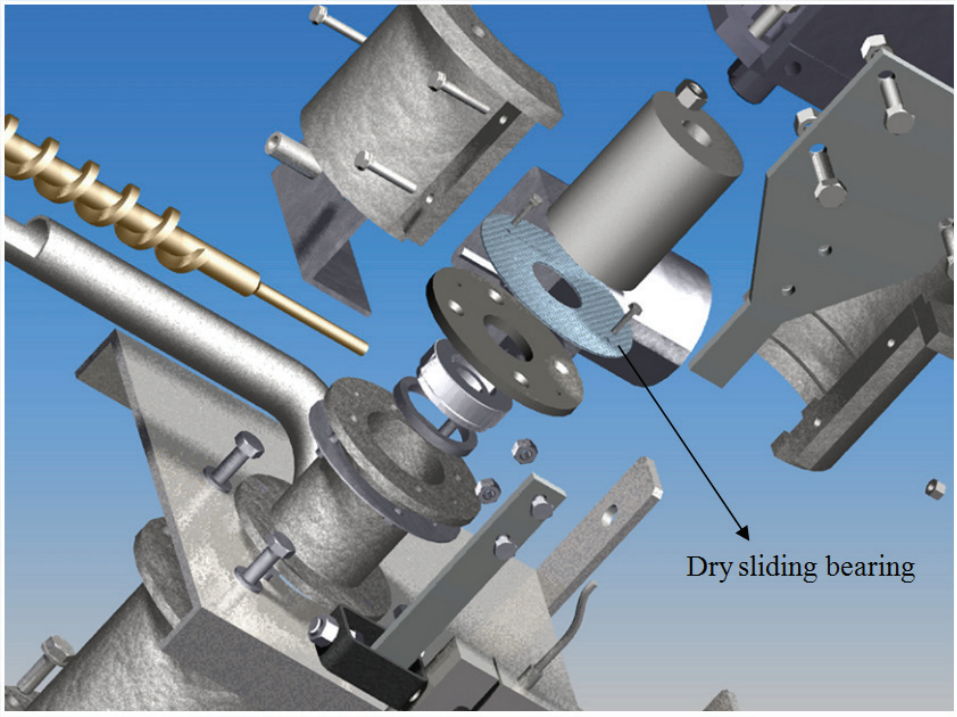

Figure 19. Close view to the bearing system of *prototype* I.

As an alternative use of the screw rheometer, it would be of interest to investigate how the screw rheometer could perform continuous flow measurements of powders (i.e.

flow-ability). The barrel could be modified to have a larger gap screw flight-barrel and with a closed discharge or with the gap as it is made today, but with a larger restriction to produce a controlled powder density at the outlet. Impellers in rotational rheometers have been used to determine the flow properties of powders under conditions of dynamic shear in laboratories. During dynamic testing the rotational and axial forces acting on a helical blade are measured as it passes through a sample. Basic flow energy is determined from these data and is regarded as a measure of the rheology or resistance to flow of the powder [66]. The screw rheometer could be as a result a good instrument to measure flow properties of powders during processing since it is capable to convey materials continuously.

7.2 PROTOTYPE II

Prototype II can be improved by adding pressure measurements at the downstream of the screw. Pressure measurements can extent the flexibility of the screw-recirculation cup for research uses (see example in Figure 20). Another reason of adding pressure measurements is to calculate the flow rate in the annular gap which in turn is related to the shear rate, so analysis of flow in annuli could be conducted.

In this thesis it was demonstrated that the shear stress information can be taken from either torque in **Paper I**, downstream pressure in **Paper II** or normal force in **Paper III**.

For extrusion researchers and engineers, *Prototype* II could be adapted to be assembled in a standard pressure cell for rheometers. By doing that, the screw rheometer could be able to perform measurements under a shear and a pressurized environment similar to the one found in extruders.

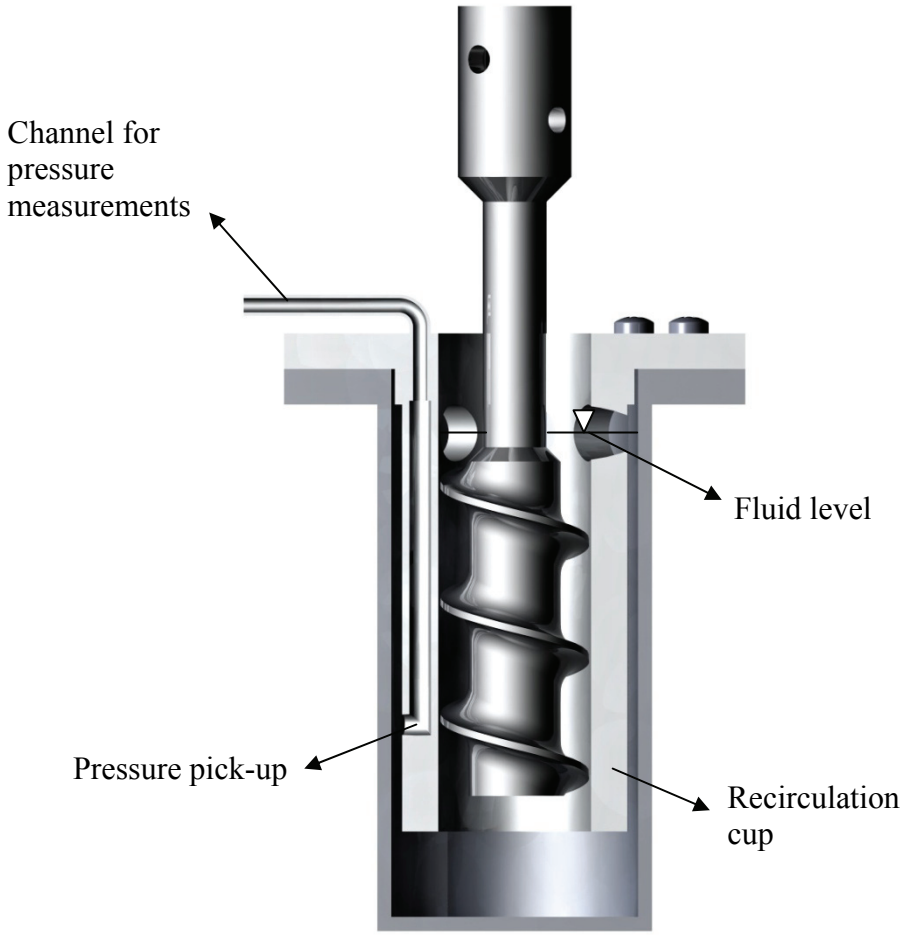

Figure 20: Improvements on the screw-recirculation cup to include pressure reading from the annular gap of the recirculation cup.

7.3 PROTOTYPE III

One of the aspects to improve in the laboratory pellet press is the implementation of more measurements to decrease uncertainties and to obtain more material properties. A possible more sophisticated press alternative is shown in Figure 21. As it was explained in **Paper IV**, the source of error when measuring the compressing stress or vertical stress (σ_{v1}) at the driven rod only, is that the friction between the material and the side walls of the channel reduces the stress from top to bottom. This can result in a wood pellet having a density gradient [55].

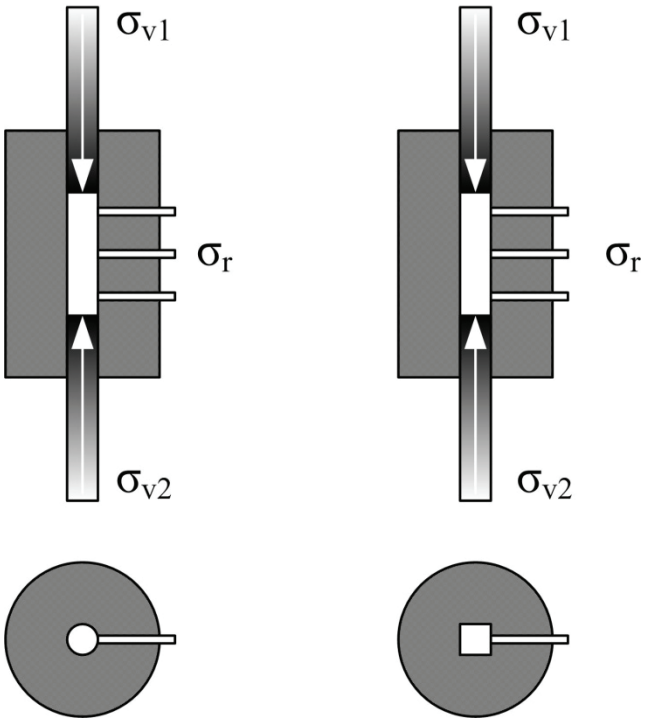

Figure 21. Improved die compacting equipment.

To measure the stresses experienced by the material at the top (σ_{v1}) and bottom (σ_{v2}) of the compressing channel, the pelleting device can be upgraded with a force transducer at the bottom too. Another uncertainty is the die-wall friction which is the one that actually generates density variations leading to an inhomogeneous test. To estimate the die-wall friction when the die compaction is performed, the die equipment can be instrumented so that the radial stresses (σ_r) can be measured during compaction. Figure 21 shows how small pins in contact with the powder and connected to a force transducer can provide information regarding the die-wall friction. Three pins are shown in the figure to show that theoretically is possible to obtain the information regarding the radial stress distribution along the compact height.

Figure 21 shows two alternatives, one at the left using a circular channel and at the right a rectangular or cubic channel. Using a circular channel can lead to the advantage that the shape of the pellets is more similar to what is obtained today from pellet presses. The other alternative with a rectangular channel is to provide the advantage of producing rectangular pellets that can be of interest to test the physical strength. Because the different sides of the pellets can have a known contact area between the compressing probe and the

pellet (area of stress). Since many compacts are non-isotropic, especially the wood pellets that were tested in **Paper IV**, it is especially attractive to measure the strength through any of the arrangements shown in Figure 22 and to compare the stresses causing failure when the compacts are positioned differently.

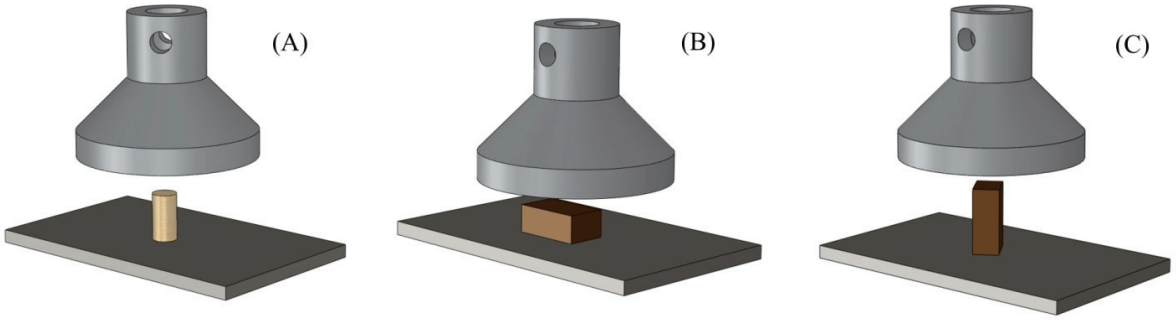

Figure 22. Three possible measurement set-up for compression tests of compacts. (A) is an alternative to the diametral compression test of cylindrical pellets, (B) and (C) are alternatives for rectangular pellets.

The arrangements shown in Figure 22 were not possible to make in **Paper IV** because the goal was to compare the strength with the pellets produced in an industrial pellet press, these cylindrical pellets did not have defined ends as the one shown in Figure 22 (A).

To avoid direct contact between the pin and the compressed material (Figure 21), the axial pressure measurements can be done using a vertical thin pipe touched by the pins shown in Figure 23. According to stress analysis of an on-going project, using a 8 mm inner diameter stainless steel pipe with 1 mm thickness, a pressure inside the pipe of 300 MPa would result in a force in the pin of around 140 N. At this pressure, the pipe will deflect only 10^{-3} mm so a load cell with small deflection has to be used. The ongoing test showed that is also possible to connect the pins to a length gauge and to relate the displacements in the pipe to the pressure inside the pipe, however it must be considered a prudent time to obtain a full relaxation in the pipe between each tests.

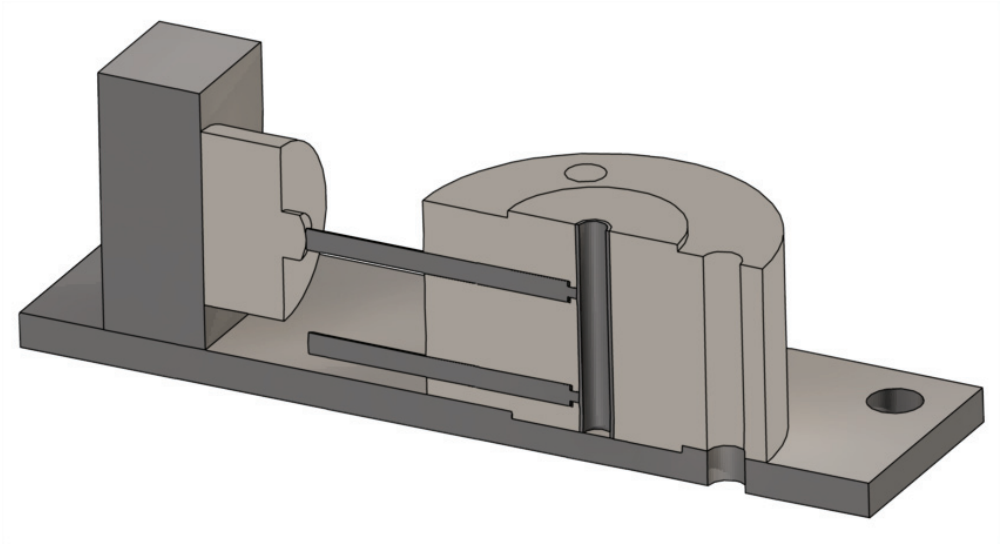

Figure 23: Testing of axial pressure measurements through indirect contact. Ongoing development.

ARTICLES MADE DURING THE PHD STUDIES

The following is a list of all the publications that were made by the author of this thesis during the period of the PhD studies. All articles below are classified as class 1 according to the Norwegian research council.

[i] Salas-Bringas C, Jeksrud WK, Lekang OI, Schüller RB: Noncontact Temperature Monitoring of a Pelleting Process Using Infrared Thermography, Journal of Food Process Engineering 30 (2007) 24-37.

[ii] Salas-Bringas C, Jeksrud WK, Schüller RB: A New On-Line Process Rheometer for Highly Viscous Food and Animal Feed Materials, Journal of Food Engineering 79 (2007) 383-391.

[iii] Salas-Bringas C, Plassen L, Lekang O-I, Schüller RB: Measuring Physical Quality of Pelleted Feed by Texture Profile Analysis, a New Pellet Tester and Comparisons to Other Common Measurement Devices, Annual Transactions of the Nordic Rheology Society 15 (2007) 149-157.

[iv] R. B. Schüller RB, Orr R, Salas-Bringas C: Finite Element Modelling of the Fluid Temperature in a Plate-Plate Rheometer in Oscillatory Tests, Annual Transactions of the Nordic Rheology Society 15 (2007) 261-265.

[v] Schüller RB, Salas-Bringas C: Fluid Temperature Control in Rotational Rheometers with Plate-Plate Measuring Systems, Annual Transactions of the Nordic Rheology Society 15 (2007) 159-163.

[vi] Salas-Bringas C, Lekang OI, Schüller RB: Rheology in Feed Production, Annual Transactions of the Nordic Rheology Society 16 (2008) 229-237.

[vii] Schüller RB, Løkra S, Salas-Bringas C, Egelandsdal B, Engebretsen B: Emulsion Stability Measurements by Single Electrode Capacitance Probe (Secap) Technology, Measurment Science and Technology 19 (2008) 1-7.

[viii] Schüller RB, Salas-Bringas C: Modelling Rheological Cone-Plate Test Conditions, Annual Transactions of the Nordic Rheology Society 16 (2008) 263-268.

[ix] Rukke E-O, Salas-Bringas C, Lekang O-I, Schüller RB: Rheological Characterization of Liver Paste with a New Capillary Rheometer That Uses Direct Pressure Measurements in the Capillary, Annual Transactions of the Nordic Rheology Society 17 (2009) 243-248.

[x] Salas-Bringas C, Lekang O-I, Rukke EO, Schüller RB: Development of a New Capillary Rheometer That Uses Direct Pressure Measurements in the Capillary, Annual Transactions of the Nordic Rheology Society 17 (2009) 39-47.

[xi] Salas-Bringas C, Lekang OI, Schüller RB: Time Variations and Calibration of a Screw Type Process Rheometer, Applied Rheology 20 (2009) 34526-134526-11.

[xii] Salas-Bringas C, Filbakk T, Skjevrak G, Lekang OI, Høibø O, Schüller RB: Compression Rheology and Physical Quality of Wood Pellets Pre-Handled with Four Different Conditions, Annual Transactions of the Nordic Rheology Society 18 (2010) 87-94.

[xiii] Salas-Bringas C, Filbakk T, Skjevrak G, Lekang OI, Høibø O, Schüller RB: Assessment of a New Laboratory Die Pelleting Rig Attached to a Texture Analyzer to Predict Process-Ability of Wood Pellets. Energy Consumption and Pellet Strength, Annual Transactions of the Nordic Rheology Society 18 (2010) 77-86.

[xiv] Salas-Bringas C, Lekang OI, Schüller RB: Data Analysis from Capillary Rheometry Can Be Enhanced by a Method That Is an Alternative to the Rabinowitsch Correction, Annual Transactions of the Nordic Rheology Society 18 (2010) 95-100.

[xv] Salas-Bringas C, Rukke EO, Saga L, Lekang OI, Schüller RB: Rheological Properties of Buttermilk Pellets Manufactured by a New Die Pelleting Rig of a Texture Analyzer, Annual Transactions of the Nordic Rheology Society 18 (2010) 101-106.

[xvi] Salas-Bringas C, Lekang O-I, Schüller RB: Analysis of a Screw Type Process Rheometer to Determine Viscoelastic and Flow Properties of Non-Newtonian Fluids, Applied Rheology (2011) Submitted.

NOMENCLATURE USED IN THE PAPERS

Table 4: Nomenclature used in **Paper I**

Variable	Symbol	Unit
Actual viscosity	A_η	Pa s
Angular velocity	ω	rad s^{-1}
Area	A	m^2
Constant equal to the ratio k_1/k_2	K	-
Constant to convert M to $_\sigma$	k_1	-
Constant to convert N to an average $\dot{\gamma}$	k_2	-
Gap between rotating screw and barrel	δ	m
Intercept of the curve fit N versus M	b	Nm
Local shear stress	τ	Pa
Mean shear stress in rheometer	σ	Pa
Number of samples	n	-
Power	P	W
Predicted viscosity	P_η	Pa s
Radius	r	m
Shear rate	$\dot{\gamma}$	s^{-1}
Shear stress	τ	Pa
Slope of the curve N versus M	a	Nm/rpm
Speed of rotating shaft	N	rpm
Torque	M	Nm
Velocity	v	m/s
Viscosity	η	Pa s

Table 5: Nomenclature used in **Paper II**

Variable	Symbol	Unit
Actual viscosity	A_η	Pa s
Area below the curve fit *N* versus *M*	*MA*	Nm rpm^{-1}
Area below the curve fit *N* versus ΔP	*PA*	MPa rpm^{-1}
Constant to convert *M* to $\sigma_{rheometer}$	k_1	-
Die diameter	*d*	m
Errors or residuals	*E*	Pa s
Gap between rotating screw flight and barrel	δ	m
Intercept of the curve fit *N* versus *M*	e	Nm
Intercept of the curve fit N versus ΔP	c	MPa
Isotropic pressure at the boundary of the barrel walls	ΔP_{xyz}	Pa
Number of samples	*n*	-
Overall shear stress in the rheometer	$\sigma_{rheometer}$	Pa
Predicted viscosity	P_η	Pa s
Pressure amplitude	Δp	MPa
Pressure between screw and die (downstream pressure)	ΔP	MPa
Radius	*r*	m
Root mean square error of prediction	*RMSEP*	Pa s
Shear rate	$\dot{\gamma}$	s^{-1}
Shear stress at the barrel walls	σ_b	Pa
Slope of the curve *N* versus *M*	*a*	Nm/rpm
Slope of the curve *N* versus ΔP	*b*	MPa rpm^{-1}
Speed of rotating shaft	*N*	rpm
Torque	*M*	Nm
Torque amplitude	ΔM	Nm
Variance	*p*	-

Table 6: Nomenclature used in **Paper III**

Variable	Symbol	Unit
Actual viscosity	A_η	Pa s
Constant to convert M to σ_M	k_1	-
Constant to convert N to $\dot{\gamma}$	k_2	-
Constant to convert N_F to σ_{NF}	K_{NF}	m^{-2}
Errors or residuals	E	Pa s
Gap between two concentric cylinders	δ	m
Height of the analogue cylinder	h	m
Loss modulus	G''	Pa
Normal force in the screw shaft	N_F	Pa
Paar Physica bob-cup CC27-SN20666	CC27	-
Paar Physica bob-cup Z4	Z4	-
Paar Physica cone-plate MK22 (50 mm diameter, 1°, 50 μm)	MK22	-
Paar Physica plate-plate PP50 (50 mm diameter)	PP50	-
Paar Physica stirrer ST24-2D/2V/2V-30-SN18211	ST24	-
Predicted viscosity	P_η	Pa s
Radius of the analogue cylinder	r	m
Radius of the cup	r_{cup}	m
Screw – recirculation cup	Screw	-
Shear rate	$\dot{\gamma}$	s^{-1}
Shear stress	σ	Pa
Shear stress from normal force	σ_{NF}	Pa
Shear stress from torque	σ_M	Pa
Slope of the curve N versus M	a	Nm/rpm
Speed of rotating shaft	N	rpm
Storage modulus	G'	Pa
Torque	M	Nm
Viscosity	η	Pa s

Table 7: Nomenclature used in **Paper IV**

Variable	Symbol	Unit
Ground Scot pine dried with air at 75 °C and stored for 11 months	LT Stored	-
Ground Scot pine dried with air at 75 °C and stored for 3 months	LT Fresh	-
Ground Scot pine dried with flue gas 450 °C and stored for 11 months	HT Stored	-
Ground Scot pine dried with flue gas at 450 °C and stored for 3 months	HT Fresh	-
Linear regression in Figure 5	Linear	-
Normal force	F	kN
Number of samples	n	-
Power law curve in Figure 3	Power	-

Table 8: Nomenclature used in **Paper V**

Variable	Symbol	Unit
Ground Scot pine dried with air at 75 °C and stored for 3 months	LT Fresh	-
Ground Scot pine dried with flue gas at 450 °C and stored for 3 months	HT Fresh	-
Ground Scot pine dried with air at 75 °C and stored for 11 months	LT Stored	-
Ground Scot pine dried with flue gas 450 °C and stored for 11 months	HT Stored	-
Variance	p	-
Length of the die	L	m
Radius of the die	R	m
Pressure at the end of the relaxation time	ΔP_{min}	MPa
Yield stress	τ_0	MPa

8 REFERENCES

[1] Roberts I: In-Line and on-Line Rheology Measurement, In Instrumentation and Sensors for the Food Industry, Eds. Kress-Rogers E, Brimelow CJB, CRC Press, Boca Raton, Fla (2001).

[2] Sinnott RK: Chemical Engineering Design, Elsevier Butterworth-Heinemann, (2005).

[3] Lipták BG: Process Measurement and Analysis, CRC Press, Boca Raton, FL (2003).

[4] Kok Kiong T, Sudjana Putra A: Drives and Control for Industrial Automation, Springer, New York (2011).

[5] Figura LO, Teixeira AA: Food Physics, Springer, Berlin (2007).

[6] Bourne M: Food Texture and Viscosity, Academic Press, London (2002).

[7] Heldman DR, Lund DB: Handbook of Food Engineering, CRC Press/Taylor & Francis, Boca Raton, Fla (2007).

[8] Salas-Bringas C, Jeksrud WK, Schuller RB: A New on-Line Process Rheometer for Highly Viscous Food and Animal Feed Materials, Journal of Food Engineering 79 (2007) 383-391.

[9] McKenna BM, Lyng JG: Rheological Measurements of Foods, In Instrumentation and Sensors for the Food Industry, Eds. Kress-Rogers E, Brimelow CJB, CRC Press, Cambridge (2001).

[10] Steffe JF: Rheological Methods in Food Process Engineering, Freeman Press, East Lansing, Mich. (1996).

[11] Collins M, Schowalter WR: Behavior of Non-Newtonian Fluids in the Inlet Region of a Channel, AICHE Journal 9 (1963) 98-102.

[12] Salas-Bringas C, Lekang OI, Schüller RB: Rheology in Feed Production, Annual Transactions of the Nordic Rheology Society 16 (2008) 229-237.

[13] Doraiswamy D: The Origins of Rheology, http://www.ae.su.oz.au/rheology/Origin_of_Rheology.pdf. (Last access in 05/11/2010).

[14] Cristescu N: Rock Rheology, Springer, Boston (1988).

[15] Karato S-i: Rheology of the Earth's Mantle: A Historical Review, Gondwana Research 18 (2010) 17-45.

[16] Skalak R, Chien S: Handbook of Bioengineering, McGraw-Hill Book Company, New York (1987).

[17] Tattersal GH, Bandfill PFG: Rheology of Fresh Concrete, Pitman Publishing Inc., Boston (1983).

[18] Edwards DA, Brenner H, Wasan DT: Interfacial Transport Processes and Rheology, Butterworth-Heinemann, Stonheam, MA. (1991).

[19] Keedwell MJ: Rheology and Soil Mechanics, Spon Press, (1990).

[20] Vyalov SS: Rheological Fundamentals of Soil Mechanics (Developments in Geotechnical Engineering), Elsevier Science Ltd, Oxford (1986).

[21] Callister WD: Material Science and Engineering, John Wiley & Sons, New York (1991).

[22] Dealy JM, Wissbrun KF: Melt Rheology and Its Role in Plastics Processing - Theory and Applications Kluwer Academic Publishers, The Netherlands (1999).

[23] Block H, Kelly JP: Electro-Rheology, Journal of Physics D: Applied Physics 21 (1986) 1661-1677.

[24] Nielsen LE: Mechanical Properties of Polymers and Composites Marcel Dekker, Inc., New York (1993).

[25] Yanovsky YG: Polymer Rheology: Theory and Practice, Chapman & Hall, New York (1993).

[26] Drake B: Food Psychorheology, In Food Texture, ed. Moskowitz HR, Marcel Dekker, New York (1987).

[27] Laba D: Rheological Properties of Cosmetics and Toiletries in Vol. 13, Marcel Dekker, New York (1993).

[28] Patton TC: Paint Flow and Pigment Dispersion, Interscience Publishers, New York (1964).

[29] Saunders SR, Hamann DD, Lineback DR: A Systems Approach to Food Material Adhesion, Lebensm.-Wiss.u.-Technol. 25 (1992) 309-315.

[30] Dintefass L: Blood Viscosity, Hyperviscosity & Hyperviscosaemia, MTP Press Limited, Boston, MA. (1985).

[31] Yoo B, Rao MA, Steffe JF: Yield Stress of Food Dispersions with the Vane Method at Controlled Shear Rate and Shear Stress, Journal of Texture Studies 26 (1995) 1-10.

[32] Drozdek KD, Faller JF: Use of a Dual Orifice Die for on-Line Extruder Measurement of Flow Behavior Index in Starchy Foods, Journal of Food Engineering 55 (2002) 79-88.

[33] Conrradini MG, Peleg M: Solid Food Foams, In Food Materials Science, Eds. Aguilera JM, Lillford PJ, Springer, NY (2008).

[34] Dogan H, Kokini JL: Rheological Properties of Foods, In Handbook of Food Engineering, Eds. Heldman DR, Lund DB, CRC Press/Taylor & Francis, Boca Raton, Fla (2007).

[35] Vergnes B, Valle GD, Colonna P: Rheological Properties of Biopolymers and Applications to Cereal Processing, In Characterization of Cereals and Flours, Eds. Kaletunc G, J BK, Marcel Dekker Inc, NY (2003).

[36] Rukke E-O, Salas-Bringas C, Lekang O-I, Schüller RB: Rheological Characterization of Liver Paste with a New Capillary Rheometer That Uses Direct Pressure Measurements in the Capillary, Annual Transactions of the Nordic Rheology Society 17 (2009) 243-248.

[37] Singh N, Smith AC: Rheological Behaviour of Different Cereals Using Capillary Rheometry, Journal of Food Engineering 39 (1999) 203-209.

[38] Ortega-Rivas E, Juliano P, Yan H: Food Powders, Springer, NY (2005).

[39] Levine L: Estimating Output and Power of Food Extruders, Journal of Food Process Engineering 6 (1982) 1-13.

[40] Padmanabhan M, Bhattacharya M: Effect of Extrusion Processing History on the Rheology of Corn Meal, Journal of Food Engineering 18 (1993) 335-349.

[41] Tamura MS, Henderson JM, Powell RL, Shoemaker CF: Analysis of the Helical Screw Rheometer for Fluid Food, Journal of Food Process Engineering 16 (1993) 93-126.

[42] Aarseth KA, Perez V, Bøe JK, Jeksrud WK: Reliable Pneumatic Conveying of Fish Feed, Aquacultural Engineering 35 (2006) 14-25.

[43] Thomas M, van Zuilichem DJ, van der Poel AFB: Physical Quality of Pelleted Animal Feed. 2. Contribution of Processes and Its Conditions, Animal Feed Science and Technology 64 (1997) 173-192.

[44] Thomas M, van der Poel AFB: Physical Quality of Pelleted Animal Feed 1. Criteria for Pellet Quality, Animal Feed Science and Technology 61 (1996) 89-112.

[45] Aarseth KA, Prestlokken E: Mechanical Properties of Feed Pellets: Weibull Analysis, Biosystems Engineering 84 (2003) 349-361.

[46] Salas-Bringas C, Plassen L, Lekang O-I, Schüller RB: Measuring Physical Quality of Pelleted Feed by Texture Profile Analysis, a New Pellet Tester and Comparisons to Other Common Measurement Devices, Annual Transactions of the Nordic Rheology Society 15 (2007) 149-157.

[47] Aarseth KA: Attrition of Feed Pellets During Pneumatic Conveying: The Influence of Velocity and Bend Radius, Biosystems Engineering 89 (2004) 197-213.

[48] Finell M, Arshadi M, Gref R, Scherzer T, Knolle W, Lestander T: Laboratory-Scale Production of Biofuel Pellets from Electron Beam Treated Scots Pine (Pinus Silvestris L.) Sawdust, Radiation Physics and Chemistry 78 (2009) 281.

[49] Arshadi M, Gref R, Geladi P, Dahlqvist S-A, Lestander T: The Influence of Raw Material Characteristics on the Industrial Pelletizing Process and Pellet Quality, Fuel Processing Technology 89 (2008) 1442.

[50] Ståhl M, Granstrom K, Berghel J, Renstrom R: Industrial Processes for Biomass Drying and Their Effects on the Quality Properties of Wood Pellets, Biomass and Bioenergy 27 (2004) 621-628.

[51] Mani S, Tabil LG, Sokhansanj S: Effects of Compressive Force, Particle Size and Moisture Content on Mechanical Properties of Biomass Pellets from Grasses, Biomass and Bioenergy 30 (2006) 648-654.

[52] Nielsen NPKN, L; Strobel, B.V.; Felby, C: Effect of Storage on Extractives from Particle Surfeces of Softwood and Hardwood Raw Materials for Wood Pellets, European Journal of wood products (2009)

[53] Nielsen NPK, Gardner DJ, Felby C: Effect of Extractives and Storage on the Pelletizing Process of Sawdust, Fuel 89 94.

[54] Samuelsson R, Thyrel M, Sjöström M, Lestander TA: Effect of Biomaterial Characteristics on Pelletizing Properties and Biofuel Pellet Quality, Fuel Processing Technology 90 (2009) 1129.

[55] Salas-Bringas C, Filbakk T, Skjevrak G, Lekang OI, Høibø O, Schüller RB: Compression Rheology and Physical Quality of Wood Pellets Pre-Handled with Four Different Conditions, Annual Transactions of the Nordic Rheology Society 18 (2010) 87-94.

[56] Salas-Bringas C, Filbakk T, Skjevrak G, Lekang OI, Høibø O, Schüller RB: Assessment of a New Laboratory Die Pelleting Rig Attached to a Texture Analyzer to Predict Process-Ability of Wood Pellets. Energy Consumption and Pellet Strength, Annual Transactions of the Nordic Rheology Society 18 (2010) 77-86.

[57] Chhabra RP, Richardson JF: Non-Newtonian Flow in the Process Industries, Butterworth-Heinemann, Oxford (1999).

[58] Rauwendaal C: Polymer Extrusion, Hanser Gardner Publications, Inc., Krugzell, Germany (2001).

[59] Kraynik AM, Aubert JH, Chapman RN, Gyure DC: Helical Screw Rheometer: A New Concept in Rotational Rheometry in Annual Technical Conference Society of Plastics Engineers, (1984).

[60] Tamura MS, Henderson JM, Powell RL, Shoemaker CF: Evaluation of the Helical Screw Rheometer as an on-Line Viscometer, Journal of Food Science 54 (1989) 483-484.

[61] Collyer AA, Clegg DW: Rheological Measurement - Second Edition, Springer, London (1998).

[62] Shackelford D: Rheological Test Apparatus and Method Using a Helical Screw Rheometer. United States Patent Number 5,209,108 in (1993).

[63] Winter HH: Viscosity Measuring Device and Method. United States Patent Number 4,077,251 in (1978).

[64] Kemblowski Z, Sęk J, Budzyński: The Concept of a Rotational Rheometer with Helical Screw Impeller, Rheologica Acta 27 (1988) 82-91.

[65] Shinohara K: Fundamental and Rheological Properties of Powders, In Handbook of Powder Science and Technology, Eds. Fayed ME, Otten L, Springer, NY (1997).

[66] Schulze D: Powders and Bulk Solids: Behavior, Characterization, Storage and Flow, Springer, NY (2007).

[67] Pietsch W: Agglomeration Processes, Wiley-VCH, Darmstadt, Germany (2002).

[68] McEllhiney RR: Feed Manufacturing Technology Iv, American Feed Industry Association, Arlington, Va. (1994).

[69] Schofield EK: Feed Manufacturing Technology V, American Feed Industry Association, AFIA, Arlington, Va (2005).

[70] Fairfield D: Pelleting Cost Center, In Feed Manufacturing Technology Iv, ed. McEllhiney RR, American Feed Industry Association, Arlington, Va (1994).

[71] Dominy WG, Tan RKH, Akiyama D, Bewley WH: The Pelleting Process for Shrimp Feeds, In Feed Manufacturing Technology Iv, ed. McEllhiney RR, American Feed Industry Association, Arlington, Va (1994).

[72] Salas-Bringas C, Jeksrud WK, Lekang OI, Schüller RB: Noncontact Temperature Monitoring of a Pelleting Process Using Infrared Thermography Journal of Food Process Engineering 30 (2007) 24-37.

[73] Jirjis R: Storage and Drying of Wood Fuel, Biomass and Bioenergy 9 (1995) 191-190.

[74] Stjørdal S: Feedstock Situation for Wood-Pellets Production in Southern Norway in Østlandsforskning, (2006).

[75] Brewin PR, Coube O, Doremus P, Tweed JH: Modelling of Powder Die Compaction, Springer, London (2008).

[76] Doremus P: Model Input Data - Plastic Properties, In Modelling of Powder Die Compaction, Eds. Brewin PR, Coube O, Doremus P, Tweed JH, Springer, London (2008).

[77] Sinka LC, Pitt KG, Cocks ACF: The Strength of Pharmaceutical Tablets, In Particle Breakage, Eds. Salman AD, Ghadiri M, Hounslow MJ, Elsevier, Oxford UK (2007).

[78] Salas-Bringas C, Rukke EO, Saga L, Lekang OI, Schüller RB: Rheological Properties of Buttermilk Pellets Manufactured by a New Die Pelleting Rig of a Texture Analyzer, Annual Transactions of the Nordic Rheology Society 18 (2010) 101-106.

[79] Doremus P: Model Input Data - Failure, In Modelling of Powder Die Compaction, Eds. Brewin PR, Coube O, Doremus P, Tweed JH, Springer, London (2008).

[80] Design Analysis Software Simulation - User Manual, SolidWorks Corp., (2010).

[81] Salas-Bringas C, Lekang O-I, Rukke EO, Schüller RB: Development of a New Capillary Rheometer That Uses Direct Pressure Measurements in the Capillary, Annual Transactions of the Nordic Rheology Society 17 (2009) 39-47.

[82] Esbensen KH, Guyot D, Westad F, Houmøller LP: Multivariate Data Analysis in Practice, Camo, Oslo (2001).

INDEX

H

I

L

M

N

O

P

R

S

T

U

V

W

Y

ERRATUM TO PAPER IV: Compression rheology and physical quality of wood pellets pre-handled with four different conditions

Carlos Salas-Bringas[1], Tore Filbakk[2], Geir Skjevrak[3], Odd-Ivar Lekang[1], Olav Høibø[4] and Reidar Barfod Schüller[5]

[1]Dep. Of Mathematical Sciences and Technology, Norwegian University of Life Sciences, P.O. Box 5003, N-1432 Ås, Norway
[2]Norwegian Forest and Landscape Institute, P.O. Box 115, N-1431 Ås, Norway
[3]Dep. of Energy and Process engineering, Norwegian University of Science and Technology, N-7491 Trondheim, Norway.
[4]Dep. of Ecology and Natural Resource Management, Norwegian University of Life Sciences, P.O. Box 5003, N-1432 Ås, Norway
[5]Dep. Of Chemistry, Biotechnology and Food Science, Norwegian University of Life Sciences, P.O. Box 5003, N-1432 Ås, Norway

Published in: Annual Transactions of the Nordic Rheology Society, 2010 Vol. 18, 87-93

Page 90. In the phrase "The results showing the normal force (KN)…", the units should be changed to (N)

Page 91. In the phrase "…presents the smallest slope between 200-600 KN of normal force…", the units should be changed to (N)

Page 91. In Figure 4, the units in the *y*-axis should be changed from KN to N

Page 91. In the phrase "…increases the slopes between 200-600 KN…", the units should be changed to N

PAPER I

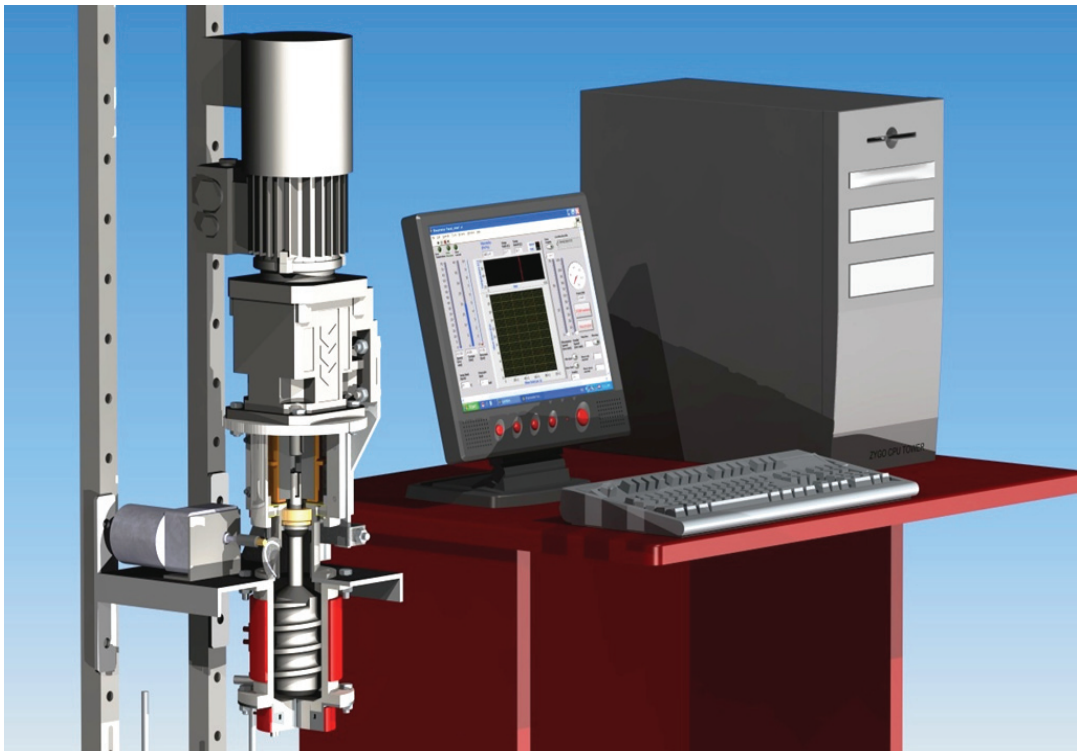

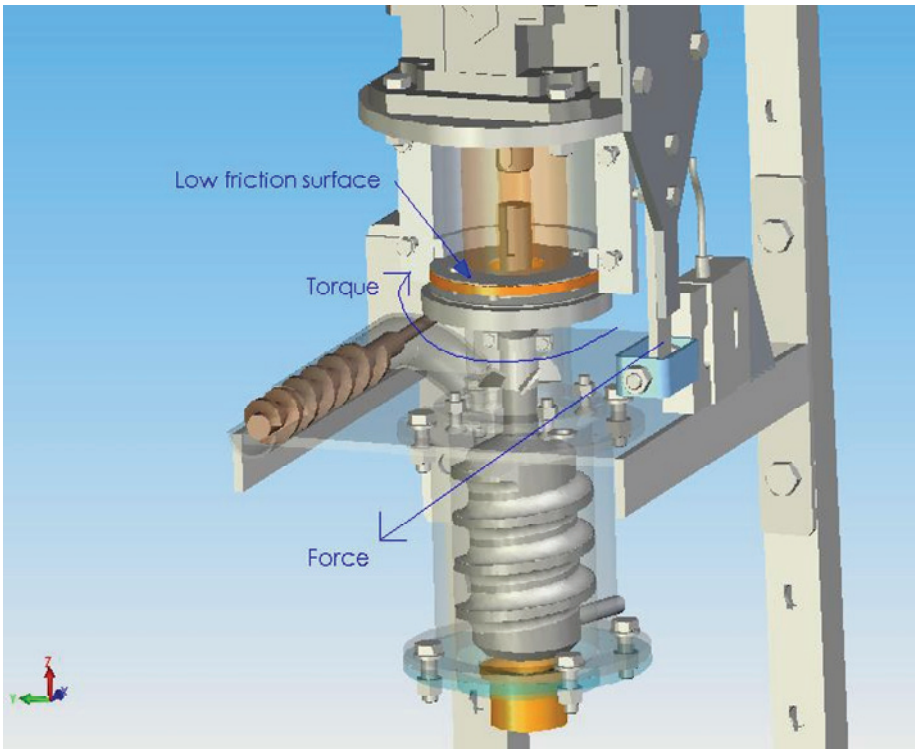

Available online at www.sciencedirect.com
ScienceDirect
Journal of Food Engineering 79 (2007) 383–391
JOURNAL OF FOOD ENGINEERING
www.elsevier.com/locate/jfoodeng

A new on-line process rheometer for highly viscous food and animal feed materials

C. Salas-Bringas [a,*], W.K. Jeksrud [a], R.B. Schüller [b]

[a] Department of Mathematical Sciences and Technology, Norwegian University of Life Sciences, P.O. Box 5003, N-1432 Aas, Norway
[b] Department of Chemistry, Biotechnology and Food Science, Norwegian University of Life Sciences, P.O. Box 5003, N-1432 Aas, Norway

Received 3 November 2005; accepted 1 February 2006
Available online 20 March 2006

Abstract

Rheological characterization of food and animal feed materials during manufacture is necessary to optimize processes, also to achieve better quality of products. Existing laboratory instruments measure accurately rheological parameters, but the complex rheological behavior of food/feed materials depends upon time, shear, temperature, pressure and process history that restricts the validity of results when retrieving information to the process. A new rheometer is developed having a similar working principle to the ones used during manufacturing process. The system allows measurement of materials taken form the process in a continuous manner. The developed rheometer uses torque and rotational speed to predict viscosity by means of an average shear stress and a mean shear rate. From a first prototype, it was possible to predict viscosity with an accuracy of ±25 Pa s over a large range of viscosities (30–450 Pa s), using polybuthene-1 as the process fluid. More research and developments are needed to describe additional capabilities given by an exchangeable die that can extend the range of viscosity measurements.
© 2006 Elsevier Ltd. All rights reserved.

Keywords: Rheometer; Rheology; Control process; Dough; Fluid; On-line; Measurement method

1. Introduction

The rheological characteristics of food products influence many aspects of the fluid performance during processing (pumpability, droplet breakup in spray drying, emulsion formation, flow into molds, formability, etc.), and the quality of finished products (texture, flavour release, stability, appearance, etc.). Knowledge of rheological properties of materials during processing is important in process design, process control and optimization, and for the production of a consistent quality of products (Roberts, 2001).

Food rheology is often confined to the behavior of liquid foodstuffs. However, there is an increasing tendency to consider the response of both solid and liquid materials to applied stresses and strains as being two extremes of the same science. There are in fact some foods that will exhibit either behavior depending on the stress applied, thus solid-like behavior at low stresses and a liquid-like behavior at high stresses (McKenna & Lyng, 2001). Food and animal feed materials can both be defined as complex materials with similar constitution and rheological properties; they consist in a mixture of solid and fluid structural components, i.e. they are viscoelastic.

Rheology is a relatively new field of study that has existed no more than 80 years (Steffe, 1996). It is important to understand food and feed conformational changes that occur during process involving pelleting or extruding. Rheology can characterize the physical and/or structural behavior of these biomaterials under the applied stresses. These rheological properties have been widely described as having a direct correlation with the physical characteristics of the final products (Arhaliass, Bouvier, & Legrand, 2003; Bouzaza, Arhaliass, & Bouvier, 1996; Hoseney,

* Corresponding author. Tel.: +47 64965474; fax: +47 64965401.
E-mail address: carlos.salas.bringas@umb.no (C. Salas-Bringas).

0260-8774/$ - see front matter © 2006 Elsevier Ltd. All rights reserved.
doi:10.1016/j.jfoodeng.2006.02.002

William, Lai, & Guetzlaff, 1992; Li, Campanella, & Hardacre, 2003; McKenna & Lyng, 2001; Roberts, 2001; Smith, 1992; Steffe, 1996; Tabilo-Munizaga & Barbosa-Canovas, 2005; Thomas & van der Poel, 1996; Thomas, van Vliet, & van der Poel, 1998). This can be explained because viscosity correlates with composition and molecular distribution, and hence the characteristics of the material.

Rheological testing equipment and methods are used for determining properties of compositions including viscosity. By determining viscosity, it is possible to quantify changes in flowing compositions with respect to time. By monitoring the changes over time, one can adjust the composition of the flowing media in order to achieve optimum flowing and product characteristics.

Determining rheological characteristics can be performed off-line or on-line in a process. Off-line measuring was typically used in early rheological testing, and conducted in a laboratory after taking samples from the flowing composition. In recent years, on-line rheological measuring has become an important feature in controlling and optimizing the characteristics of flowing material in a process.

Despite the abundant information and wide utilization of rheology in many fields, feed producers and technologists generally pay little attention to these types of measurements. To understand this issue we need to note that many rheometers are based on different working principles, making it difficult to use their valuable information to adjust the process. Steffe (1996) points out that the rheological properties are independent of the instrument, so different instruments will yield the same results, but this is a theoretical concept and different instruments rarely yield identical results. Roberts (2001) mentioned that the highly complex rheological behavior of food material depends upon time, shear, temperature, pressure, and process history which severely restricts the validity of off-line rheological measurements to provide information pertinent to the processing conditions. As it is observed, there are indications of a general need for industrial-instruments based on similar working principles to the ones used during the manufacturing process, as well as a need for instruments capable of performing on-line measurements, allowing easier and more reliable data interpretation and utilization.

The present rheometer relates to an apparatus and system developed for determining rheological properties of highly viscous materials. The rheometer is created to perform its measurements during a manufacturing process, intended for feed and food bio-based materials and having an exchangeable die (Salas, 2004; Salas & Jeksrud, 2005), which could have the same die profile as the manufacturing die. This article will focus on the working principle of the rheometer and future research will address the use of the exchangeable die.

There are different types of rotational rheometers operating under different principles, the most similar instruments to the rheometer we have developed will be described. The rheometer according to the present development comprises a rotational rheometer, Searle type, having a cylindrical shearing gap. Shackelford (1993) developed an instrument belonging to the same category, this rheometer uses a helical screw into a barrel. A pressure transducer is installed at the outlet of the rheometer, and a solenoid valve is used to close the outlet downstream from the pressure transducer. In a test, fluid flows into the rheometer. With the screw stopped and the discharge closed, a pressure transducer measures a static pressure, and a computer resets this to a zero reference value. The screw in the rheometer is then rotated at a constant speed with the discharge closed, and the pressure transducer measures dynamic pressure at the outlet. The test is repeated at different speeds. A computer then calculates, in response to the differential pressure values and speeds, the shear rate and shear stress.

Winter (1978) developed a rotational viscometer of a modified Couette-type for continuous measurements of viscosity of non-Newtonian fluids. The fluid flows in an annular gap between concentric cylinders in circumferential direction. In order to bring about an axial flow through the annulus, the geometry of one of the cylinders is modified such that a small axial pressure gradient is formed. The modification consists of small grooves while the main part of the cylinder surface remains unchanged. This invention does not have a die.

The rheometer presented in this article, is fitted with a headed shaft with helical flights and assembled in a vertical position to measure the rheological characteristics and process parameters. The torque from the helical headed shaft is used to measure the mean shear stress, and the rotational speed is used to measure the mean shear rate. A rheometer according to the present development allows continuous measurements of highly viscous materials composed of solid particles like fibers. The use of process parameters like power consumption, allows the comparison between the rheological values with manufacturing parameters.

Several benefits can be achieved. The incorporation of a new tool for quality control with potential to be used for process control (automation) will result in economical benefits. Research institutions need to receive the benefits of the incorporation of new industrial instruments where the measurements are closely related with the production values. As an example fish feed producers are currently struggling to incorporate new raw materials into fish feed diets, which demands selected amount of thermo-mechanical treatment depending on specific feedstuffs. As a result, there is a need for mapping the "rheological stage" of the product, so measurements are needed. There is a general constant worldwide demand for better product quality and increasing regulations for monitoring processes.

2. Materials and methods

2.1. Design features

To help to understand the rheometer we have developed, a detailed description is given with reference to Fig. 1.

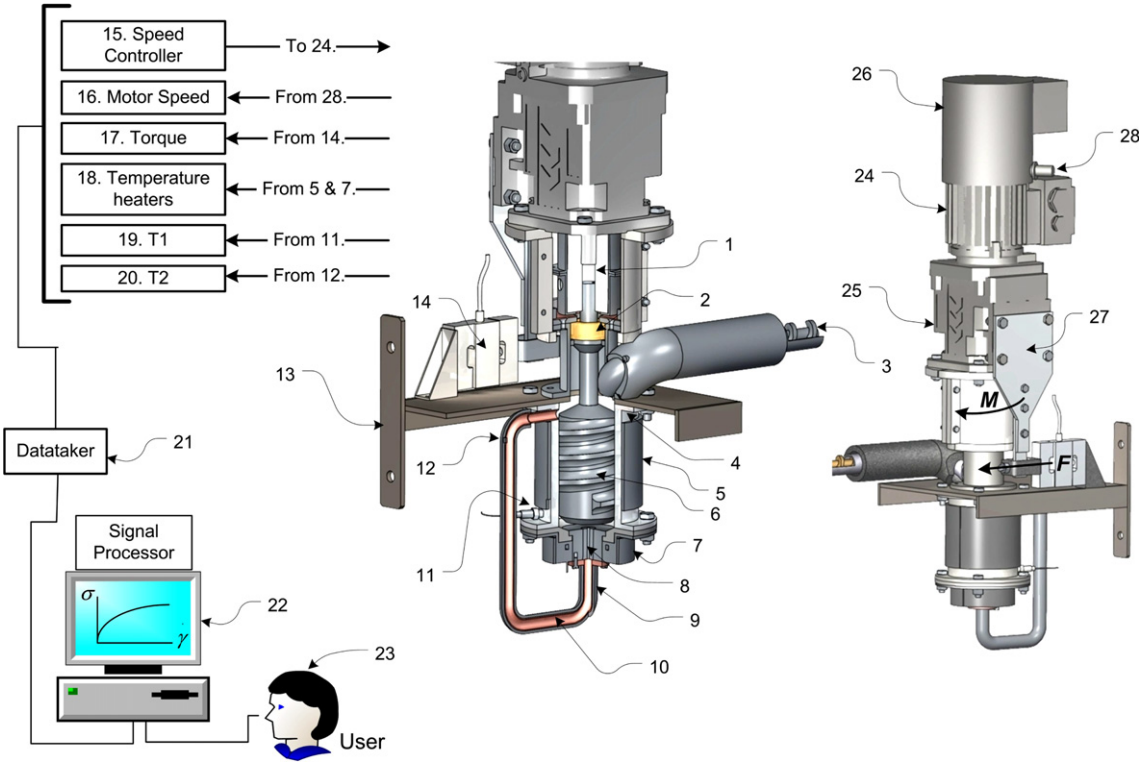

Fig. 1. Sketch of the rheometer for highly viscous materials. Items are indicated by numbers: (24) motor, (26) cooling fun, (25) gear box, (28) proximiter, (27) arm, M represents momentum, F force, (1) coupling, (2) dry sliding bearing, (4) barrel, (5, 7, 9) heaters, (6) shaft, (8) die, (10) circulation path, (11, 12) temperature sensors, (13) bracket, (14) load cell and (22) a standard PC with data card.

Fig. 1 shows the basic principle of the rheometer. The main elements comprise a barrel (4) mounted in a vertical position with an upper and lower end, housing a vertical shaft (6) connected to a geared (25) 250 W AC motor (24) in the upper end. A changeable die is attached at the lower end of the barrel. The vertical shaft rotates relatively frictionless due to a spherical plain thrust bearing (2) (SKF, Gothenburg, Sweden), located in the upper part of the barrel. The feeder for on-line measurements (3) described in the drawing will not be used for the experiment presented in this article.

In order to characterize the steady state of the material, temperature measurements T1 and T2 (11, 12) are performed for the incoming and out coming material through Pt1000 elements. The rheometer is based on a mechanical principle that allows it to perform constant measurements of power consumption to compare the energy costs for processing (mechanical and electrical energy). The rheometer has an electric jacket-heater (5) connected to the barrel (4) section, another jacket-heater (7) is connected to the die section (8) and a third electric heater (9) covers a removable circulation path (10) for calibration and off-line measurements. All the heaters are connected to individuals PID controllers.

The rheometer is provided with a bracket (13) to mount it in a vertical position. A load cell (14) is provided for torque measurements (17). An arm (27) is attached to a gearbox that is free to rotate due to the use of a dry sliding strip (29, Fig. 2) as a bearing to hold axial loads (SKF, Gothenburg, Sweden). The torque (M) is generated by the material resistance to flow, and it is measured through the force (F) perceived by a load cell (14), then the force (F) and the distance to the center of the shaft axis (6) gives the torque. Item 28 is a proximiter for speed measurement of the motor which is related to the shearing speed, and item 1 is a coupling to connect the shaft to the gear box. The motor has a cooling fan (26) for cooling the 250 W AC motor (24) which is connected to a gear box (25).

The signal processor of the rheometer, a standard PC (22), is equipped with a data card with a 12 bit resolution, 2 analogue outputs, 4 analogue inputs ($\pm$10 V) and 10 DOI (National Instruments, Texas, USA). Enabling the user can control and record the information through the software LabView graphical programming (National Instruments, TX, USA). The data acquisition was set to log10 data per second.

The intention is to measure the fluid resistance to flow between the upper parts of the barrel (4) to the exit of the die (8). A circulation path (12 mm diameter copper tube from outlet to inlet, see Fig. 1, item 10) was made with a much bigger diameter than the die (5.5 mm diameter–28 mm length) to create a "bottle neck" situation at the die (8), neglecting the friction in the circulation path (10). A detailed view of the die and the bearing is presented in Fig. 2.

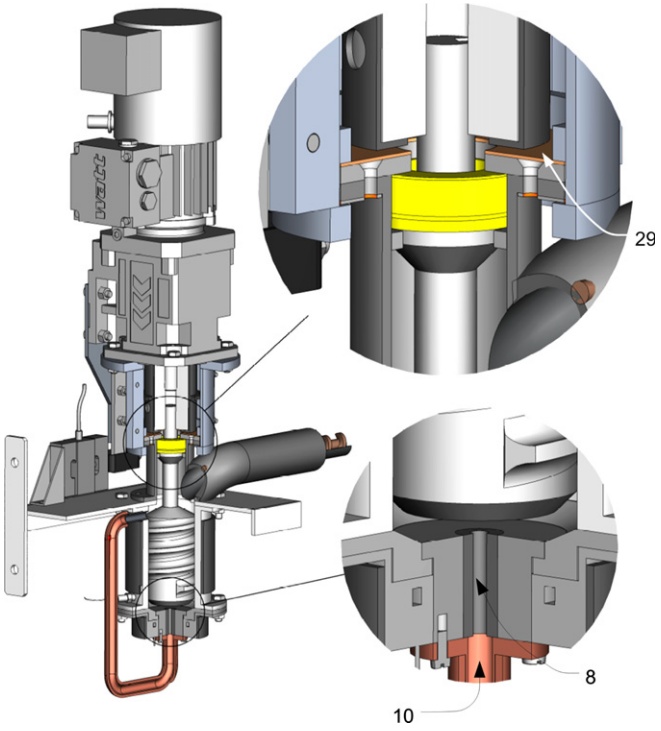

Fig. 2. Close up of the bearing and die configuration in the process rheometer for high viscous food and feed materials. Item 29 is a dry sliding strip, 8 is an exchangeable die and 10 a circulation path.

2.2. Experimental procedure for rheological measurements

Rheometers are instruments that can perform rheological measurements at different shear rates. In this case, the process rheometer will operate from a maximum speed of 75 rpm until 0 rpm, running the instrument every 5 rpm for about half a minute, gathering 10 data points per second. Then, averages of torque (related to the shear stress) and rotational speed (related to the shear rate) will be calculated, ensuring a high population of data ($n > 150$ at least). As the viscous standard is a Newtonian fluid, a linear regression will be applied between rotational speed and torque. This procedure is made in duplicate, and repeated every 5 °C between 40 °C and 85 °C to cover a wide range of viscosities.

2.3. Development of a model to predict viscosity

The rheometer has a complex geometry, especially due to the headed shaft with helical flights. This characteristic, together with a pressure gradient along the barrel, creates difficulties to analytically determine the shear stress and shear rate by means of the torque and speed. However, from the behavior or relation between speed and torque, it is possible to predict viscosity throughout a calibration experiment using a Newtonian standard with known viscosities. The next equations and figure (Fig. 3) will clarify this method.

As it is shown in Fig. 3, local shear stresses (τ) and local shear rates ($\dot{\gamma}$) depend on position. The torque (M) in the shaft (6) is the integral of the shear stress times radius over an infinitely small area dA, thus

$$M = \int \tau r \mathrm{d}A \tag{1}$$

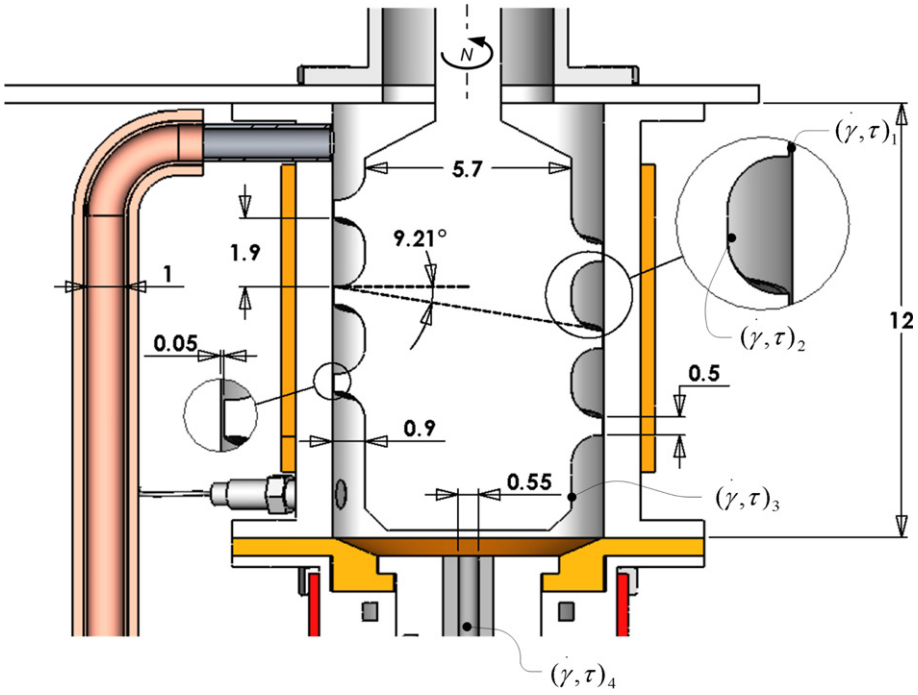

Fig. 3. Cross-section of the barrel. The figure indicates local shear stresses (τ) and local shear rates ($\dot{\gamma}$) which depend on position. All dimensions are in centimeters.

On the other hand, the local shear rate for Searle flow (Steffe, 1996; Tabilo-Munizaga & Barbosa-Canovas, 2005) is defined as

$$\dot{\gamma} = \frac{dv}{dx} = \frac{v}{\delta} = \frac{\omega \cdot r}{\delta} \tag{2}$$

where δ is the distance between the rotating shaft and the stationary barrel that varies along the shaft, v is the peripherical velocity of the shaft that consequently varies (see Fig. 4). ω is the angular speed of the shaft and r is the radius of the shaft that varies as well.

For concentric cylinders with constant radius and gap size, we have that the angular speed ω (rad s^{-1}) can be calculated by

$$\omega = \frac{2 \cdot \pi \cdot N}{60} \tag{3}$$

where N is the rotational speed (rpm), thus

$$\dot{\gamma} = \frac{2 \cdot \pi \cdot N}{60} \cdot \frac{r}{\delta} \tag{4}$$

Then, the local shear rate is represented by

$$\dot{\gamma} = \frac{2 \cdot \pi \cdot r}{60 \cdot \delta} \cdot N \tag{5}$$

where r and δ, depends on position.

Eq. (6) comes from the definition of viscosity (η) as a function of shear stress (σ) and shear rate ($\dot{\gamma}$)

$$\eta = \frac{\sigma}{\dot{\gamma}} \tag{6}$$

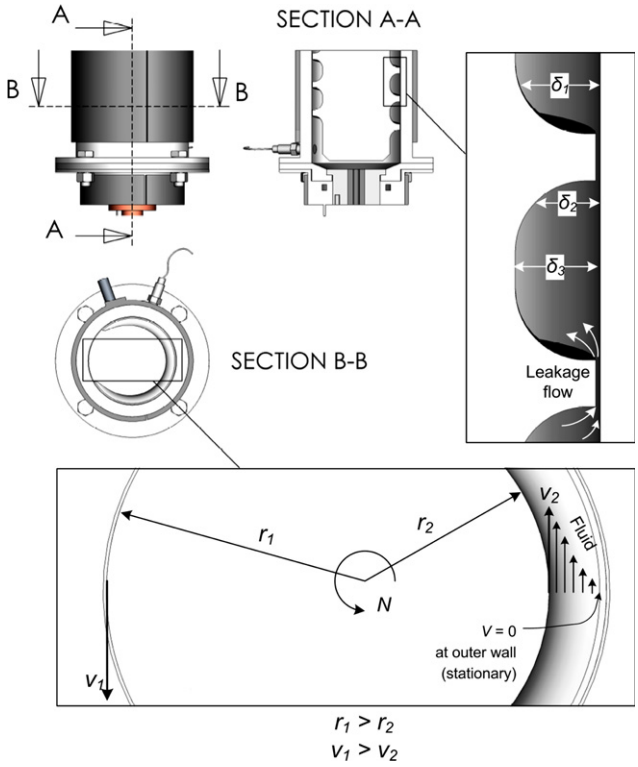

Fig. 4. Transversal and longitudinal sections at the barrel. The rotating shaft is assembled concentrically with the barrel.

In this rheometer, the torque comes from the material resistance to flow, which is proportional to the shear stress. This resistance is present near the barrel walls and along the channels in the helical flights, also the die indirectly affect the torque by the pressure gradient. Therefore to simplify this estimation the mean shear stress is used. Something similar occurs with the estimation of the shear rate. In this way, a constant which should characterize the system is needed to extract the average shear rate and average shear stress from the speed and torque, and thus to predict viscosity. Eq. (7) describes this situation:

$$\eta = \frac{\sigma}{\dot{\gamma}} = \frac{M \cdot k_1}{N \cdot k_2} \tag{7}$$

Here, M is torque (N m) and N is the number of revolution per minute of the shaft. k_1 is the constant needed to convert torque to mean shear stress, and k_2 is the constant to convert the rotational speed to an average shear rate. To reduce the number of constants to estimate, k_1 and k_2 can be expressed in terms of another constant K where

$$\eta = \frac{M \cdot k_1}{N \cdot k_2} = \frac{M}{N} \cdot K \tag{8}$$

In consequence, to predict viscosity it will be necessary to find the constant K. To find this value, a Newtonian certified viscosity standard (polybuthene-1 – 100%) was introduced into the system. This is a temperature dependent polymer and three of its viscosities were documented by the manufacturer. Consequently it was necessary to use a calibrated rheometer (Physica UDS200, Germany) to determine a wider range of viscosities according to different temperatures.

Operation of the rheometer at different speeds, gives a relation between shear stress and shear rate over different degrees of shear, and therefore shows the characteristics of the material in study (viscosity and whether it is a Newtonian or non-Newtonian fluid). Using a Newtonian fluid, a proportional relation is expected between the rotational speed and torque, therefore applying the best curve using the equation of a linear fit (Eq. (9)) should result in

$$M = a \cdot N + b \tag{9}$$

where a is the slope of the curve and b is the constant where the curve intersect the axis of the dependent variable. Using Newtonian fluids, the curve intersects the origin and consequently b is set to zero. Then, Eq. (9) in Eq. (8) results in

$$\eta = \frac{M}{N} \cdot K = a \cdot K \tag{10}$$

Polybuthene-1 is a thermo dependent polymer. Its viscosity changes at an exponential rate when the temperature changed; this behavior was assessed using both rheometers (Figs. 5 and 6). Thus K and the slope a, vary in proportional way when the viscosity changes, owing to the changes in temperature (Fig. 7). K is then extracted from the best curve between K versus a, therefore a new equation is created from this relation where

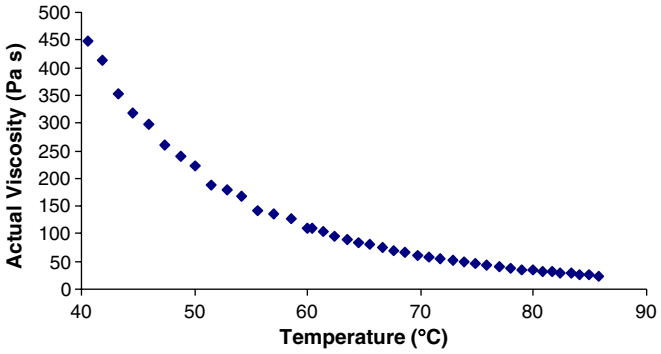

Fig. 5. Viscosities of polybuthene-1 at different temperatures measured in a calibrated rheometer (Physica UDS 200), which will be used as actual viscosities (A_η).

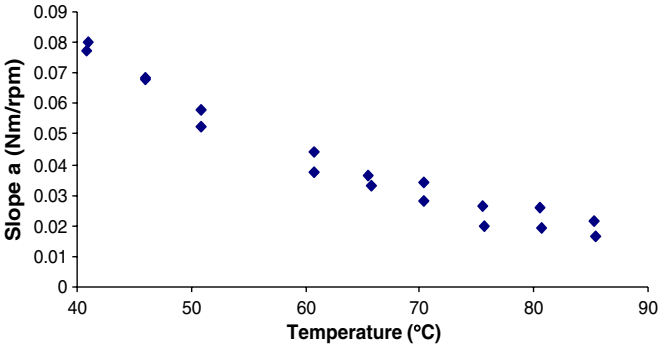

Fig. 6. Slope responses measured in the rheometer for highly viscous materials at different temperatures (two repetitions), which are related with the viscosities of polybuthene-1. Slope a, is described in Eq. (9).

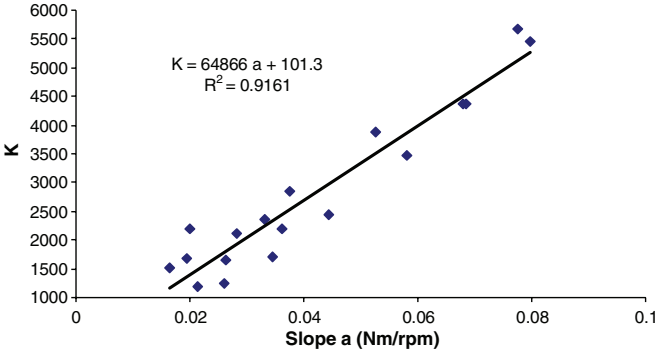

Fig. 7. Linear correlation to estimate $K(a)$, according to Eq. (11). K is the factor between the slope a, and the actual viscosity (Pa s) for different temperatures (see also Figs. 5 and 6).

$$\eta = a \cdot K = a \cdot K(a) \tag{11}$$

Therefore, the model that will come from Eq. (11) will be used to predict viscosity, and it is specific for the geometry of the developed rheometer.

2.4. Prediction of viscosity and accuracy estimation

The results coming from Eq. (11), which are based in the utilization of the slope a into the prediction model, will be presented as predicted viscosity (P_η). Subsequently, these results will be plotted together with the viscosity evaluated in the calibrated rheometer, termed as actual viscosity (A_η).

To determine the accuracy of the rheometer through the prediction model, the differences between P_η and A_η will be plotted as errors versus actual viscosity. The following equation represents this:

$$\text{Error} = P_\eta - A_\eta \tag{12}$$

2.5. Estimation of power

The relatively similar shape of the rheometer to an extruder or to a screw-pumping device, allows us to compare the rheological characteristics of the fluid with the power consumption or energetic costs for processing.

Here we have that

$$P = M \cdot \omega \tag{13}$$

where P is the power in watts, M is the torque in N m and ω is the angular speed in rad s^{-1}. To convert the angular speed from rad s^{-1} to rpm, the following formula is required:

$$P = M \cdot \frac{2 \cdot \pi \cdot N}{60} \tag{14}$$

3. Results and discussion

3.1. Experimental procedure for rheological measurements

Due to the large number of experiments (rotational speed vs torque) that were repeated twice every 5 °C between 40 °C and 85 °C, the results will not be represented in a graph. However, the slopes coming from the linear regressions between rotational speed and torque are presented and used as a base to build the model to predict viscosity.

3.2. Development of a model to predict viscosity

Each data point in Fig. 6, comes from a linear regression of 16 averages (e.g. avg. for 75, 70, 65 rpm, etc. which has $150 < n < 270$ and standard error of the mean < 0.02) obtained between rotational speed and torque.

The curves of Figs. 5 and 6 are both exponential, but with different curvature. These differences in responses between instruments may be caused by diverse flow patterns that vary at different viscosities. The pressure build up due to the small die opening, may generate backwards movements between the helical flights and the barrel (see Fig. 4); the level of leakage flow is also influenced by the viscosity of the fluid, this can be explained since when using

similar pressure and the same clearance between the helical flights and barrel, the fluid with lower viscosity will leak more than the fluid with higher viscosity. Moreover, if there is any slip at the barrel wall as the screw rotates then, the downstream component of the flow of the melt is demised and the efficiency of the screw decreases.

The predictive model for viscosity is given in Eq. (11), where the constant, K, is a function of the slope, a. Fig. 7 shows a plot of K versus a, defining the relationship; $K = 64866a + 101.3$

This relates torque (N m) and rotational speed (rpm), at different degrees of shear

$$P_\eta = 64866 \cdot a^2 + 101.3 \cdot a \tag{15}$$

This model covers all ranges of speeds (0–75 rpm) and all viscosities (0–450 Pa s) used during the experiments. Phenomena like backwards movements that occur inside the rheometer that depends on viscosity, speed, torque and pressure are included in the model (all factors influencing the slope a).

Future research will document how to use the instrument utilizing different dies.

3.3. Prediction of viscosity and accuracy estimation

The viscosities obtained from the prediction model, that were gathered at different temperatures (40–85 °C) and speeds (0–75 rpm), are plotted with the actual viscosity in Fig. 8.

The model from Eq. (15) to predict viscosity resulted in a good prediction ($R^2 = 0.9854$), considering the wide range of viscosities, speed and pressures plus the simplicity of the model (Fig. 9).

The maximum error (43 Pa s) is obtained at a temperature of 40.8 °C (439 Pa s of A_η). This maximum error it is not that big considering that the viscosity of polybuthene-1 at about 40 °C can vary 45 Pa s changing only 1.5 °C, because it is a very temperature sensitive material. The rheometer was filled with about 300 cm^3 of polybuthene-1 and this error can be due to changes in temperature

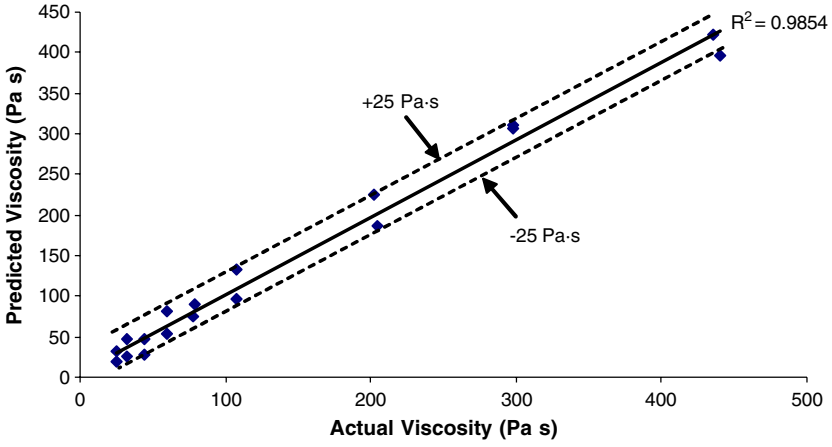

Fig. 8. Correlation between predicted viscosity (Pa s) and actual viscosity (Pa s). Actual viscosity is measured using the calibrated rheometer (Physica USD 200) and the predicted viscosity comes from the prediction model (Eq. (15)).

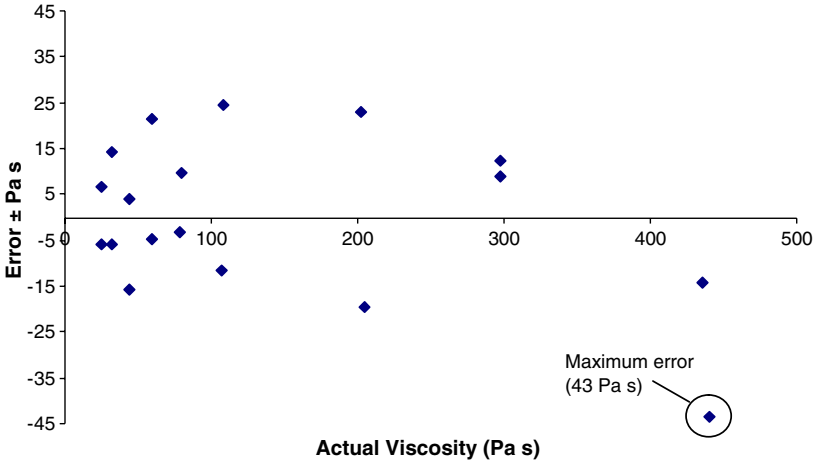

Fig. 9. The graph shows the errors associated with the viscosities of the material (from differences between predicted and actual viscosity).

during the run which affected the slope a. This is the first prototype of the process rheometer and improvements in the construction and especially in its bearing system will possibly reduce these errors. As previously explained, the process rheometer utilizes two dry sliding bearings (2 of Fig. 1 and 29 of Fig. 2) and the friction of these types of bearings, change according to different loads that could possibly influence the accuracy. Commercial rotational rheometers usually use air or magnetic bearings, which has much lower friction that normally can be neglected.

The authors tried to build a simple predictive model in order to keep a straight forward physical relationship between shear rate and shear stress. More sophisticated mathematical models can be built in the future to obtain higher accuracies if required.

The graph of Fig. 10 describes how the torque is affected by changes in viscosity at different speeds. The torque (proportional to the shear stress) presents a logarithmic behavior at all speeds when viscosity changes. The differences in correlation (R^2) are due to the errors associated with different speeds (see Fig. 11). The graph of Fig. 10 was intended to show how the shear stress (from torque) changes when the viscosity changes at constant shear rate (related to rotational speed).

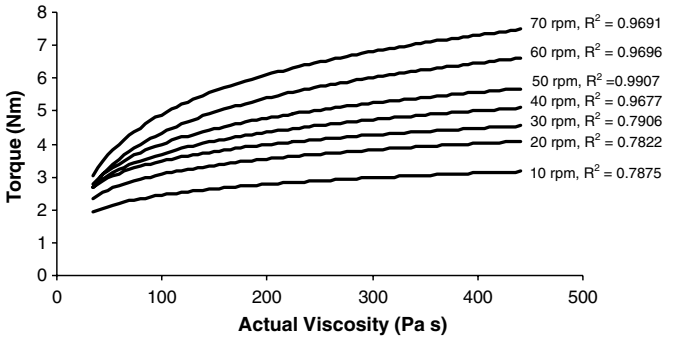

Fig. 10. Correlation between torque responses (related to the mean shear stress) under different speeds (related to the mean shear rate) at different viscosities.

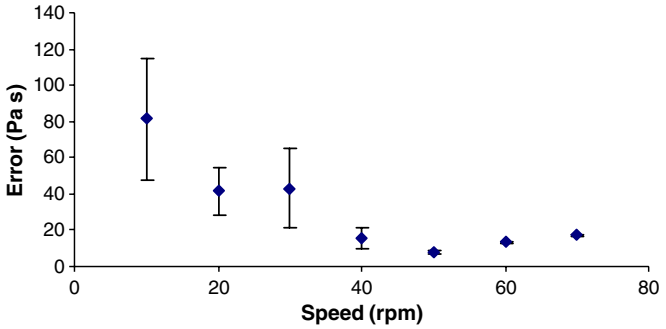

Fig. 11. Averages of errors (Pa s) associated with different speeds. Every data point comes from the average errors at a particular speed and from different viscosities ± standard error of the mean (±SE), from the difference between A_η and P_η.

Fig. 11 shows a clear difference between the average error between the predicted viscosity and the actual measured viscosity at low and at high speeds. At lower speeds, the rheometer shows the worse accuracy. Considering all viscosities, the minimum errors are found between 40 and 60 rpm with the best accuracy at 50 rpm according to the prediction model. Then from Figs. 10 and 11, it can be concluded that the instrument has the best accuracy when run with a rotational speed between 40 and 60 rpm for all viscosities. The reason for these differences of accuracy is probably due to a combination of factors, like the increase of friction in the bearing system at high speeds and loads (>60 rpm) and to the low sensitivity of the load cell for measuring low forces at low speeds (<40 rpm). All these factors are related to the devices installed in the prototype and can be improved. The present load cell and bearing limit the lower operational range to approximately 30 Pa s.

One of the most important measurements during a manufacturing process is to detect viscosity changes with respect to time. This measurement will demand the running of the process rheometer at constant speed (constant shear rate) to monitor any change in torque (shear stress) that will indicate a change in viscosity. Thus, the rheological monitoring can be performed at a constant rotational speed of 50 rpm where it was found the highest accuracy.

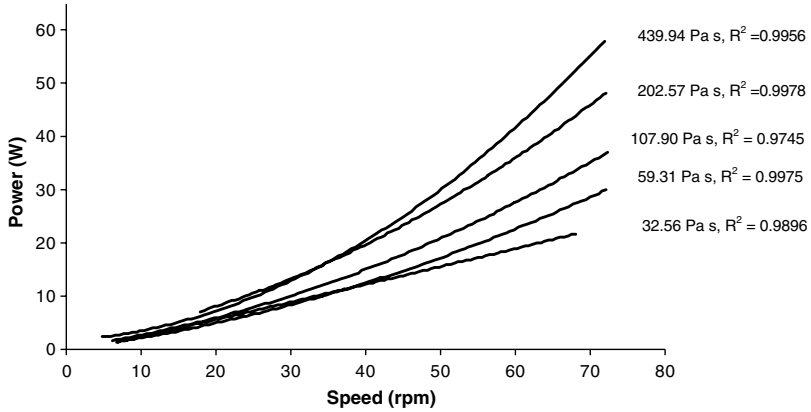

Fig. 12. Power at different speeds and under different viscosities.

Therefore, the errors related to speed will not affect the accuracy of the rheological monitoring.

3.4. Estimation of power

The viscosity of the fluid, as shown in Fig. 12, influences the power required to move a material inside the rheometer. Higher viscosities resulted in higher power consumed by the rheometer at similar speeds. This can be explained since the viscosity is a measure of a fluid resistance to flow. A higher resistance to flow will lead to a higher power requirement. At low viscosities the power changes in a more proportional way when increasing the rotational speed (related to shear rate).

These power results are interesting if we extrapolate this situation when extruding a Newtonian polymer or if we analyze what could happens when pumping with a screw device at different viscosities. In large manufacturing processes, determinations of power consumption are fundamental when high efficiencies and lower manufacturing costs are required.

4. Conclusions

A new process rheometer is developed to measure highly viscous food and animal feed materials. By using torque and rotational speed it was possible to predict viscosity by means of an average shear stress and a mean shear rate. From the first prototype, it was possible to have a good prediction of viscosity with an accuracy of ± 25 Pa s over a large range of viscosities (30–450 Pa s), with a simple model. Higher accuracies can be obtained by more complex models. The working principle of the rheometer allows measurement of materials taken from the process in a continuous manner. More research and developments are needed to describe additional capabilities when using different dies to extend the range of measurements and utilization during the process.

Acknowledgements

The authors would like to thank Andreas Flø, Tom Ringstad, Tore Ensby and to the Workshop from the Department of Mathematical Sciences and Technology for their help in the development of the prototype, also to Trond Storebakken from the Aquaculture Protein Centre for his initial help describing problems in the animal feed industry. The financial support received for this research, which comes from the Business Liaison Office of the Norwegian University of Life Sciences, is gratefully acknowledged.

References

Arhaliass, A., Bouvier, J. M., & Legrand, J. (2003). Melt growth and shrinkage at the exit of the die in the extrusion-cooking process. *Journal of Food Engineering, 60*, 185–192.

Bouzaza, D., Arhaliass, A., & Bouvier, J. M. (1996). Die design and dough expansion in low moisture extrusion-cooking process. *Journal of Food Engineering, 29*, 139–152.

Hoseney, R. C., William, R. M., Lai, C.-S., & Guetzlaff, J. (1992). Factors affecting the viscosity and structure of extrusion-cooked wheat starch. In J. L. Kokini, C.-T. Ho, & M. V. Karwe (Eds.), *Food extrusion science and technology* (pp. 277–305). New York: Marcel Dekker.

Li, P. X., Campanella, O. H., & Hardacre, A. K. (2003). Using an in-line slit-die viscometer to study the effects of extrusion parameters on corn melt rheology. *Cereal Chemistry, 81*, 70–76.

McKenna, B. M., & Lyng, J. G. (2001). Rheological measurements of foods. In E. Kress-Rogers & C. J. B. Brimelow (Eds.), *Instrumentation and sensors for the food industry*. 1-59124-341-6 (pp. 425–452). Boca Raton, FL: CRC Press.

Roberts, I. (2001). In-line and on-line rheology measurement. In E. Kress-Rogers & C. J. B. Brimelow (Eds.), *Instrumentation and sensors for the food industry*. 1-59124-341-6 (pp. 403–422). Boca Raton, FL: CRC Press.

Salas, C., 2004. Development of an on-line rheometer and die tester for feed/food quality control. Master Thesis, Norwegian University of Life Sciences, Ås, pp. 84.

Salas, C., Jeksrud, W., 2005. Norway Patent Number (Application) P19447NO00.

Shackelford, D. W., 1993. United States Patent number 5,209,108.

Smith, A. C. (1992). Studies on the physical structure of starch-based materials in the extrusion cooking process. In J. L. Kokini, C.-T. Ho, & M. V. Karwe (Eds.), *Food extrusion science and technology*. 0-8247-8542-8 (pp. 573–618). New York: Marcel Dekker.

Steffe, J. F. (1996). *Rheological methods in food process engineering* (2nd ed.). 0-9632036-1-4. East Lansing, MI, USA: Freeman Press.

Tabilo-Munizaga, G., & Barbosa-Canovas, G. V. (2005). Rheology for the food industry. *Journal of Food Engineering, 67*, 147–156.

Thomas, M., & van der Poel, A. F. B. (1996). Physical quality of pelleted animal feed 1. Criteria for pellet quality. *Animal Feed Science and Technology, 61*, 89–112.

Thomas, M., van Vliet, T., & van der Poel, A. F. B. (1998). Physical quality of pelleted animal feed 3. Contribution of feedstuff components. *Animal Feed Science and Technology, 70*, 59–78.

Winter, H. H., 1978. United States Patent number 4,077,251.

PAPER II

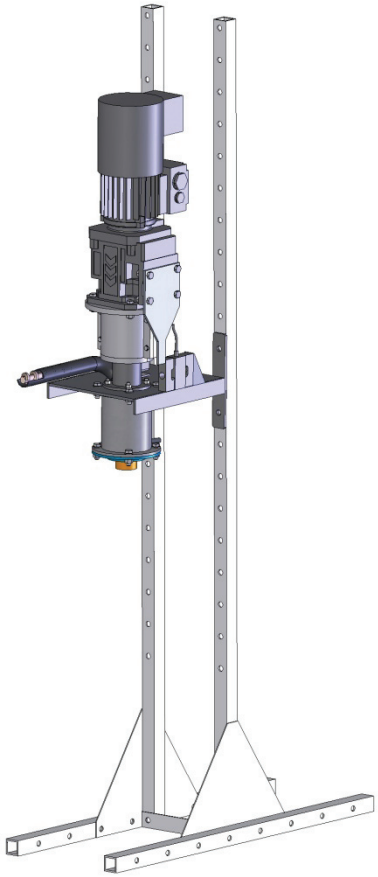

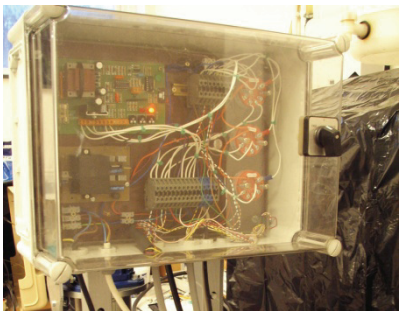

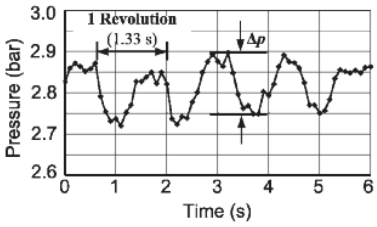
1 Revolution
(1.33 s)
Δp
Pressure (bar)
Time (s)
3.0
2.9
2.8
2.7
2.6
0
1
2
3
4
5
6

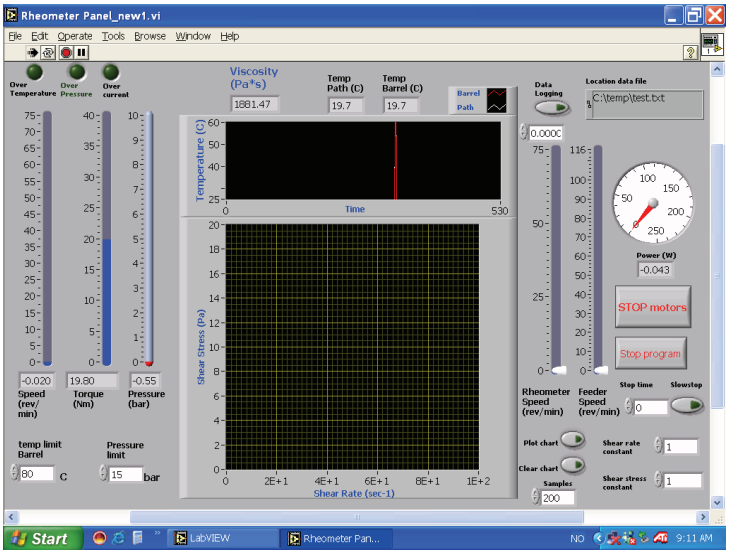
Rheometer Panel_new1.vi
File Edit Operate Tools Browse Window Help
Viscosity (Pa*s)
1881.47
Temp Path (C)
19.7
Temp Barrel (C)
19.7
Data Logging
Location data file
C:\temp\test.txt
Temperature (C)
Time
Shear Stress (Pa)
Shear Rate (sec-1)
Speed (rev/min)
Torque (Nm)
Pressure (bar)
-0.020
19.80
-0.55
temp limit Barrel
80
C
Pressure limit
15
bar
Power (W)
-0.043
STOP motors
Stop program
Rheometer Speed (rev/min)
Feeder Speed (rev/min)
Stop time
Slowstop
Plot chart
Clear chart
Shear rate constant
Shear stress constant
Samples
200
Start
LabVIEW
Rheometer Pan...
9:11 AM

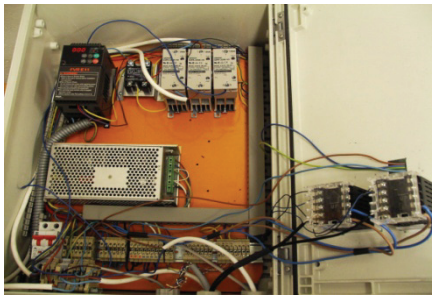

Time Variations and Calibration of a Screw Type Process Rheometer

C. Salas-Bringas[1]*, O.-I. Lekang[1] and R.B. Schüller[2]

[1] Department of Mathematical Sciences and Technology, [2] Department of Chemistry, Biotechnology and Food Science, Norwegian University of Life Sciences, P. O. Box 5003, 1432 Ås, Norway

* Email: carlos.salas.bringas@umb.no
Fax: x47.64965401

Received: 2.9.2009, Final version: 16.12.2009

Abstract:
The present article describes and analyzes different calibration methods for a screw type process rheometer, Searle type, having a die hole at the downstream of a barrel. The work also quantifies the effect of time dependent flows due to the screw on the measurement performance. Time variations in torque and pressure become more notorious at increased resistances to flow (higher fluid viscosities and smaller die diameters). Screw speeds seem to do not affect these variations. Shear stress in the system is related to pressure and torque, and by using any of them, is possible to predict an average viscosity. Similar prediction errors were found when using torque or pressure. A section of practical applications is added to understand the use of a screw type process rheometer better.

Zusammenfassung:
Der vorliegende Artikel untersucht und beschreibt unterschiedliche Kalibrationsmethoden für ein Prozess-Schneckenrheometer nach dem Searle-Prinzip, das eine Lochdüse am Zylinderauslass hat. Ausserdem wurde in dieser Arbeit der Effekt der Zeitabhängigkeit des Flusses aufgrund der rotierenden Schnecke zur Messleistung. Zeitschwankungen in Drehkraft und Druck werden deutlicher, wenn der Widerstand zum Fluss erhöht wird (durch Flüssigkeiten höhrer Viskosität und einen geringeren Düsendurchmesser). Die Scherspannung in einem System ist abhängig von Druck und Drehmoment und durch Messung eines der beiden Parameter lässt sich die durchschnittliche Viskosität vorhersagen. Der Prädiktionsfehler für die Viskosität war für Druck und Drehmoment ähnlich. Ein Abschnitt über praktische Anwendungen für diese Art Prozess-Schneckenrheometer wurde dem Artikel hinzugefügt, um dessen Nutzung besser zu veranschaulichen.

Résumé:
Cet article décrit et analyse différentes méthodes de calibration pour un rhéomètre de type procédé-vis, type Searle, qui possède une filière en forme de trou monté au bout d'un canon. L'étude quantifie également l'effet des écoulements transitoires associés à la vis sur la performance de la mesure. Les variations temporelles du couple et de la pression deviennent plus prononcés lorsque la résistance à l'écoulement est accentuée (fluides de viscosité plus élevée, et diamètre de filière plus petit). Les vitesses de la vis ne semblent pas affecter ces variations. La contrainte de cisaillement dans ce système est reliée à la pression et au couple, et en utilisant l'une ou l'autre, il est possible de prédire une viscosité moyenne. Des erreurs de prédiction similaires sont trouvées que ce soit en utilisant le couple ou la pression. Un paragraphe décrivant des applications pratiques est ajouté afin de mieux comprendre l'utilité de ce type de rhéomètre.

Key words: rheometer, viscometer, process, viscosity, measurement method, time variation

1 INTRODUCTION

Process rheometers, process viscometers and consistency analyzers, are normally used to keep steady the rheological properties of the feed during processing. Process rheometers and viscometers are normally used to measure the viscosity of a representative portion of the product stream. Consistency analyzer are used to measure the consistency, that is expressed as a percentage by dividing the mass of a solid material by the total mass of a wet sample, most of them measure mechanically the resistance to deformation, and thus is related to apparent viscosity. Consistency analyzers are used for wood pulp, dough, tomato paste, paint, gelatin or drilling mud [1]. Some of the industrial viscometers used by the process industry are: differential pressure type capillary viscometers, back pressure type, falling-piston viscometer, falling slug or falling ball viscometers, float viscometers, oscillating

© Appl. Rheol. 20 (2010) 34526

DOI: 10.3933/ApplRheol-20-34526

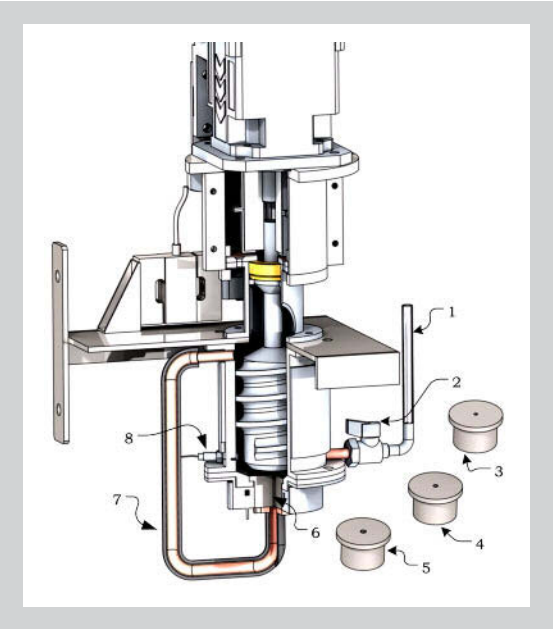

Figure 1:
The process rheometer with its exchangeable dies. Items are indicated by numbers: (1) transparent tube to measure the level of the fluid in the barrel, (2) valve to avoid overflow in the meter during running, (3, 4, 5) are the three different die holes used in the experiment, (6) an assembled die, (7) a circulation path used for calibration only and (8) the location of the pressure and temperature sensors.

viscometers, plastometers, rotary viscometers, vibrating-reed viscometer and coriolis mass flow meter with viscosity measurements capabilities [2]. The consistency analyzers used by the industry are: probe type, blade type, rotating sensors and optical sensors [1].

This article presents a new robust screw type process rheometer. The apparatus is a rotational rheometer, Searle type, having a cylindrical shearing gap assembled in a vertical position. The rotating element is a specially designed screw. At the end of the cylindrical shearing gap (barrel), an exchangeable die is located to evacuate the fluid or semi-solid material from the system (see Figure 1). An extensive description of the system and comparisons to the closest rheometers was previously made by Salas-Bringas et al [3]. Since the screw of the rheometer act as a screw conveyor, it is also possible for the rheometer to convey a viscous material whiles measures viscosity in a process. This is ideal for continuous measurements and low fouling levels in the instrument. The equipment can also handle fluids having particles or fibers which have been described as a problem in most rheometers [4].

The resistance of a fluid to be sheared can be measured in two ways in this rheometer, by using the torque that is required to rotate the screw, or by using the pressure that is formed downstream the screw, before the restriction or die. It is expected that a screw type process rheometer is able to measure a wide range of viscosities. Laboratory rheometers use air or magnetic bearings to detect minute torques (e.g. nNm). Because the screw type process rheometer is a robust industrial equipment that is expected to work in harsh environments, relatively low cost bearings are added. This causes limitations to detect low torques. For this reason, when the screw exert low resistances to rotate (e.g. in the presence of a low viscous fluid), it is recommended the use of a large restriction downstream the screw to increase the resistance of the fluid to flow and thus to increase torque or pressure.

If a screw rheometer is made to measure viscosity of different fluids, it is mandatory to develop a calibration procedure and system allowing the use of different restrictions or dies. Extrusion literature is the only close information that can be obtained today from the behavior of a screw type rheometer. From extrusion is known that the die determines in great manner the behavior of extruders (e.g. pressure and torque) [5, 6]. Therefore, a calibration method that accounts the effects given by different dies sizes plus that accounts the complex flows that might be present in the rotating screw is required. It is expected from extruder behavior that among the main time variations that can be present in the rheometer, are the ones produced by the geometry of the screw. Time variations can be caused by pressure difference across the screw flight. This can cause a cyclic pressure change (e.g. oscillatory change over time) that can be detected if the extruder has accurate pressure readout [6].

Nowadays, it is increasingly found that the control of a process relies extensively on instrumentation. If viscosity or consistency is decided to be the controlled variable, it is desirable that this parameter should be kept within relatively tight given limits during process [7]. If the feed doesn't change with time, it is as well demanded that the instrumentation should deliver a constant viscosity reading (or an electrical signal) over time, so the process can be modified only when the viscosity changes overpass the instrumental uncertainty. Consequently, this article will cover the effect (e.g. time variations in torque and pressure) of three different die diameters (3.5, 4.5 and 5.5 mm), viscosities (13.5 - 106.8 Pa·s) and speeds (10, 15, 20, 25, 30, 35, 40 and 45 rpm) in a screw type process rheometer, together with developing and analyzing four different calibration procedures. Early description of the system [3, 8] included only a procedure for calibration using torque, but pressure was neither measured nor used in the rheometrical procedure. Also the effects of different restrictions and fluctuations in torque and pressure in a screw type process rheometer have not been described on literature.

2 MATERIALS AND METHODS

2.1 DESIGN FEATURES

The process rheometer used in these experiments, is the same as the one used and described in detail by Salas-Bringas et al. [3] which is mounted on its own assembly. A practical application section is included in the article to show how the rheometer can be assembled in a process.

For this research, the rheometer was upgraded and the new features will be described in Figure 1. A transparent tube (see item 1) was incorporated to measure the level of the fluid inside the barrel and to ensure that the barrel and screw were fully and equally covered by the fluid for all tests with different dies. The valve which is indicated in the Figure 1 (item 2) was closed during each run to avoid overflow in the meter. Items 3, 4 and 5 are the three different dies having 3.5, 4.5 and 5.5 mm diameter, respectively, and the same length (30 mm). Item 6 is an assembled die. Item 7 is the circulation path for calibration only which is covered with a PID controlled jacket heater to keep a steady temperature through the tests since the viscosity of our testing fluid, polybutene oil (isobutylene/butane copolymer, Newtonian certified viscosity standard N450000, Cannon Instrument Co., PA), is highly temperature dependent. Cannon Instrument Co., disclosure the physical state of N450000 as a viscous liquid [9]. The circulation path is made with a much bigger diameter (10 mm) than the biggest die (5.5 mm) to produce a bottle neck situation at the die, neglecting the friction in the circulation path. Item 8 is the position of temperature (Pt1000 element) and pressure (Dynisco, PT467E, Heilbronn, Germany) sensors.

The control system of the rheometer (described in Salas-Bringas et al. [3]), LabView graphical programming software (National Instruments, TX, USA), was re-programmed this time to incorporate a PID control over the 250 W AC motor, so better speed control was obtained this time. Also LabView was re-programmed to read and log the new pressure measurements.

2.2 EXPERIMENTAL PROCEDURE FOR DETECTION OF TIME VARIATIONS

The process rheometer has essentially three different sensors that can detect time variations, the pressure, the torque and the speed measuring unit. Time variations will be studied by logging these sensors data at 10 Hz.

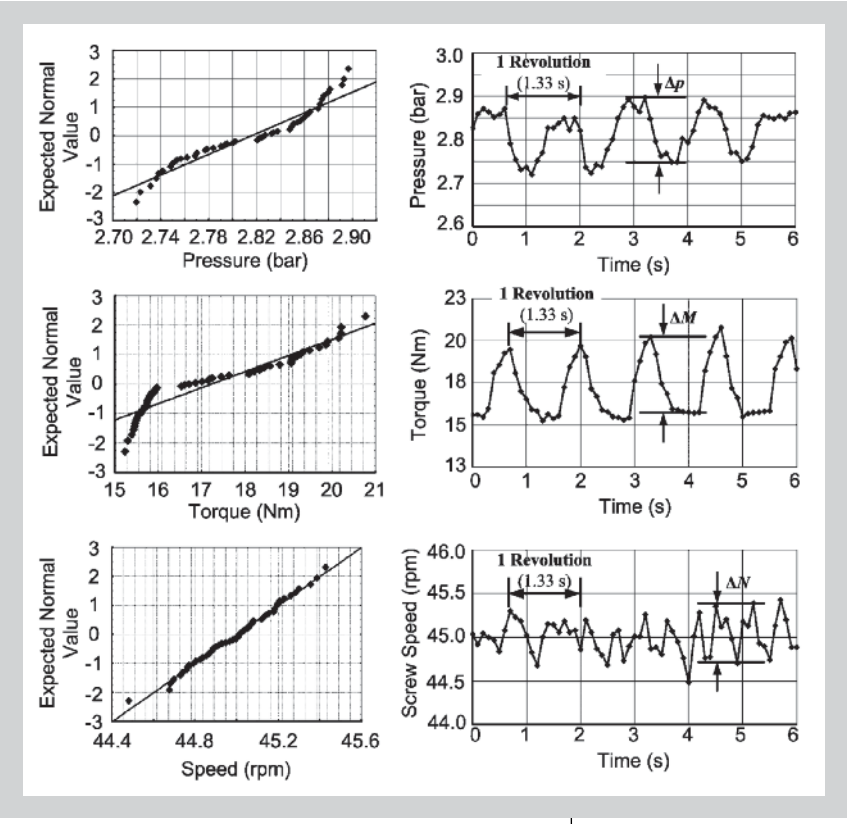

Figure 2: Normally distributed pressure, torque, and speed oscillations at 45 rpm (45.004 avg.) and 55.6°C (145 Pa·s of viscosity)

2.3 EXPERIMENTAL PROCEDURE TO DETECT CHANGES IN THE AMPLITUDE OF PRESSURE, TORQUE AND SPEED

A first exploratory view to the amplitudes of pressure, torque and speed (ref. Figure 2), is included to show that these parameters oscillate with time and that they are normally distributed. To compare amplitude differences among different running conditions, a representative amplitude will be determined using the standard deviation times three. This method is used in statistical process control and is simple to calculate. It indicates the dispersion of 99.7 % of the data keeping the original units [10].

2.4 EXPERIMENTAL PROCEDURE TO DETECT VARIATIONS IN PRESSURE, TORQUE AND SPEED OVER TIME

To study how often pressure, torque and speed oscillate, the data will be analyzed by using Single Spectrum (Fourier) Analysis (Statistica 8.0, StatSoft, Inc., Tulsa, USA), the results will be presented in 2D surface plots (Dplot 2.2. Hydesoft Computing, LLC. MS, USA) for 3 different cases; an experiment having a fluid/equipment configuration including the largest resistance to flow (3.5 mm die and 60°C), another with moderate resistance to flow (4.5 mm die and 70 °C) and a last having the lowest resistance to flow (5.5 mm

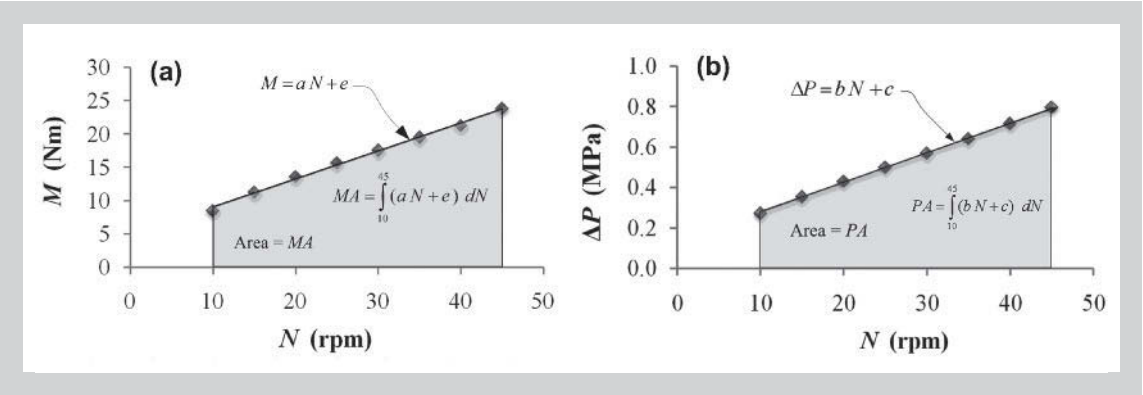

Figure 3: Rheograms taken from two experimental data plots using die pressure (MPa) and torque (Nm) as a function of the screw speed (rpm). (a) shows how the Slope a (Nm/rpm) and the area MA (Nm/rpm) were obtained. (b) shows how the Slope b (MPa/rpm) and area PA (MPa/rpm) were obtained

die and 90°C). The plots will be made by using either the pressure or torque frequencies (Hz) in the *x* axis, average speeds in the *y* axis and the spectral densities from the *z* axis drawn in a 2D surface plot.

2.5 EXPERIMENTAL PROCEDURE FOR RHEOLOGICAL MEASUREMENTS

The rheometer was operated from a maximum speed of 45 rpm to a minimum speed of 10 rpm, and it was run at speed intervals of 5 rpm for about half a minute each. Averages of torque (related to the shear stress), die pressure (also related to the shear stress) and rotational speed (related to the shear rate) were calculated ensuring a high population of data ($n > 150$). These sets of data were used to create different prediction models covering a range of shear rates. The experiments were repeated six times at each temperature (60, 65, 70, 80 and 90°C). Experiments at 65°C were included since N450000 standard largely changes its viscosity between 60 – 70°C and in a much lower degree between 70 – 90°C. N450000 manufacturer disclosure only three viscosities at three different temperatures (1631 Pa·s at 25°C, 106.8 Pa·s at 60°C and 2.6 Pa·s at 135°C) and therefore it was previously necessary to give a detailed information of its viscosities at different temperatures in Salas-Bringas et al. [3]. The viscosity of N450000 standard has been reported to remain Newtonian over a wide range of shear rates [11, 12].

2.6 DEVELOPMENT OF FOUR DIFFERENT PREDICTION MODELS FOR VISCOSITY

Four different alternatives to predict viscosity using the same experimental data will be described. The prediction errors or residuals (*E*) generated though the models will be compared

2.7 PREDICTION OF VISCOSITY USING SLOPE A (NM/RPM)

A proportional relationship is expected between speed and torque using a Newtonian fluid for calibration in a test running the rheometer at different speeds, therefore applying the best curve using the equation of a linear fit, Equation 1 is obtained (Figure 3a):

$$M = aN + e \quad (1)$$

where *a*, is the slope of the curve (Nm/rpm) and *e* (Nm) is the intercept with the axis of the dependent variable. Using Newtonian fluids (e.g. Polybuthene-1/N450000), the curve should intersect the origin and consequently *e* is set to zero.

The model that will be used to predict viscosity from a Slope *a* (Nm/rpm), given by the screw type process rheometer, will be built from the experimental results coming from the plot of Slope *a* (Nm/rpm), versus the viscosities of Polybuthene-1 that were previously measured [3] in a calibrated rheometer (Physica UDS 200, Germany), see Figure 4.

2.8 PREDICTION OF VISCOSITY USING AN AREA MA (NM RPM)

In this research it was observed that when using the smallest die ($d = 3.5$ mm) and the lowest temperature within our experimental range (60°C), the intersect *e* (Nm) was not zero as it is expected from a Newtonian fluid. Despite of this, the intersect *e* (Nm) was zero when the rheometer was run at higher temperatures, so Polybuthene-1 presented lower viscosities, and the rheometer lower pressures and torques. A similar situation ($e = 0$) happened when using bigger die diameters. We believe that the situation ($e \neq 0$) occurring when using small die holes is associated with a particular problem in the bearing system which was also described previously [3]. Here, high thrusts pressures increased the friction in the spherical plain thrust bearing (GX-17, SKF Inc., Gothenburg), assembled with the screw. This bearing has a sliding contact surface made of a combination steel/PTFE composite.

This phenomenon occurring in the system resulted in the development of another type of prediction method using the intersect *e* obtained from the curve fit described on Equation 1 and shown in Figure 3a to obtain the area below the

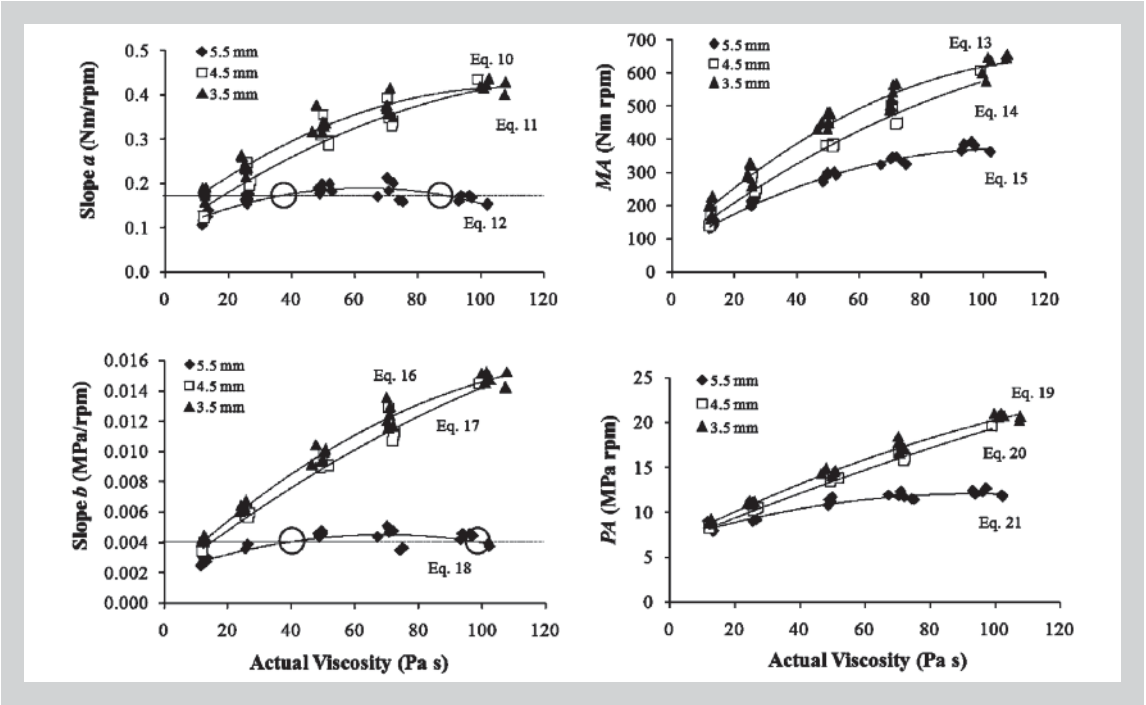

Figure 4: Viscosities of Polybuthene-1 (Pa·s) at different temperatures versus the averages (6 rheograms) of slope a (Nm/rpm), MA (Nm/rpm), slope b (MPa/rpm) and PA (MPa/rpm)

curve. The area below the linear fit curve (*MA* (Nm/rpm)) can be expressed as follows:

$$MA = \int_{10}^{45} (aN + e)\,dN \tag{2}$$

MA (Nm/rpm) represents the integrated power that is needed to rotate the shaft of the rheometer. The prediction model will come from a plot between *MA* (Nm/rpm) and the viscosities of Polybuthene-1 obtained in the calibrated rheometer (Figure 4). This method takes into account all bearing effects at different running conditions.

2.9 PREDICTION OF VISCOSITY USING A SLOPE B (MPA/RPM)

It was found that high torque was coupled with high pressures in all tests. High pressures and torques were found when higher resistances to flow were present (e.g. when using the smallest die holes or using the highest viscosities). A plot between *M* and ΔP always resulted in a linear fit with high correlations ($R^2 \geq 0.98$). Therefore it was experimentally seen that the magnitude of the pressure in the barrel (between screw and die) is proportional to the magnitude of torque. Previously, Salas-Bringas et al. [3, 8] analytically showed that on the rheometer, the torque is proportional to a mean shear stress as follows:

$$\sigma_{rheometer} = k_1 M \tag{3}$$

where $\sigma_{rheometer}$ is an overall shear stress in the rheometer and k_1 is the rheometer constant to convert torque to an overall shear stress in the system. Moreover, by assuming an isotropic pressure at the boundary of the barrel walls (ΔP_{xyz}), between the screw and the die, a shear stress at the barrel walls (σ_b) can be obtained using direct pressure measurements (~ flush mounted sensor). Since it is also known that the pressure gradient along a rotating screw depends on screw speed [6, 13], and because it is experimentally known that *M* is proportional to ΔP_{xyz}, it is analytically expressed a proportionality between $\sigma_{rheometer}$ and σ_b as follows:

$$\frac{\sigma_{rheometer}}{k_1 M} = \frac{\sigma_b}{\Delta P_{xyz}} \tag{4}$$

Given that *M* is proportional to ΔP_{xyz}, a new prediction model using barrel pressure instead of torque (*M*) versus the screw speed (*N*) will be created to predict viscosity, Figure 3 b, this will result in the following curve fit:

$$\Delta P = bN + c \tag{5}$$

where $\Delta P = \Delta P_{xyz}$ (used further for simplification). Previously it was mentioned that *M* versus *N* curves have an intersect $e \neq 0$ when high resistance to the flow was caused by both increased viscosity of the fluid and reduced die diameter. Nevertheless, when using the absolute die pressure in a plot of ΔP versus *N*, all intersects *c* were equal to 0.1 MPa (atmospheric pressure, see Figure 3b), so *c* was neglected from this prediction model and only the slopes *b* (MPa/rpm) were plotted versus the previously measured viscosities of Polybuthene-1.

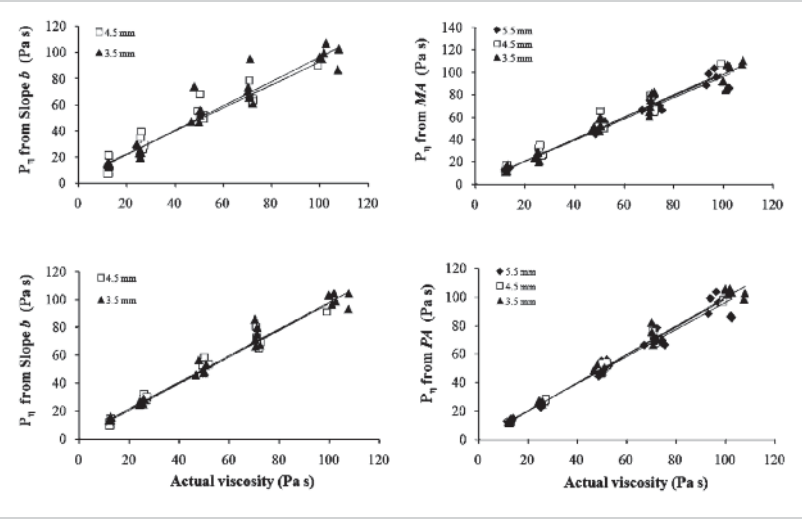

Die diameter	Equation ID	Prediction model (curve fit) Predictor	Trinomial	R^2
3.5 mm	Eq. 10	Slope a (Nm/rpm) =	$-2E-05\eta^2 + 0.0055\eta + 0.1163$	0.9570
4.5 mm	Eq. 11	Slope a (Nm/rpm) =	$-2E-05\eta^2 + 0.0051\eta + 0.0861$	0.9257
5.5 mm	Eq. 12	Slope a (Nm/rpm) =	$-3E-05\eta^2 + 0.0032\eta + 0.0903$	0.7695
3.5 mm	Eq. 13	MA (Nm rpm) =	$-0.0346\eta^2 + 8.7105\eta + 93.324$	0.9733
4.5 mm	Eq. 14	MA (Nm rpm) =	$-0.0208\eta^2 + 7.0772\eta + 75.605$	0.9580
5.5 mm	Eq. 15	MA (Nm rpm) =	$-0.0264\eta^2 + 5.603\eta + 73.148$	0.9856
3.5 mm	Eq. 16	Slope b (Mpa/rpm) =	$-7E-07\eta^2 + 0.0002\eta + 0.0017$	0.9865
4.5 mm	Eq. 17	Slope b (Mpa/rpm) =	$-4E-07\eta^2 + 0.0002\eta + 0.0016$	0.9805
5.5 mm	Eq. 18	Slope b (Mpa/rpm) =	$-5E-07\eta^2 + 7E-05\eta + 0.0019$	0.7642
3.5 mm	Eq. 19	PA (Mpa rpm) =	$-0.0004\eta^2 + 0.1809\eta + 6.6434$	0.9906
4.5 mm	Eq. 20	PA (Mpa rpm) =	$-0.0002\eta^2 + 0.1494\eta + 6.4779$	0.9942
5.5 mm	Eq. 21	PA (Mpa rpm) =	$-0.0006\eta^2 + 0.1108\eta + 6.9111$	0.9419

Figure 5 (left above): Viscosities of Polybuthene-1 (Pa·s) at different temperatures versus the predicted viscosities using the four types of prediction models; Slope a (Nm/rpm), MA (Nm/rpm), Slope b (MPa/rpm) and PA (MPa/rpm)

Figure 6 (right): Root mean square error of prediction (RMSEP) for all models and for the three dies. RMSEP expresses the average error to be expected associated with the future predictions. The models having different letters above the columns are significantly different ($p < 0.05$) p is the variance

Table 1: Four different types of prediction models for the three die diameters

2.10 PREDICTION OF VISCOSITY USING AN AREA PA (MPA RPM)

A similar procedure as the one to obtain *MA*, will be used here, but instead of using the area below the curve $M = aN + e$, the area below the curve $\Delta P = bN + c$ will be used as follows (Figure 3b):

$$PA = \int_{10}^{45} (bN + c)\, dN \tag{6}$$

where *PA* (MPa/rpm) represents the integrated pressure generated at the inlet of the die when the rheometer is run between 10 to 45 rpm. The prediction model will come from a plot between *PA* (MPa/rpm) and the viscosities of Polybuthene-1.

2.11 ACCURACY ESTIMATION AND COMPARISON OF MODELS

The results coming from Equations 1, 2, 5, and Equation 6 that will be obtained from the experimental results shown in Table 1, are presented and plotted in Figure 5 as predicted viscosities (P_η) versus the viscosities of Polybuthene-1 that will be referred as actual viscosities (A_η). These plots will include the results obtained using the three different dies. The errors or residuals will be estimated using the experimental data and models (Equations 10 to 21 in Table 1) as follows:

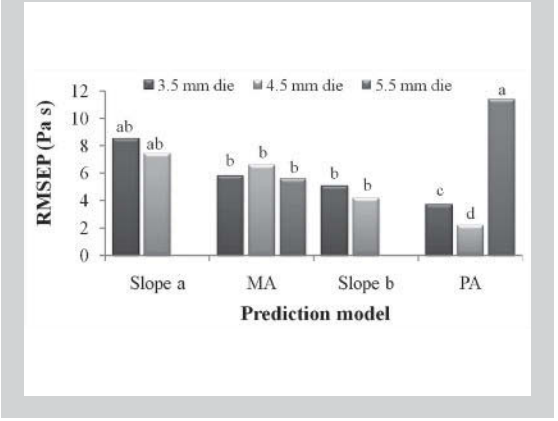

$$E(Pa \cdot s) = P_\eta - A_\eta \tag{7}$$

To obtain an estimation of the most expected errors (in Pa·s) when using the models to predict new viscosities, we will use the root mean square error of prediction (RMSEP) that is estimated by the following equation [14], where *n* is the number of samples:

$$RMSEP(Pa \cdot s) = \sqrt{\frac{\sum_{i=1}^{n} (P_\eta - A_\eta)^2}{n}} \tag{8}$$

Besides using RMSEP (Pa s) to give an indication of the majority of the expected errors when using the prediction models again, it will be investigated whether one prediction model should be preferred over the others. Since all the models had a distribution of errors (Equation 7) with zero mean and normally distributed, the comparisons among them will be based in a test of variance ($p < 0.05$) using *F* distribution with $n - 3$ of degrees of freedom due to the trinomial type of models. For this purpose, it was plotted one rheogram for a speed range that includes 10, 15, 20, 25, 30, 35, 40 and 45 rpm (see two rheograms in Figure 3), this was repeated six times for each die diameter (3.5, 4.5 and 5.5 mm) and for each temperature (60, 65, 70, 80 and 90°C). The data came from each sensor (pressure, torque and speed). Therefore a total number of 180 rheograms were built in this research. The *F* distributions were calculated using statistical software (Minitab 14.2 Statistical Software, USA). The results are presented in Figure 6.

3 RESULTS AND DISCUSSION

3.1 EXPERIMENTAL PROCEDURE TO DETECT CHANGES IN THE AMPLITUDE OF PRESSURE, TORQUE AND SPEED

Torque amplitudes are plotted in Figure 7. All plots made for 3.5, 4.5 and 5.5 mm die shows the general trend that lower torque amplitudes appeared when using lower viscosities. Screw speeds do not have any clear effect over torque amplitudes as can be seen in all three plots, however, it seems to be a slight tendency to encounter lower torque amplitudes as the die diameter increases. From the effects on torque amplitude from viscosity and in a smaller degree from die size, it can be concluded that higher torque amplitudes are likely to be present when using higher resistances to flow.

Pressure amplitudes can be found in Figure 7. As happens to torque amplitudes, here lower pressure amplitudes appeared when using lower viscosities, and similarly as in torque, pressure amplitudes do not have a clear relation with screw speeds. Excluding the 106.8 Pa·s (60°C) and 75.9 Pa·s (65°C) pressure curves from the 5.5 mm die plot, one could notice a slight reduction in pressure amplitudes as it increases the die diameter for all viscosities, and this shows a similar trend to the one found for torque amplitudes, but due to these two curves, and the small differences, it cannot be concluded this statement. However, since lower pressures amplitudes are found at lower viscosities, it can be concluded as in torque amplitudes that the smaller the resistance to the flow, the smaller the pressure amplitudes.

3.2 EXPERIMENTAL PROCEDURE TO DETECT VARIATIONS IN PRESSURE, TORQUE AND SPEED OVER TIME

From all plots from torque and pressure in Figure 8, is possible to see frequencies that match the speed of the screw, for example see in all plots how a peak appear at approximately 0.33 Hz with 20 rpm. A screw is a non symmetric shaft as can be seen in Figure 1. On one side, the screw presents four flights while on the other side only three flights and this possibly creates a different pressure gradient along the length of the barrel and thus different backwards flows in the gap

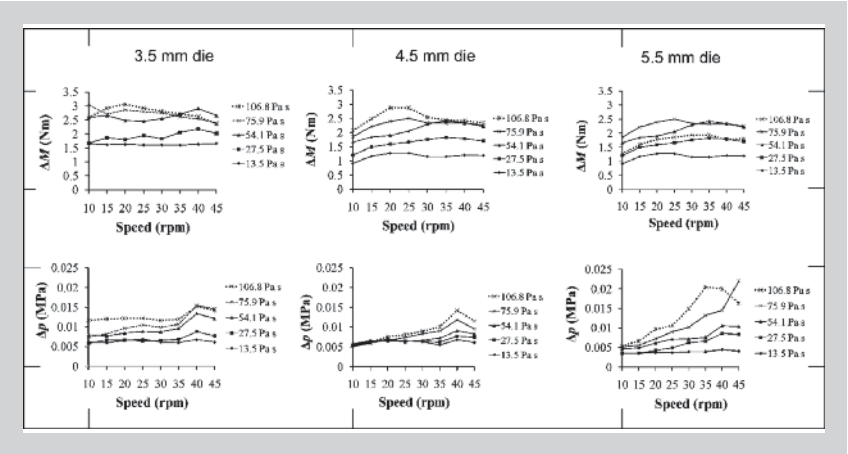

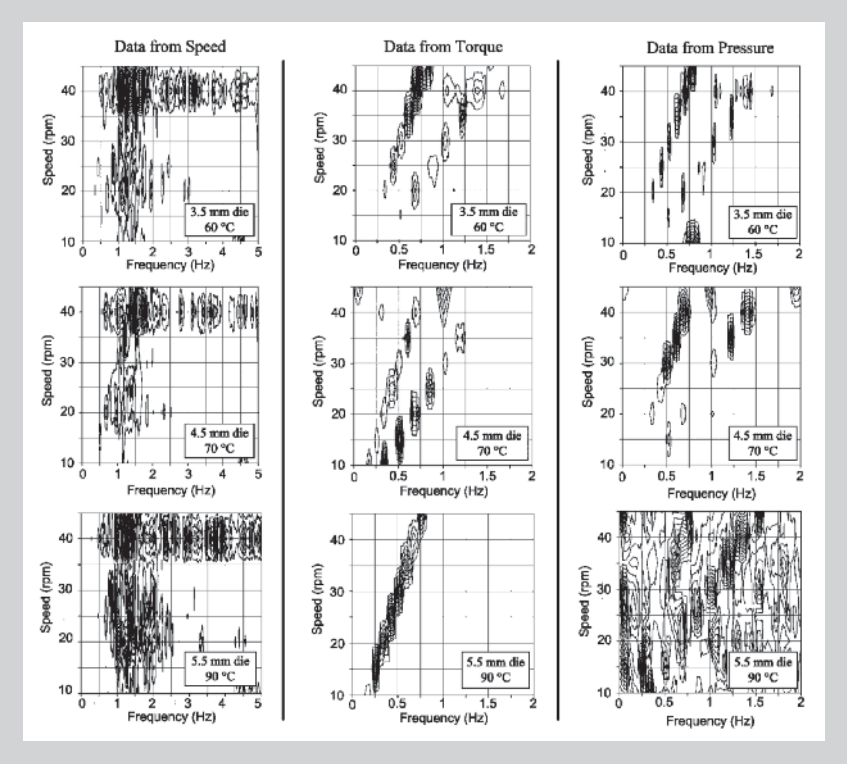

screw flight – barrel. In consequence, pressure and torque vary while the screw rotates. It is also likely that a great influence to this variation comes from the last section of the screw flight which is close to the die where the highest pressure is present. On each revolution, the last section of the screw flight could create pressure waves in the fluid that are recorded in the pressure and torque sensor each time passes nearby. Pressure waves can also lead to intermittent back flows in the clearance between the screw flight and barrel and also oscillating throughputs. A second set of frequencies, that tends to double the first frequency, can also be observed in almost all plots, for example at about 0.66 Hz another peak appears at 20 rpm.

In the present rheometer, the frequencies measured in the speed sensor located in the motor were not clearly coupled with the fluctuations showed by the pressure and torque sen-

Figure 7 (above): Torque and pressure amplitudes. The graphs are aligned and equally scaled.

Figure 8 (below): 2D Spectral density plots for three resistances to flow. Largest resistance to flow (3.5 mm die and 60°C), a medium resistance to flow (4.5 mm die and 70°C), and a lowest resistance to flow (5.5 mm die and 90°C). The plots present the frequencies analyzed for speed, torque and pressure.

sors (see Figure 8). As it can be observed from this figure regarding torque and pressure, in the three different flow resistances, no clear spectral peaks were linked to the spectral peaks of motor speed. However, changes in pressure and torque can produce speed changes in a motor connected directly to a frequency converter, but in the case of the present rheometer, the frequency converter is controlled by a PID which compensate for the pressure and torque fluctuations. Therefore in this research, pressure and torque fluctuations are likely to be caused by the screw geometry and its effect over the fluid, specifically the last flight affecting the regions of higher pressures close to the die.

Another possibility for time variations is the one produced by the contact screw flight-barrel due to the small gap (δ = 0.0001 m), but it is unlikely that this would have been a main cause of fluctuations in pressure and torque, because pressure and torque fluctuate similarly. Furthermore, if friction between the screw flight and barrel is the only cause of time variations, it should not appear a connection between the spectral peaks of pressure and torque as it was obtained in this research. Running on empty, the rheometer presented zero torque.

3.3 EXPERIMENTAL PROCEDURE FOR RHEOLOGICAL MEASUREMENTS

Previously the rheometer was tested in a speed range between 75 to 5 rpm when using a stainless steel die with 5.5 mm of diameter. At this time, the maximum speed was changed because the fluid, Polybuthene-1, increased its temperature owing to the high shear when using the smallest die (d = 3.5 mm), making it difficult to achieve a steady temperature at high viscosities. In this way, reducing the magnitude of shear rate by reducing the maximum speed of the shaft (from 75 to 45 rpm), it was possible to obtain a steady low temperature for all tests. This situation was only observed with the smallest die (d = 3.5 mm). From this experience, it can be concluded that the recommended range of viscosity measurements and shear rates in the rheometer should be in accordance with the size of the die. Previously the limitation in power from the motor was described. The motor capacity is anyway not a critical limiting point in the rheometer because a bigger motor can be installed, but a simpler solution is to increase the die diameter to decrease the power demands.

Detailed results from each rheogram, apart from Figure 3, will not be presented due to the large number of experiments (180). However, averages from the six repetitions using the slopes coming from the linear regressions between rotational speed versus torque, and rotational speed versus absolute pressure plus the averages of the areas below their curves will be presented. The maximum torques and absolute pressures found in the experiments running the rheometer at 45 rpm and using the smallest die of 3.5 mm diameter, were 23.9 Nm and 0.88 MPa abs, respectively. A maximum shear rate will be present at the tip of the screw flight (maximum radius). It is possible, by using the following equation

$$\dot{\gamma}=\frac{2\pi N}{60}\frac{r}{\delta} \tag{9}$$

to estimate that 176.24 s^{-1} is the maximum local shear rate at the tip of the screw when the rheometer is run at 45 rpm (r = 0.0374 m, δ = 0.0001 m) [3].

3.4 DEVELOPMENT OF FOUR DIFFERENT PREDICTION MODELS FOR VISCOSITY

The four different alternatives to predict viscosity based on the same experimental data (180 rheograms) are presented in Figure 4. This figure shows the four different predictors (Slope *a*, *MA*, Slope *b* and *PA*) versus the viscosities of Polybuthene-1 presented as actual viscosity. A trinomial curve was chosen to model the results from all dies (d = 3.5, 4.5 and 5.5 mm) and predictors (Slope *a*, *MA*, Slope *b*, *PA*) because it is a very flexible equation that fitted well to all the behaviors (Equations 10 to 21 in Figure 4). The equations from the models are presented in Table 1, and they only model the data within the range of our experimental viscosities.

When plotting the actual viscosities of N450000 versus the Slopes (*a*, *b*) and the areas below the curves (*MA*, *PA)*, it was found a small difference for the smaller die holes (3.5 and 4.5 mm) and a larger difference between 4.5 and 5.5 mm die. These differences can be caused by leakage flows (backwards flows) that occur in the gap screw flight – barrel (0.5 mm). In single screw

extruders is experienced pure drag flow caused by the conveying effect of the screw when no die or very large dies are used, and on the other extreme a drag flow of the same magnitude to the leakage flow exists when using a blank die. In between these two extremes is situated the process rheometer when using the 3.5, 4.5 and 5.5 mm die. The small differences in pressure and torque between 3.5 and 4.5 mm die are probably caused by excess leakage flow. The 4.5 mm die is 16.7 times smaller than the barrel (75 mm diameter) and possibly large leakage flows occur, decreasing the pressure at the die entry and therefore affecting the torque since torque and pressure were coupled in all experiments. In a hypothetical case of using a blank die, it would not be surprising to find a curve close to the 3.5 mm die. On the other hand, it might be found an even a larger difference to the 5.5 mm die, if a 6.5 mm die had been used because less leakage flow and more drag flow could be present.

3.5 ACCURACY ESTIMATION AND COMPARISON OF MODELS

The viscosities obtained from the prediction models (Equations 10 to 21 in Table 1) are plotted versus the actual viscosities in Figure 4. All models from Equations 10 to 21 to predict viscosity resulted in a relatively good correlation (R^2) considering the wide range of viscosities, speeds and pressures (Table 1). It is possible to observe that when applying a linear fit in the plots between the predicted and the actual viscosities, most of the curves overlap which is a positive sign of the suitability of the different models, see Figure 5. However it was not possible to model the data from the d = 5.5 mm die using both the Equation 12 (slope a) and Equation 18 (slope b), because some part of the curves presents two x-values (actual viscosity) for a given slope (slope a or slope b), see the circles over Equation 12 and Equation 18 in Figure 4.

Previously, in Salas-Bringas et al. [3] an accuracy in the system of ± 25 Pa·s was found based on the maximum errors or residuals, however, this value did not take into account the distribution of errors as indicated earlier. In this research, the root mean square error of prediction will be used to indicate where the most of possible future expected errors will be. Because previous reported errors did not account for the distribution of errors and that this time the speed control of the motor was done by a PID. Figure 6 shows that the expected errors are much smaller than previous reported errors. The maximum RMSEP (11.4 Pa s) was found in the model *PA* for the biggest die (d = 5.5 mm) but it was not significantly different (p < 0.05) to the RMSEP found when modeling the data based on the slope a using both the smaller and medium die size (d = 3.5, 4.5 mm) because the data were very disperse (Figure 6). The large dispersion of data in *PA* is possible linked to the larger pressure variations (Δp) found at the higher viscosities (Figure 7). From Figure 6 is possible to observe that were no significant differences (p<0.05) in errors among the three dies modeled through Slope a, *MA* and Slope a.

The smallest errors (2.2 and 3.7 Pa·s) are expected to be found when using the models based on *PA* for the d = 3.5 and 4.5 mm die (Equations 19 and 20), however this is not the case for d = 5.5 mm die. The best prediction can be obtained using the model PA with a 4.5 mm die, which is significantly different to all others RMSEP (p < 0.05), but the difference in RMSEP between d = 3.5 mm and 4.5 mm die is only 1.5 Pa s, and is because the data were distributed in a narrower range. The two extreme RMSEP (Pa·s) were found using *PA*. These differences were not due to a bigger maximum error, but due to the sum of residuals "$\Sigma(P_\eta - A_\eta)$". The maximum errors found in these experiments were ± 25 Pa·s, the same value as previously reported by Salas-Bringas et al. [3], but most of the errors were distributed far below this value, a reason why all RMSEP (Pa·s) on Figure 6 appear below 12 Pa·s.

The sensors data (e.g. torque) obtained when running the rheometer with N450000 standard using a d = 5.5 mm die reported by Salas-Bringas et al. [3] and the ones obtained in this article for the same die opening, are not comparable since these two dies were made in different materials, resulting in different coefficients of friction (for some authors indicated as different die conductance [15]). In addition, the filling degree with N450000 was not measured in the previous work. It was only estimated and thus it is possible that the filling degree was lower than the one used in this newer research. Future use of the rheometer must always ensure the same level of the fluid to establish experimental comparisons.

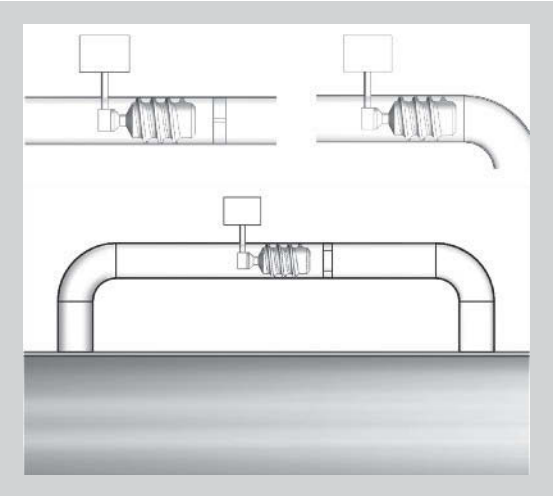

Figure 9:
Possible installation for a screw type process rheometer to measure fluids from a product stream.

The differences in torque and pressure among repeated tests leading to the described errors, may partly be due to small temperature differences between the repetitions since the viscosity of Polybuthene-1 is very sensitive to temperature. In the lower temperature range of our experiments, changes in a fraction of a degree Celsius, can lead to changes in several viscosity units (Pa·s). Previously, it was commented that slow temperature fluctuations were not displayed in the spectral plots because they focused on higher frequencies. Schüller and Salas-Bringas [16] found even larger errors to the ones seen in this research when using a Physica UDS200 rheometer with the same fluid, Polybuthene-1, during rapid transient tests using plate-plate measuring system. This is caused by a temperature gradient in the fluid when is only heated by a Peltier plate at the bottom.

4 PRACTICAL APPLICATIONS

Example of possible process installations of the screw type process rheometer are shown in Figure 9. On the top left side of Figure 9, it is shown how the rheometer could be positioned in a straight pipe having a restriction. This set up can be a good solution when measuring low viscosity fluids. On the top right side of Figure 9 the screw is positioned before a bend, this figure does not include a restriction to show that any natural pressure loss might be enough to generate a sufficient pressure or torque reading. At the bottom of Figure 9 it is represented a bypass that can be used to extract part of the fluid from the main process stream. In this last alternative, a smaller restriction is drawn to shown how the set up can vary according to the specific requirements. For a practical use of the rheometer by a control unit (e.g. PLC, PID, etc), viscosity (Pa·s) or consistency (%) units are not important, but an electrical signal that can indicate the extent of torque or pressure, in this way the process will be regulated by the control unit to keep the electrical signal from the rheometer constant. However viscosity and consistency values are important to certify quality or traceability.

For cases requiring viscosity measurements using Non-Newtonian fluids, an average or apparent viscosity can be used since different strain rates are present in the screw, as it is similarly obtained today from mixer, parallel plate and bob type of rheometers. An average viscosity or sometimes presented as equivalent Newtonian viscosity [17] can be obtained by following any of the calibration procedures described in this research. In some fluids, elongational flow might be present at the die. To eliminate this type of flow, it is been shown on literature that the entry angle of a die can be manipulated to produce pure shear flow [18]. It is possible to encounter offsets for viscosity using these calibration methods based on N450000 standard for fluids having yield stress. For example, the velocity profile in capillary flow (die region) between a fluid with and without yield stress are different [19], and therefore different shear stresses (linked to torque and pressure) are present. Also it has been reported for Couette flow that a Newtonian assumption for the wall shear rate can lead to errors, especially when increasing the gap size and yield stress [20, 21]. Traditionally the complex flows occurring between a rotating screw and a stationary barrel has been approximated to Couette flow [6]. However, for process control applications where a steady consistency of the fluid is the goal, this should not present any obstacle. Yield stress can be estimated by performing a stress relaxation test by stopping the process rheometer after running at constant speed. The residual pressure difference between the inlet and exit of the restriction must be registered. For circular channels the following equation can be used: $\tau_o = \Delta P_{Min} R/(2L)$, where τ_o is the yield stress, ΔP_{Min} residual pressure, R channel radius and L channel length [22, 23].

5 CONCLUSIONS

Time variations in pressure and torque seem to be mainly caused by time dependent flows produced by the non-symmetric geometry of the screw. These variations can become more notorious (e.g. increased amplitude of torque and pressure oscillations) at higher resistances to flow produced by either an increased viscosity or

to a lesser extent by reductions in die diameter. The most notorious fluctuations occur at a half, and on each shaft revolution. The influence of different running speeds does not seem to affect the variations in amplitudes of torque and pressure. The range of viscosities that can be predicted in this rheometer can be widened by changing and selecting different die sizes. It is possible to predict viscosity using different dies by using prediction models based on calibration experiments. The RMSEP (± Pa·s) based on the prediction models using Slope *a*, *MA* and Slope *b* were not significantly different ($p < 0.05$). By using Slope *a* and Slope *b*, it was not possible to successfully model the data at low die restrictions (5.5 mm). The models based on *PA* gives the significantly ($p < 0.05$) smallest RMSEP (± Pa·s), except for the model using the lowest die restriction (5.5 mm), which was not significantly different to the Slope *a*. Because of the complex flows and the different shear rates present in the rheometer, it is not possible to compute a unique shear viscosity when Non-Newtonian fluids are used. However, is possible to obtain an average or representative viscosity using the prediction models presented in this research. Keeping the same degree of filling will be mandatory to use the same prediction models in the future.

REFERENCES

[1] Brodgesell A, Lipták BG: Consistency Analyzers, In Process Measurements and Analysis, CRC Press, Boca Raton (2003).

[2] KIM CH, Lipták BG, Jamison JE: Viscometers-Industrial, In Process Measurements and Analysis, CRC Press, Boca Raton (2003).

[3] Salas-Bringas C, Jeksrud WK, Schuller RB: A New on-Line Process Rheometer for Highly Viscous Food and Animal Feed Materials, J. Food Eng. 79 (2007) 383-391.

[4] Roos H, Bolmstedt U, Axelsson A: Evaluation of New Methods and Measuring Systems for Characterization of Flow Behavior of Complex Foods, Appl. Rheol. 16 (2006) 19-25.

[5] Levine L, Miller C: Extrusion Process, In Handbook of Food Engineering, CRC Press, Boca Raton (2007).

[6] Rauwendaal C: Polymer Extrusion, Hanser Gardner Publications, Germany (2001).

[7] Dunn WC: Fundamentals of Industrial Instrumentation and Process Control, McGraw-Hill (2005).

[8] Salas-Bringas C, Jeksrud WK, Lekang O-I, Schüller RB: A Calibration Method for a New Type of Rheometer, Annu. Trans. of the Nord. Rheol. Soc. 14 (2006) 197-201.

[9] Canon Instrument Co. Material Safety Data Sheet (Msds Ref Ciio9-012) http://www.canoninstrument.com/MSDS.htm.

[10] Montgomery DC, Runger GC: Applied Statistics and Probability for Engineers, John Wiley & Sons, (2003).

[11] Mastropierro J. Personal Communication, Quality Assurance and Viscosity Standards Cannon Instrument Company (2009).

[12] Moran K, Yeung A, Masliyah J: Shape and Relaxation of an Elongated Viscous Drop, J. Colloid Interface Sci. 267 (2003) 438-493.

[13] Heldman DR, Lund DB: Handbook of Food Engineering, CRC Press/Taylor & Francis, Boca Raton (2007).

[14] Esbensen KH, Guyot D, Westad F, Houmøller LP: Multivariate Data Analysis in Practice, Camo, Oslo (2001).

[15] Forte D, Young G: Causes and Effects of Extruder Instabilities, In Food and Feed Extrusion Technology, Foostream Pty Ltd, Dennis Forte & Associates Pty Ltd and Shanaglen Technology Pty Ltd, Cleveland (2007).

[16] Schüller RB, Salas-Bringas C: Fluid Temperature Control in Rotational Rheometers with Plate-Plate Measuring Systems, Annu. Trans. of the Nord. Rheol. Soc. 15 (2007) 159-163.

[17] Barnes HA: On-Line or Process Viscometry - a Review, Appl. Rheol. 9 (1999) 102-107.

[18] Mitsoulis E, Hatzikiriakos SG: Bagley Correction: The Effect of Contraction Angle and Its Prediction, Rheol. Acta 42 (2003) 309-320.

[19] Chhabra RP, Richardson JF: Non-Newtonian Flow in the Process Industries, Butterworth-Heinemann, Oxford (1999).

[20] Kelessidis VC, Maglione R: Shear Rate Corrections for Herschel-Bulkley Fluids in Couette Geometry, Appl. Rheol. 18 (2008) 34482.

[21] Chatzimina M, Georgiou G, Alexandrou A: Wall Shear Rates in Circular Couette Flow or a Herschel-Bulkley Fluid, Appl. Rheol. 19 (2009) 34288.

[22] Salas-Bringas C, Lekang O-I, Rukke EO, Schüller RB: Development of a New Capillary Rheometer That Uses Direct Pressure Measurements in the Capillary, Annu. Trans. of the Nord. Rheol. Soc. 17 (2009) 39-47.

[23] Steffe JF: Rheological Methods in Food Process Engineering, Freeman Press, East Lansing (1996).

PAPER III

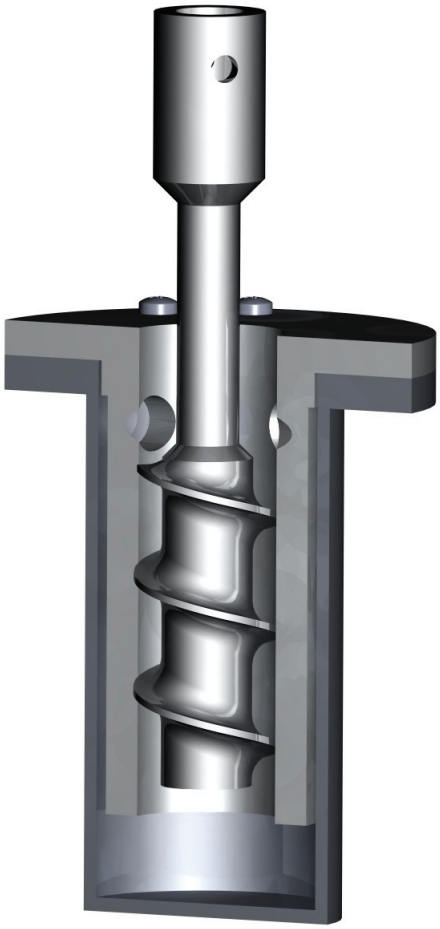

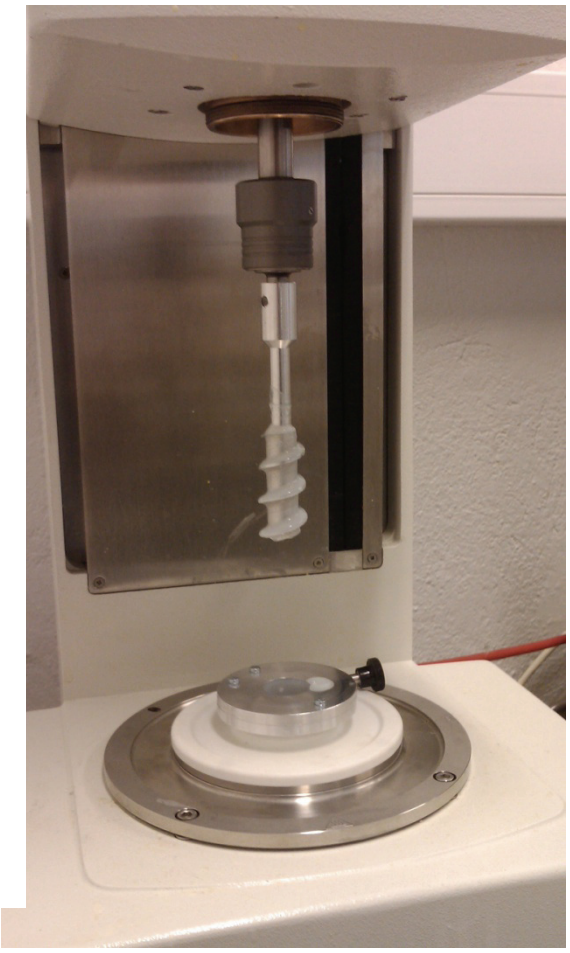

Analysis of a Screw Type Process Rheometer to determine Viscoelastic and Flow Properties of Non-Newtonian Fluids

C. Salas-Bringas[a*], O.-I. Lekang[a] and R.B. Schüller[b]

[a]*Department of Mathematical Sciences and Technology, Norwegian University of Life Sciences, P.O. Box 5003, N-1432 Ås, Norway*

[b]*Department of Chemistry, Biotechnology and Food Science, Norwegian University of Life Sciences, P.O. Box 5003, N-1432 Ås, Norway*

+47 64965474

+47 64965401

www.umb.no

Abstract

The present article shows how a coaxial cylindrical analogue performs to represent a screw concentrically assembled in a stationary cup having a recirculation channel to determine the storage, loss modulus and flow curves of non-Newtonian fluids. The screw-recirculation cup is connected to a Paar Physica UDS 200 rheometer and its results are compared with cone-plate, plate-plate, bob-cup and a standard Paar Physica stirrer that is used on sedimenting fluids. The results indicate that is possible to determine the storage, loss modulus and the flow curves of non-Newtonian fluids, both time independent and time dependent fluids. The flow curves from the screw-recirculation cup are closer to the flow curves from cone-plate and bob-cup than the ones from a Paar Physica stirrer. Storage and loss modulus given by the screw-recirculation cup are of relatively similar magnitude to the ones obtained from plate-plate and bob-cup systems.

Zusammenfassung

In dem vorliegendem Artikel untersuchen wir ein Modell eines Schneckenrheometers zur Bestimmung des Speicher- und Verlustmoduls sowie der Strömungskurven von nicht-newtonschen Flüssigkeiten. Das untersuchte System besteht aus einer Schnecke, die konzentrisch in einem stationärem Zylinder mit Rezirkulationskanal rotiert. Eine Nachbildung eines solchen Prozess-Schneckenrheometers wird mit einem Paar-Physica UDS 200 Rheometer verbunden. Die Ergebnisse werden mit denen eines Kegel-Platte-, Platte-Platte- und koaxialen Zylinder-Messsystems sowie eines Standard Paar-Physica-Rührers verglichen, welcher für sedimentierende Flüssigkeiten verwendet wird. Die Studie zeigt, dass mit Hilfe des untersuchten Modells Speicher- und Verlustmodul sowie Strömungskurven von nicht-newtonschen zeitunabhängigen und zeitabhängigen Flüssigkeiten bestimmt werden können. Die Strömungskurven des Prozess-Schneckenrheometers liegen näher an denen des Kegel-Platten- und koaxialen Zylinder-Messsystems als an denen des Systems mit Standard Paar-Physica-Rührer. Speicher- und Verlustmodul des Schnecken-Rezirkulationszylinders sind von ähnlicher Grössenordnung wie beim Platte-Platte- und koaxialen Zylinder-Messsystem.

Keywords: Rheometer · Viscometer · Process · Viscosity · Viscoelasticity · Measurement method

[*] Corresponding author. Tel.: +47 64965474; fax: +47 64965401. *E-mail address:* carlos.salas.bringas@umb.no (C. Salas-Bringas).

1 INTRODUCTION

There is a wide agreement about the need in the industry for process rheometers and viscometers that can be used to control the process and fluid composition [1-14]. Problems in on-line rheometry can occur when measuring suspensions, especially if the suspensions contain settling particles. In most cases the common viscometric methods are unsuitable because of effects like phase separations caused by gravity and centrifugal forces, effect of wall slip, blocking of the measuring gap by particle aggregates, etc [7]. These problems can be avoided using the Metzner-Otto approach [7, 15] that considers the utilization of an impeller with different shape, e.g. paddle, anchor, turbines, etc. The measurement uses the torque on the shaft of the impeller as a function of its rotational speed. Helical screw type rheometers have been grouped as impeller type [7].

Salas-Bringas et al [11-13] have presented a screw type process rheometer that consists of a screw concentrically assembled inside a cylinder, Searle type, having a downstream restriction. The system can measure an average viscosity using the slope formed between the rotational speed of the screw (related to the shear rate) and the torque (related to the shear stress) [11-13], the method is further referred to as slope method. Because of the relatively low cost bearing system of the prototype used previously [11-13] compared to an air or magnetic bearing, the flow curve rotational speed versus torque did not converge to the origin using a Newtonian fluid, this led to the development of a second method that uses the area bellow the flow curve between torque and speed [13]. However, the second method only allows relative comparisons of resistance to flow for non-Newtonian fluids. Because of this limitation, a third method was developed in the same study which uses the downstream pressure to replace torque following the same slope procedure. The use of downstream pressure to represent the overall shear stress in the system resulted in the best method to deal with bearing friction.

As an alternative to the use of pressure transducers, the pressure at the downstream side of the screw can hypothetically be obtained dividing the normal force of the screw shaft with the cross-sectional area of the screw [16], which is one of the issues investigated in the present article. By confirming the proportionality of the normal force with shear stress, it is possible to expand the flexibility of the screw type process rheometer to perform shear stress measurements using the normal force along the screw shaft.

The slope method [11-13] is simple and suitable to indicate in real time changes of viscosity during a manufacturing process. However, this method does not convert torque or downstream pressure into a mean shear stress or the rotational speed into an average shear rate, because it only uses directly the slope between torque or downstream pressure over the rotational speed to calculate viscosity. As a consequence a method that can be used to convert torque or downstream pressure into shear stress units and the rotational speed into shear rate units is sought.

Kemblowski et al [7] using a helical screw impeller concentrically assembled into a draught tube which is also assembled into a tank, developed an analytical method based on a coaxial cylindrical analogue that would not require a calibration procedure to determine the flow curve of fluids. There is a great advantage using analytical methods to determine directly shear stress and shear rate, but this analytical method cannot be used with the screw type process rheometer used by Salas-Bringas et al [11-13] because is based on a different working principle. The method used by Kemblowski et al [7] does not have a restriction at the downstream side of the screw and consequently it does not produce a considerable pressure gradient. It has been documented that when using the screw type process rheometer with different downstream restrictions, the screw produces different pressure gradients that lead to different torques for the same speed and fluid viscosity [13]. As a consequence a method that can find the dimensions of a coaxial cylindrical analogue for a given restriction is also sought.

The present article explores the use of an experimental method to estimate the dimensions of an analogue coaxial cylinder, Searle type to represent the complex geometry of the screw having a restriction at the downstream side of the screw. The aim is to determine an average shear stress and a mean shear rate directly from torque and speed. The geometry of a screw inside a barrel is quite similar to the coaxial cylinder set-up in rheometers. The difference is the presence of the helical flight wrapped around the core of the cylinder [16]. Because of the helical flights a Couette flow is expected with “leakage flows” or back flows in the gap screw flight-cup as shown by Salas-Bringas et al [12], together with a longitudinal component of flow that gives the

conveying effect. At high rotational speeds other secondary flows can also appear as the one indicated inside the screw channel in Figure 1 which has been described for single screw extruders by Rauwendaal [16]. Non-Newtonian fluids will present different viscosities at the different sections of the screw depending of the level of shear rate. It is for this reason that this study compares the flow curves of non-Newtonian fluids from the screw type process rheometer using the coaxial cylindrical analogue, with the flow curves given by other standard rotational methods.

Despite of the large number of methods and probes to determine the flow characteristics of a fluid, there are few methods to determine the viscoelasticity of fluids. Viscoelastic measurements are generally done through oscillatory tests, and the success of this technique can be regarded as the method is relatively simple and suitable for a wide range of fluids. This success is obtained despite of today's expensive costs of low friction bearings and the need for an accurate driven control of the probe. Other methods have not been as widespread as the oscillatory ones. Within these "alternative methods", viscoelasticity data can be obtained using high frequency techniques that usually involves wave propagation, generally producing small strains [3]. The storage modulus (G') in plane-harmonic shear-wave propagation in a linear medium is a function of the density, the shear wave length, the exponential damping velocity and the shear wave phase velocity [3]. These measurements require more complex and limited calibrations that an oscillatory measurement could demand.

The present article describes and analyses a method that enables the determination of an average shear stress and a mean shear rate in a screw type process rheometer using a coaxial cylindrical analogue. The working principle of a screw type process rheometer is this time tested with a more precise driven system compared to the one used by Salas-Bringas et al [11-13], because it is assembled in a Paar Physica UDS 200 rheometer which allows measurement of fluids at considerable much smaller ranges of torque (± 0.002 mNm) and speeds. Also mounting a replicate of the screw type process rheometer in the Paar Physica UDS 200 Rheometer (referred as screw-recirculation cup) could bring an insight of how the screw type process rheometer could carry viscoelastic measurements during an industrial process. Satisfactory viscoelastic measurements could bring the screw type process rheometer to the next level of instruments capable of performing viscoelastic measurements during process (storage and loss modulus). Consequently, the results from the working principle of a screw type process rheometer replicated in the UDS 200 rheometer are compared with standard measuring systems like cone-plate, plate-plate, bob-cup and a standard impeller to determine the flow curves of non-Newtonian fluids, both time independent and time dependent, as well as a comparison of the storage (G') and loss (G'') modulus with results from bob-cup and plate-plate systems. For the viscoelastic measurements is used a time independent viscoelastic fluid (with G'' > G'), a time dependent viscoelastic fluid (G' > G'') and a time dependent viscoelastic fluid having a phase change during the range of measurements.

Consequently the studies conducted by Salas-Bringas et al [11-13] and the study presented here can be used as the preliminary background to construct an on-line screw type process rheometer.

2 MATERIALS AND METHODS

2.1 DESIGN FEATURES AND START UP

To help understand the replicate of the screw type process rheometer mounted in a Paar Physica UDS 200 rheometer, a description is given in reference to Figure 1. The blue arrows show the flow direction when the screw provides a conveying effect. Fluid is filled into the cup until it reaches the level indicated in the drawing. *N* represents the rotational speed. All dimensions are in millimeter.

The screw-recirculation cup is assembled in a Paar Physica UDS 200 rheometer. This measuring system is built in aluminum to provide a good transfer of heat from the Peltier which is in direct contact with the bottom surface of the cup, in a similar manner as the Paar Physica UDS 200 rheometer does with the other cup systems. Aluminum also provides a good resistance to corrosion, and it is a low density material that can contribute to a

low moment of inertia. At the top of the screw shaft, a standard Paar Physica (# 300442) coupling is added to connect the screw to the rheometer (not shown in Figure 1).

Before starting the measurements the UDS 200 rheometer was programmed to calculate the moment of inertia of the screw shaft to be able to compensate for it during the measurements, especially important is this process for the oscillatory tests. The moment of inertia of the screw is compared with the moment of inertia of the other probes used in this research. The experimental inputs to measure the moment of inertia were a frequency of 10 Hz with a deflection angle of 10 mrad using 300 values to estimate a mean moment of inertia. The same procedure was used for all the probes.

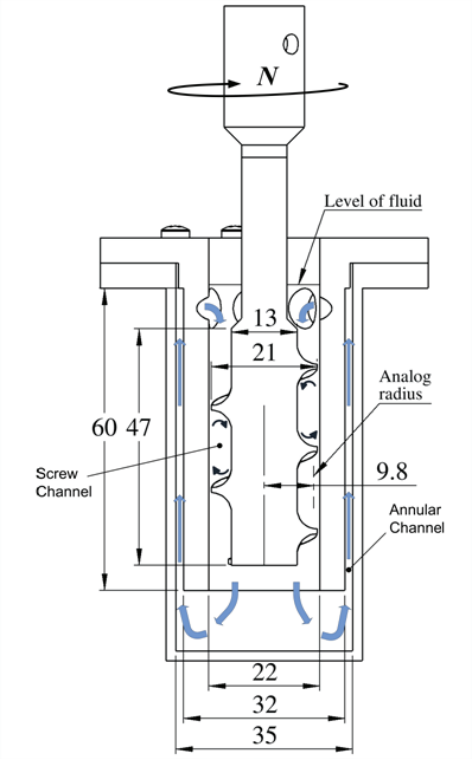

Figure 1: Cross-section of the screw-recirculation cup assembled in a Paar Physica UDS 200 rheometer. The direction of flow is shown by the blue arrows. The arrows inside the screw channel show the secondary flow that can occur at high rotational speeds in single screw extruders [16]. All dimensions are in millimeters.

2.2 ANALYTICAL DETERMINATION OF AN AVERAGE SHEAR STRESS AND A MEAN SHEAR RATE THROUGH AN ANALOGUE CYLINDER WHEN USING THE SCREW-RECIRCULATION CUP

The rheological measurements of non-Newtonian fluids can be made by calibrating the rheometer using a procedure which is analogous to Couette flow formed between two cylindrical surfaces, Searle type.

The average shear stress (σ) acting on the fluid can be obtained from the torque (M) that is neccesary to rotate the screw, or for this case from M (Nm) acting on the analogue cylinder divided with the surface of the inner cylinder as follows:

$$\sigma = \frac{M}{2\pi r^2 h} \tag{1}$$

where r (m) is the radius of the analogue cylinder and h (m) its height.

Using an analogue cylinder, the fluid is contained in the annular space, with one of the boundaries formed by the inner rotating cylinder and the other boundary formed by the static outer cylinder. Since the inner boundary is moving with respect to the outer boundary, a drag flow will be set up in the fluid and the fluid will be sheared. For concentric cylinders with constant radius and gap size, the shear rate in the fluid can be obtained using Eq. (2) through the Newtonian approximation that is frequently used by commercial rheometers [14] :

$$\dot{\gamma} = \frac{2\pi r N}{60\delta} \tag{2}$$

where $\dot{\gamma}$ (s^{-1}) is the rate of shear, N (rpm) the rotational speed and δ (m) the gap between the two concentric cylinders.

For Newtonian fluids it is known that the viscosity (η) is defined by the ratio between σ and $\dot{\gamma}$. In this way using equation (1) and (2), the following equation is obtained,

$$\eta = \frac{M}{2\pi r^2 h} \Big/ \frac{2\pi r N}{60\delta} \tag{3}$$

Eq. (3) finally leads to Eq. (4) as follows,

$$\eta = \frac{15\,\delta}{\pi^2 r^3 h} \cdot \frac{M}{N} \tag{4}$$

Where M/N is the Slope a (Nm/rpm) formed between M (Nm) and N (rpm). The Slope a (Nm/rpm) can be experimentally obtained using a Newtonian fluid with known viscosity while measuring M (Nm) and N (rpm). By obtaining the Slope a (Nm/rpm), it is possible to estimate the radius r (m) of the analogue cylinder and the gap δ (m) formed between the concentric cylinders.

The Paar Physica UDS 200 rheometer as well as other rheometers like the Paar Physica MCR 301 rheometer uses two constants, k_1 and k_2, one of them multiply directly M (Nm) to convert it into a shear stress σ_M (Pa) as follows:

$$\sigma_M = k_1 M \tag{5}$$

The other constant, k_2, multiply N (rpm) to convert it into a shear rate $\dot{\gamma}$ (s^{-1}) as indicated:

$$\dot{\gamma} = k_2 N \tag{6}$$

To find k_1 and k_2 in the screw-recirculation system, the analogy of a concentric cylinder is used as indicated by Eq. (7) and Eq. (8):

$$k_1 = \frac{1}{2\pi r^2 h} \tag{7}$$

$$k_2 = \frac{2\pi r}{60\delta} \tag{8}$$

As it can be noticed, Eq. (7) comes from Eq.(1), particularly from the geometry of the analogue cylinder. In a similar manner k_2 is obtained from Eq. (2). k_1 is in m^{-3} and k_2 dimensionless.

k_1 and k_2 are added into the Paar Physica UDS 200 rheometer software UDS200/32 V2.5 (PHYSICA Messtechnik GmbH, Ostfildern, Germany). Once this is done, the screw-recirculation cup can be used as any other measurement system without the need for extra calculation outside the Paar Physica software to obtain σ_M, $\dot{\gamma}$ and viscoelastic variables like the storage modulus (G') and the loss modulus (G'').

2.3 EXPERIMENTAL DETERMINATION OF AN AVERAGE SHEAR STRESS AND A MEAN SHEAR RATE THROUGH AN ANALOGUE CYLINDER WHEN USING THE SCREW-RECIRCULATION CUP

As it was commented earlier, Eq. (4) is used to determine the radius r (m) of an analogue cylinder representing an average shear rate in the screw. To estimate r (m) from Eq. (4) it is necessary to know h (m), δ (m) and the slope a (Nm/rpm). For this reason the Newtonian standard Brookfield 12 500 cP (Brookfield Engineering Laboratories, Inc.), its certified viscosity is 12 500 cP at 25 °C was used. The different η (Pa s) of the standard at different temperatures were measured through a cone-plate (50 mm diameter, 1°, 50 μm gap) in a Paar Physica UDS 200 rheometer, further referred to as MK22. The temperature change was done using a linear increase from 10 to 90 °C in two hours.

Once η (Pa s) was known at different temperatures, similar tests were conducted in the screw-recirculation cup by doing a temperature change in steps of 10 °C and using the same standard fluid. A resting time of 40 minutes between each temperature step was used to ensure an even temperature distribution. Each flow test lasted three minutes rotating the screw from 0 to 60 rpm in a linear increase. These tests resulted in a series of flow curves of N (rpm) versus M (Nm) with the outcome of estimating the different Slope a ($\equiv M/N$) for different η (Pa s). Thereafter the following equation that comes from Eq. (4) was used to obtain r (m):

$$r^3 = \frac{15(r_{cup} - r)}{\pi^2 \eta h} \cdot Slope\, a \tag{9}$$

where in reference to Figure 1, r_{cup} (m) is the internal radius of the cup (0.022 m) and h (m) the height of the shaft section having helical flights (0.047 m).

Eq. (9) is an ill-posed equation when trying to estimate r (m), therefore it is necessary to obtain r (m) through iterations. Testing the fluid at different temperatures, different Slope a (Nm/rpm) and η (Pa s) values are obtained, as a consequence relatively different r (m) are also obtained. The function "Goal seek" in Microsoft Excel 2007 was used to perform the iterations to find the different r (m) at different temperatures. An average r (m) was finally estimated together with its standard deviation.

To assess the accuracy of the predicted viscosity (P_η) of the Newtonian standard using the coaxial cylindrical analog, P_η was compared with the viscosity measured in MK22 that was considered as the actual viscosity (A_η) following Eq. (10).

$$E(Pa\,s) = P_\eta - A_\eta \tag{10}$$

where E (Pa s) are the errors of residuals.

2.4 ANALYTICAL DETERMINATION OF AN AVERAGE SHEAR STRESS THROUGH THE NORMAL FORCE IN THE SCREW SHAFT WHEN USING THE SCREW-RECIRCULATION CUP

It is hypothesized that the shear stress σ (Pa) acting on the fluid can also be obtained from the normal force (N_F) along the screw shaft, hence it is hypothesized the following equation:

$$\sigma_M = \sigma_{NF} \tag{11}$$

where σ_{NF} (Pa) is the shear stress calculated from N_F (N). σ_{NF} (Pa) can be obtained using Eq. (12) and Eq. (13). The constant K_{NF} (m^{-2}) is used to convert N_F (N) to σ_{NF} (Pa) as follows:

$$K_{NF} = \frac{\sigma_M}{N_F} \tag{12}$$

$$\sigma_{NF} = K_{NF} N_F \tag{13}$$

2.5 EXPERIMENTAL DETERMINATION OF AN AVERAGE SHEAR STRESS USING THE NORMAL FORCE GENERATED IN THE SCREW SHAFT

The same experimental data used to determine r (m) through the Newtonian standard was used to estimate σ_{NF} (Pa) through Eq. (11), Eq. (12) and Eq. (13). A plot was made to show the linear relationships between N_F (N) and N (rpm) at different viscosities that were expected for a Newtonian fluid.

In a similar manner as the accuracy assessment for the determination of σ_M (Pa), the accuracy assessment of the determination of σ_{NF} (Pa) was done comparing in a plot the new P_η (Pa s) calculated from σ_{NF} (Pa) with the A_η (Pa s) previously measured in MK22.

Eq. (10) was used to estimate the prediction errors or residuals, E (Pa s), where P_η (Pa s) came from σ_{NF} (Pa) using Eq. (11), Eq. (12) and Eq. (13).

Two plots are used to compare the residuals obtained through σ_M and σ_{NF}, one of them plot A_η (Pa s) versus P_η (Pa s) and it is presented in section 3.4. The other plot compares A_η (Pa s) with E (Pa s) in the same section.

2.6 COMPARISON OF FLOW CURVES BETWEEN THE SCREW-RECIRCULATION CUP USING THE CYLINDRICAL ANALOGUE AND STANDARD MEASURING SYSTEMS WITH NON-NEWTONIAN FLUIDS

To compare how the screw-recirculation cup performs to determine the flow behavior of non-Newtonian fluids, tests were made using different standard measuring systems like MK22, a Paar Physica bob-cup CC27-SN20666 (further referred as CC27) and a Paar Physica stirrer ST24-2D/2V/2V-30-SN18211 (further referred to as ST24). CC27 and ST24 were driven by a Paar Physica MCR 301 rheometer. ST24 is a stirrer that is designed to measure rheological properties of sedimenting fluids.

The chosen non-Newtonian fluids were the silicone oil HT Brookfield 100 000 cP which presented a weak pseudoplastic behavior (later discussed in section 3.5) when measured through MK22, Screw-recirculation cup and ST24, this fluid was chosen because it is a time independent fluid having non-Newtonian characteristics.

The other non-Newtonian fluid was the toothpaste Colgate “MaxWhite” (Colgate-Palmolive Co.) This fluid has particles in suspension. According to the producer [17], these particles are meant to stay intact in the toothpaste, but to dissolve instantly as the teeth are brushed. Consequently this toothpaste was chosen to see how the screw-recirculation cup performs when measuring time dependent fluids.

The flow properties of both non-Newtonian fluids were tested at different temperatures. HT Brookfield 100 000 cP was measured at 10, 20, 30, 40, 50, 60 and 80 °C. Colgate "MaxWhite" toothpaste was measured at 10, 20 and 60 °C. The flow curve of HT Brookfield 100 000 cP is not presented at 70 °C because the viscosity range from 60 - 80° C is very small and when plotted disturb the visualization of the flow curves obtained for the different methods. A similar case happened to the viscosity of the toothpaste and only the tests at 10, 20 and 60 ° C are presented.

The flow curves were made using the screw-recirculation cup filled with HT Brookfield 100 000 cP and compared with the flow curves from MK22 and ST24. The other flow curves were made filling the screw-recirculation cup with Colgate MaxWhite toothpaste and compared with CC27 and ST24.

Since this toothpaste is a time dependent fluid, the same experimental set-up was conducted for all experiments. The increase in $\dot{\gamma}$ was set from 0 to 30 s^{-1} in 1.67 minutes for the three measuring systems (screw-recirculation cup, CC27 and ST24). A "resting time" of 100 minutes between each test at different temperatures was used to allow an even temperature in the sample and also to allow any slow recovery in viscosity after shearing.

2.7 COMPARISON OF THE AVERAGE SHEAR STRESSES OBTAINED IN THE SCREW-RECIRCULATION CUP USING TORQUE AND THE NORMAL FORCE IN THE SCREW SHAFT

The comparison of σ_M (Pa) and σ_{NF} (Pa) was performed by plotting the results from the same experiments. The first experiment is the one used to compare flow curves of HT Brookfield 100 000 cP at different temperatures (described in section 2.6). The other experiment is the one made to compare the flow curves of the toothpaste "Colgate MaxWhite" at different temperatures that is also described in section 2.6.

The comparison was made in a plot of σ_M (Pa) versus σ_{NF} (Pa) in section 3.6.

2.8 COMPARISONS OF VISCOELASTIC DATA BETWEEN THE SCREW-RECIRCULATION CUP AND STANDARD MEASURING SYSTEMS

To estimate the storage (G') and loss modulus (G'') using the screw-recirculation cup, the constants k_1 (m^{-3}) from Eq. (7) and k_2 from Eq. (8) were added into the Paar Physica UDS 200 rheometer software UDS200/32 V2.5 .

To estimate how the screw-recirculation cup performs to measure G' and G'' from viscoelastic fluids, four different fluids were chosen, two of them were created by mixing the weak pseudoplastic and time independent silicone oil HT Brookfield 100 000 cP with two different concentration of Avicel HFE-102 - Microcrystalline cellulose (a carbohydrate formed by MCC, cellulose gel; Mannitol: D-Mannitol, Manna sugar, 1,2,3,4,5,6-Hexanehexol). Avicel HFE-102 is sold as a pharmaceutical excipient (FMC BioPolymer, Brussels, Belgium) with the form of a white free-flowing, odorless powder.

The other two viscoelastic fluids were the toothpaste Colgate "MaxWhite" and a Norwegian cooking chocolate, sold as Kokesjokolade 100 g, Landlord (labeled ingredients are: sugar, cocoa butter, milk powder, cocoa mass, whey powder, emulsifiers, E 322 (soya lecithin) and E 476).

One of the mixtures of HT Brookfield 100 000 cP with Avicel HFE-102 was created with a concentration of 85% w/w of HT Brookfield 100 000 cP and 15% w/w of Avicel HFE-102 (further referred as mix 85/15). The other mixture had 90% w/w of HT Brookfield 100 000 cP and 10% w/w of Avicel HFE-102 (further referred as mix 90/10).

The viscoelastic measurements of the mix 85/15 and 90/10 were performed using a temperature scan from 20 to 60 °C that lasted three hours using a constant oscillation of 3 Hz at 3% strain. This setting was used to measure G' and G'' in the screw-recirculation cup, in a Paar Physica bob-cup system (Z4) driven by the UDS 200 rheometer and in a plate-plate of 50 mm diameter driven by the Paar Physica MCR 301 rheometer (further referred as PP50).

The viscoelastic measurements of the toothpaste Colgate "MaxWhite" were performed in the screw-recirculation cup and in PP50 using both a 10 Hz oscillation at 0.1 % strain during a three hours temperature scan from 10 to 60 °C. A relatively small deformation was chosen to preserve as much as possible of the internal structure of the fluid throughout the tests.

The viscoelastic measurements of the Norwegian cooking chocolate were done using an oscillation at 10 Hz with a deformation of 3% strain during a temperature scan from 60 to 15 °C in 3.5 hrs. The same setting was used by the screw-recirculation cup and by CC27 to account in a similar manner the time dependent effects. A relatively large strain and rapid oscillation is chosen to observe how the screw-recirculation cup performs in conditions that can produce slip in other standard probes, especially when the chocolate solidifies.

Blocks of chocolate were gently melted at 35 °C in the same screw-recirculation cup and in the cup used by the CC27 measuring system.

3 RESULTS AND DISCUSSIONS

3.1 MOMENT OF INERTIA OF THE SCREW SHAFT COMPARED TO THE OTHER PROBES USED IN THE EXPERIMENTS

The moment of inertia of the different probes is presented in Table 1. As can be observed from this table, the moment of inertia of the screw is low compared to the other probes used in the experiments. The reason for the low moment of inertia is because the screw was made in aluminum and its diameter in relatively low.

Table 1: Moment of inertia of the different probes used in the experiments

Probe	Type	Driven by rheometer	Moment of inertia (mNm s^2)	Weight (g)
ST24	Stirrer	Paar Physica MCR 301	0.00041	31.4
Screw	Screw	Paar Physica UDS 200	0.00249	80.3
Z4	Bob	Paar Physica UDS 200	0.00552	27.6
CC27	Bob	Paar Physica MCR 301	0.00867	107.8
PP50	Plate	Paar Physica MCR 301	0.01282	103.6
MK22	Cone	Paar Physica UDS 200	0.01454	127.9

A low moment of inertia is especially advantageous when performing oscillatory tests, especially when measuring thin fluids when torque is low. A low moment of inertia is also desired when performing tests using large strains at high frequencies.

The coupling that is used by the Paar Physica MCR 301 rheometer has a considerable lower mass than the coupling used by the Paar Physica UDS 200 rheometer.

3.2 EXPERIMENTAL DETERMINATION OF AN AVERAGE SHEAR STRESS (FROM TORQUE) AND A MEAN SHEAR RATE THROUGH AN ANALOG CYLINDER WHEN USING THE SCREW-RECIRCULATION CUP

Figure 2 shows that linear relations between M (Nm) and N (rpm) were obtained when running the screw-recirculation cup with a Newtonian fluid like the standard Brookfield 12 500 cP. Using a relatively low cost bearing system in the screw type process rheometer, Salas-Bringas et al [11-13] also obtained linear relations between M (Nm) and N (rpm). However due to the friction in a sliding bearing, the curves did not intercept at the origin as is obtained in this system driven by the UDS 200 rheometer which uses an air bearing. Figure 2 also shows the equations of the curve fit with the values of the Slope a (Nm/rpm). The high R^2 indicates that the linear fit with intercept at the origin represents well the data as it is expected from a Newtonian fluid.

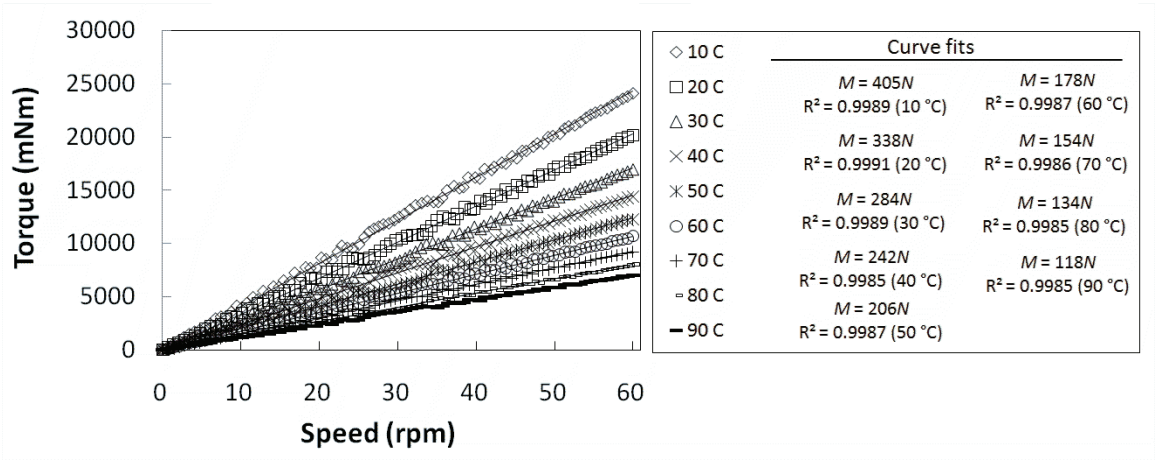

Figure 2: Relations between torque, M (Nm) and speed, N (rpm) using the screw recirculation cup and the Newtonian standard Brookfield 12 500 cP at different temperatures. On the right side are located the Slope a (Nm/rpm) that are used in the calibration procedure.

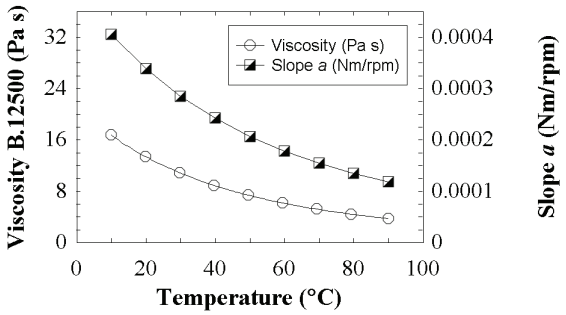

Figure 3: At the left side, viscosities of Brookfield 12 500 cP (B. 12500) at different temperatures measured in cone plate (50 mm, 1° and 50 µm central gap). At the right side, Slope a (Nm/rpm) obtained in the screw-recirculation cup at the same temperatures using the same Newtonian fluid.

The Newtonian standard Brookfield 12 500 cP is a thermo dependent fluid. Its viscosity changes at an exponential rate when the temperature changes; this behavior was assessed using both MK22 and the screw-recirculation cup through the Slope a (Nm/rpm) as shown in Figure 3.

When using Eq. (9), an average radius ± standard deviation equivalent to 0.00982 ± 0.000063 m (n = 8) is obtained based on the viscosities of the Newtonian standard Brookfield 12 500 cP when tested from 10 to 90 °C (equivalent to 4.5 to 17 Pa s). n is the number of samples.

3.3 EXPERIMENTAL DETERMINATION OF AN AVERAGE SHEAR STRESS USING THE NORMAL FORCE GENERATED IN THE SCREW SHAFT

As similarly shown for M (Nm) in Figure 2, Figure 4 shows that N_F (N) is proportional to N (rpm). The linear relation having an intercept at the origin denotes that N_F (N) can be used to describe the flow characteristics of a fluid.

Based on the relation between N (rpm) and N_F (N) shown in Figure 4 and that σ_M (Pa) is previously known for the different temperatures, it is obtained the constant K_{NF} (m^{-2}) from Eq. (12) to convert N_F (N) into σ_{NF} (Pa) following Eq. (13). Since relatively similar K_{NF} are obtained for the different tests, an average ($K_{NF} \pm$ SD) of 111 $\pm$ 1.8 (m^{-2}), using n = 9 is obtained for all tests (10 – 90 °C) using the certified Newtonian standard shown in Figure 4. Each of the nine samples representing each temperature is also an average K_{NF} from the flow curve 0 – 60 rpm.

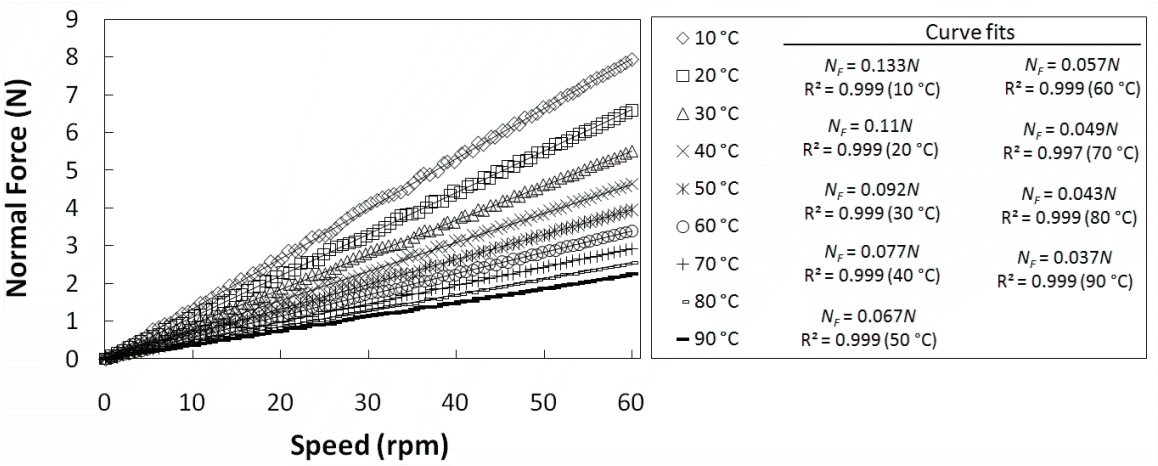

Figure 4: Relations between speed, N (rpm), and the normal force, N_F (N), in the screw shaft using the Newtonian standard Brookfield 12 500 cP at different temperatures. On the right side are shown the linear equations with intercept at the origin representing the Newtonian fluid at different temperatures.

3.4 COMPARISONS OF PREDICTIONS AND ERRORS WHEN USING THE ANALOGUE CYLINDER AND THE NORMAL FORCE IN THE SCREW WITH A NEWTONIAN STANDARD

The predictions of the viscosity of Brookfield 12 500 cP by the screw-recirculation cup versus its viscosity measured in MK22 at different temperatures using σ_M (Pa) and σ_{NF} (Pa) is presented in Figure 5. From this figure it is possible to observe that similar predictions are obtained when using either M (Nm) or N_F (N). The analysis of E (Pa s) calculated from Eq. (10) is presented in Figure 6. This figure shows that the maximum errors are around 0.95 Pa s. Slightly higher were the residuals from the predictions based on σ_M (Pa). E (Pa s) is calculated from each one of the flow curves presented in Figure 2 and Figure 4.

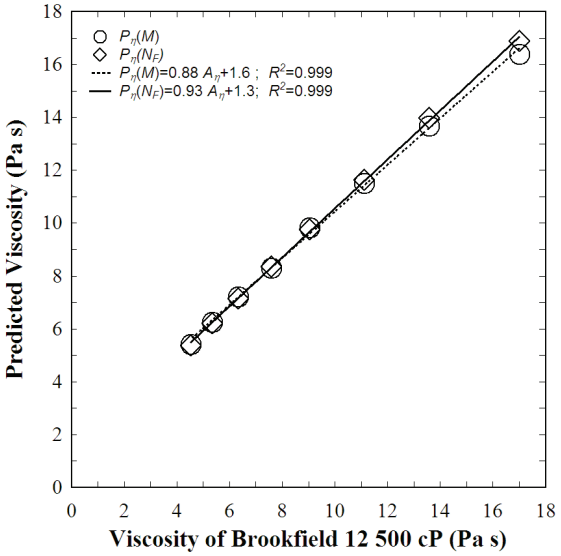

Figure 5: Correlation between predicted viscosity, P_η (Pa s) and actual viscosity, A_η (Pa s) of the standard Newtonian Brookfield 12 500 cP at different temperatures. A_η (Pa s) is obtained using cone-plate (MK22, Physica UDS 200 rheometer) and P_η (Pa s) comes from the ratio between σ_{NF} (Pa) and $\dot{\gamma}$ (s^{-1}) using the screw-recirculation cup.

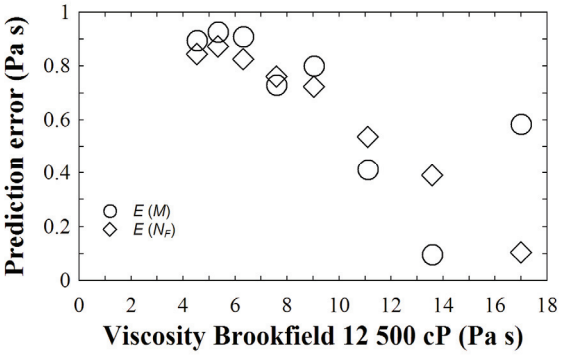

Figure 6: Prediction errors or residuals, E (Pa s), using the screw-recirculation cup and the Newtonian standard Brookfield 12 500 cP. E (M) are the errors or residuals obtained when using torque, M (Nm), to calculate shear stress, σ_M (Pa), and E (N_F) the residuals using the normal force, N_F (N), in the screw shaft to estimate shear stress, σ_{NF} (Pa)

3.5 COMPARISON OF FLOW CURVES BETWEEN THE SCREW-RECIRCULATION CUP USING THE CYLINDRICAL ANALOGUE AND STANDARD MEASURING SYSTEMS USING NON-NEWTONIAN FLUIDS

Figure 7 shows the flow curves of the silicone oil HT Brookfield 100 000 cP obtained through three different measuring systems, MK22, the screw-recirculation cup and ST24. The fluid was only measured until 30 s^{-1} in MK22 due to the centrifugal forces started to move the sample out of the cone when running at higher rotational speeds, especially this occurred when the standard was measured at the highest temperatures, and therefore lower viscosities. The screw-recirculation cup was only used at shear rates smaller than 50 s^{-1} due to viscous heating started to occur at high speeds, shown by a reduction in the shear stress from the screw as it can be observed in Figure 7, this occurred at the lowest temperatures, when the viscosity of the fluid is higher. The flow curve in

ST24 was measured until 60 s^{-1} because it was no apparent problem with the sample. However, it is expected high Reynolds number in ST24 when running at high speeds.

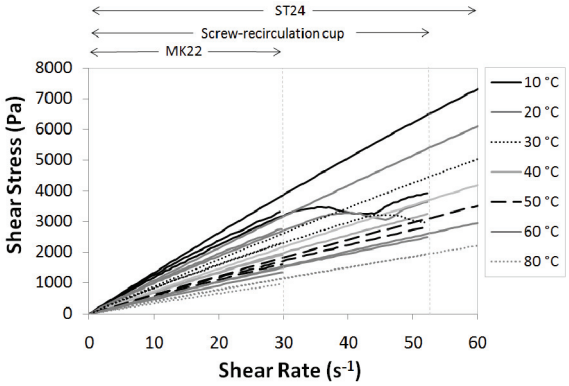

Figure 7: Flow curves of HT Brookfield 100 000 cP measured at different temperatures in cone plate MK22 (50 mm diameter, 1°) from 0 to 30 s^{-1}, in the screw-recirculation cup (0- 50 s^{-1}) and in a ST24 Par Physica stirrer (0-60 s^{-1}). In the screw recirculation cup, torque was used to estimate the shear stress.

From the flow curves shown in Figure 7, it can be observed that the fluid HT Brookfield 100 000 cP is a weak pseudoplastic fluid as the curve from all measuring systems tend to curve downwards (except where viscous heating occur in the screw-recirculation cup). It is known that in Newtonian fluids the apparent viscosity is equivalent to the actual viscosity, in the case of HT Brookfield 100 000 cP the apparent viscosity is found in decreasing order when moving from high shear rates to lower shear rates. Using MK22 with HT Brookfield 100 000 cP at 10 °C, the apparent viscosities decreased from 127 to 117 Pa s, at 20 °C from 101 to 96 Pa s, at 30 °C from 82 to 80 Pa s, at 40 °C from 68 to 66 Pa s, at 50 °C from 56 to 55 Pa s. At temperatures higher than 50 °C, the differences become smaller, and the fluid becomes closer to a Newtonian.

The shear stresses observed for HT Brookfield 100 000 cP, when running the rheometer using Paar Physica ST24 stirrer, are over predicted if they are compared with the MK22 measurements that can be taken as the true measurements. A similar situation happens, but in much lower magnitude, to the shear stresses given by the screw-recirculation cup (except the regions of viscous heating). Therefore, from these results shown in Figure 7, it can be concluded that the screw-recirculation cup and ST24 can present variations with respect to the shear stresses found in MK22 for weak pseudoplastic fluids. However, the flow curves from the screw-recirculation cup are closer to the flow curves of MK22 than the flow curves from the Paar Physica ST24 probe.

The ST24 probe and the screw-recirculation cup can be used to measure fluids that could be difficult to measure in other systems like fluids having relatively large particles, or suspensions that can sediment during measurements. However, further comparative studies have to be conducted to investigate how both systems perform using fluids difficult to measure in cone-plate, plate-plate and bob-cup systems. Additionally, it might be of interest in future studies to quantify how the Weissenberg effect could affect the measurements in the screw-recirculation cup compared with other measuring systems since the screw continuously drag the material downstream.

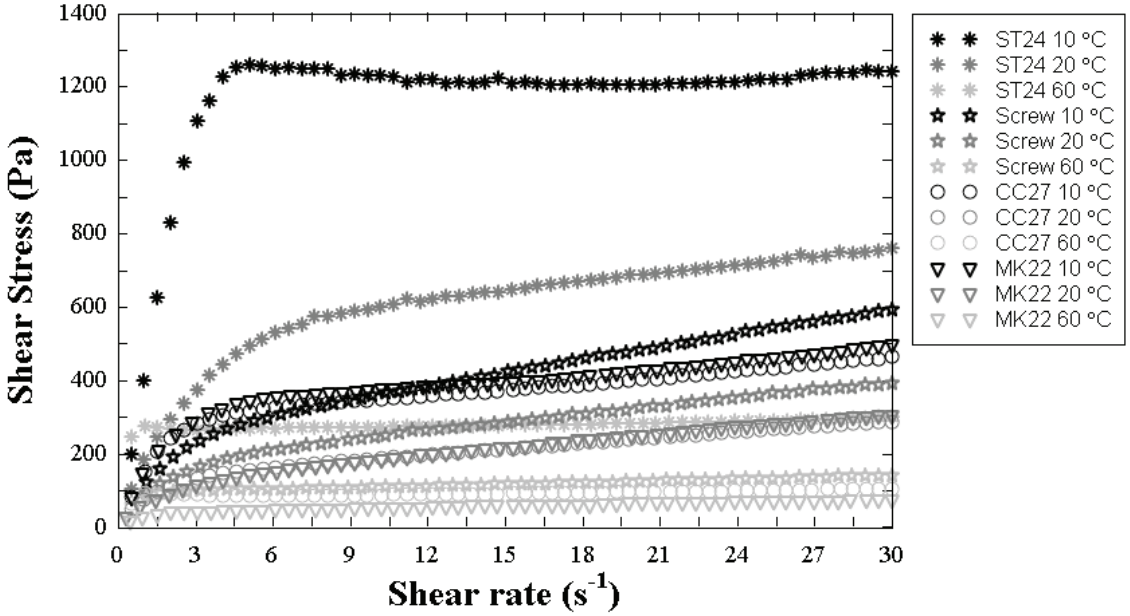

415

416 Figure 8: Flow curves of "Colgate MaxWhite" toothpaste. The measurements were made in the screw-
417 recirculation cup using torque to determine shear stress (Screw). MK22 represents the measurements in cone-
418 plate (50 mm diameter, 1°), ST24 represents the Paar Physica stirrer ST24-2D/2V/2V-30/109 and CC27 is a Paar
419 Physica bob-cup system. ST24 and CC27 were driven by the Paar Physica MCR 301 Rheometer. Screw and
420 MK22 were driven by the Paar Physica UDS 200 Rheometer.

421 In agreement with the flow curves of HT Brookfield 100 000 cP shown in Figure 7, Figure 8 shows clearly
422 that ST24 over predicts the shear stresses if the measurements from MK22 and CC27 are taken as the true
423 measurements. ST24 over predicts the shear stresses for the three different temperatures of toothpaste (10, 20
424 and 60°C). The measurements given by the screw-recirculation cup are closer to the measurements of MK22 and
425 CC27.

426 As it can be concluded from Figure 7 and Figure 8, when using one weak pseudoplastic fluid and a time
427 dependent pseudoplastic toothpaste with suspended particles, the screw concentrically assembled in a static
428 cylinder can be used to monitor changes of the "thickness" of fluids during processing by monitoring changes in
429 shear stresses which can be done through the monitoring of torque or through an electrical signal representing
430 torque.

431

3.6 COMPARISON OF THE AVERAGE SHEAR STRESSES OBTAINED IN THE SCREW-RECIRCULATION CUP USING TORQUE AND THE NORMAL FORCE IN THE SCREW SHAFT

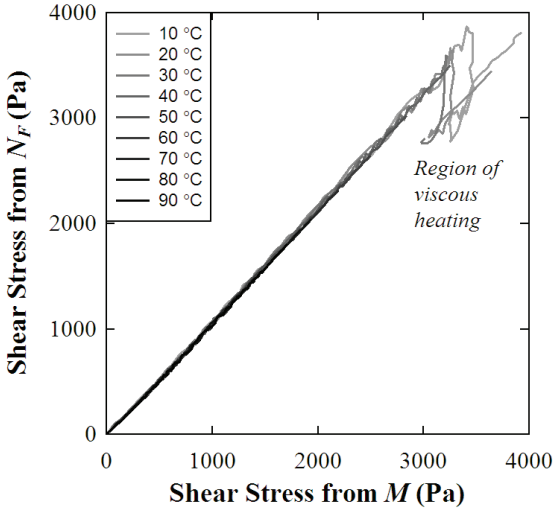

Figure 9: Comparisons of shear stresses that were determined through the torque (M) and through the normal force in the screw shaft (N_F). Fluid measured is HT Brookfield 100 000 cP.

Figure 9 shows that σ_{NF} (Pa) is proportional to σ_M (Pa) when using the weak pseudoplastic HT Brookfield 100 000 cP. The same relation is observed when measuring Colgate toothpaste in Figure 10. Therefore it can be concluded that N_F (N) can be used to estimate the shear stresses of non-Newtonian fluids according to both Figure 9 and Figure 10.

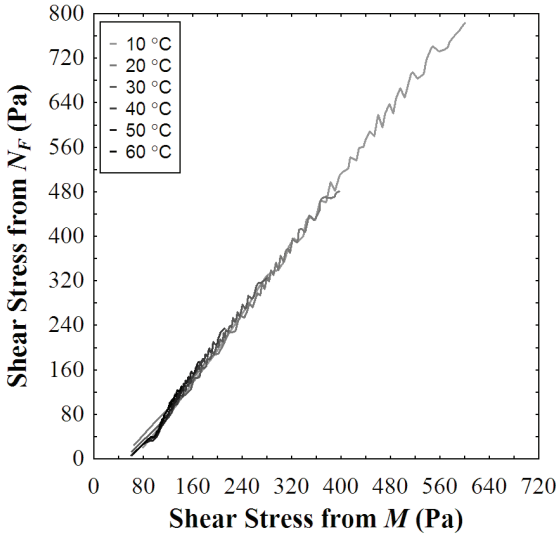

Figure 10: Comparisons of shear stresses that were determined through the torque (M) and through the normal force in the screw shaft (N_F). Fluid measured is “Colgate MaxWhite” toothpaste.

3.7 COMPARISONS OF VISCOELASTIC DATA BETWEEN THE SCREW-RECIRCULATION CUP AND STANDARD MEASURING SYSTEMS

Figure 11 shows a comparison between G' and G'' for two viscoelastic liquids using different probes. The mix 85/15 measured in bob-cup (Z4) and on the screw-recirculation cup (screw) shows a relatively good agreement. An increase in both G' and G'' is observed as the temperature decreases. Both methods determined that the mix 85/15 is a viscoelastic fluid as G'' is higher than G'. Mix 85/15 when measured in Z4 and screw resulted in relatively similar moduli.

The mix 90/10 present a reduction in both G' and G'' compared to the mix 85/15 as it can be seen in Figure 11. As similarly seen for the mix 85/15, the fluid resulted in a viscoelastic fluid with G'' > G'. Relatively good agreements can be observed in Figure 11 for G' and G'' using PP50 and the screw-recirculation cup during the temperature change.

It is believed that the relatively good agreements between the screw-recirculation cup with the bob-cup and plate-plate system are also due to the powder Avicel HFE-102 apparently did not interact enough with the silicone oil to change the rheological properties of the mixture during the approximately four weeks of experiments. The mixture resulted in a suspension. The rheological measurements of the viscoelastic suspensions using different probes were made during different weeks. The suspensions were prepared in relatively large amounts, so different samples were taken to each of the measuring systems. The similar results obtained between the different probes also demonstrate that mixing silicone oil like Brookfield 100 000 cP with microcrystalline cellulose like Avicel HFE-102 results in a rheologically stable viscoelastic suspension to compare measurement methods. The only concern using this suspension is to mix it well before each use due to Avicel HFE-102 begins to sediment in the silicone oil after some hours.

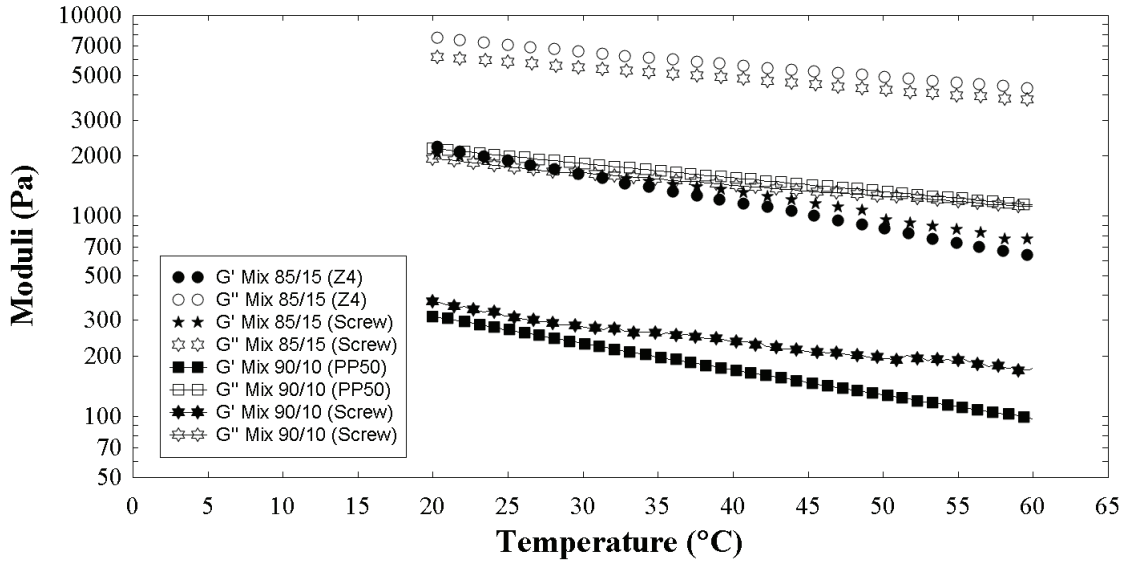

Figure 11: Storage (G') and loss modulus (G'') of a viscoelastic liquid made by mixing the silicone oil HT Brookfield 100 000 cP (85% W/W) with Avicel microcellulose powder (15% W/W), referred as Mix 85/15. Another test was made by using the same mixture with a different concentration (90% W/W of silicone oil and 10% W/W Avicel microcellulose), referred as Mix 90/10. Measurements were performed in the screw-recirculation cup (Screw) and in the Paar Physica bob-cup (Z4) measuring system. Screw and Z4 were driven by the Paar Physica UDS 200 Rheometer. The plate-plate of 50 mm (PP50) was driven by the Paar Physica MCR 301 Rheometer. All tests were performed using 3% strain and 3 Hz amplitude.

The relatively good agreements between Screw with Z4 and PP50 may be explained because the screw produces an almost if not purely Couette flow during small oscillations, so the use of an analog radius for Couette flow is appropriate to perform oscillatory tests.

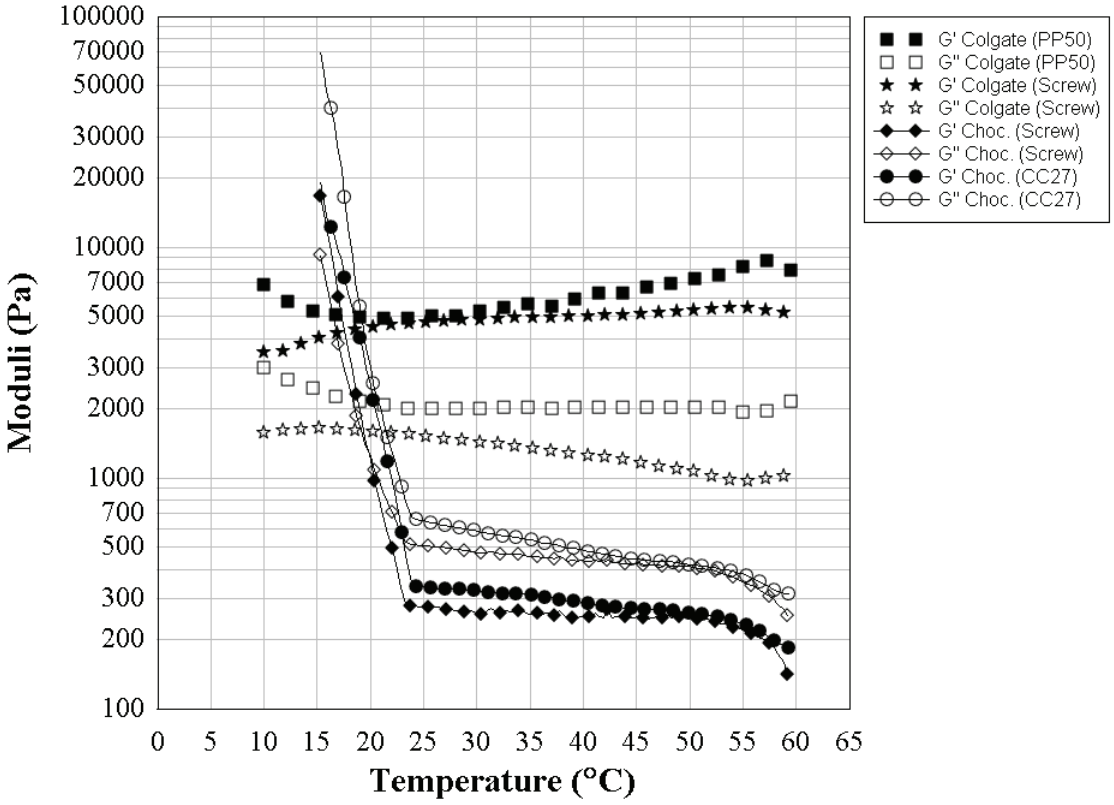

479

480 Figure 12: Storage (G') and loss modulus (G'') of "Colgate MaxWhite" toothpaste, and for the cooking
481 chocolate "Kokesjokolade Landlord 100 g" at different temperatures. The measurements were made in the
482 Screw-recirculation cup (Screw), in a 50 mm diameter plate-plate system (PP50) and in a Paar Physica bob-cup
483 (CC27). The screw and CC27 were driven by a Paar Physica UDS 200 rheometer and PP50 by the Paar Physica
484 MCR 301 rheometer.

485

486 In Figure 12 can be seen that "Colgate MaxWhite" toothpaste present a higher solid behavior (G') compared to
487 the viscous behavior (G'') when tested between 10 and 60 °C with an oscillation of 0.1 % strain at 10 Hz and
488 measured by PP50 and by the screw-recirculation cup. Both measurements the PP50 and the screw-recirculation
489 cup shows relatively similar results. However, the time dependency might have contributed to the small
490 differences.

491 The Norwegian cooking chocolate "landlord 100 g" behaves similar in both measuring systems, the screw-
492 recirculation cup and in CC27. Both moduli, G' (Pa) and G''(Pa) increased at lower temperatures with G'' (Pa)
493 higher than G' (Pa) showing that the viscous behavior dominates at high temperatures. At temperatures between
494 23-24 °C a drastic increase in both moduli (G' and G'') occur which can be explained by a phase transition in the
495 cocoa butter. Cocoa butter has four polymorphic forms; α, β, β' and γ. The α form melts at 21-24 °C and it is
496 transformed to β' form at normal storage temperatures, the β' form melts at 27-29 °C. The β form is stable and it
497 melts at 34-35 °C. The γ is the most unstable polymorphic form of cocoa butter, it is form by very fast cooling
498 and its melting point is 17 °C [6]. According to the previous description and to the measurements in CC27 and
499 the screw-recirculation cup shown in Figure 12, it is possible to conclude that the cocoa butter in the cooking
500 chocolate Landlord 100 g has the α form because of the drastic change in G' and G'' between 23-24 °C.

501 Both measuring systems, the screw-recirculation cup and CC27 agree in most of the values and behaviors,
502 however the screw-recirculation cup shows a cross over between G' and G'' at about 1300 Pa while in CC27 G'
503 approaches to G'' at around 2200 Pa and then at higher moduli (Pa) the curves separate again leaving G'' > G'.

Since the cocking chocolate solidifies at this range of temperatures it is expected a G' > G'' as it is indicated by the screw-recirculation cup. At this range of temperatures (~20 °C) the appearance of the chocolate was a brittle solid. One explanation for this difference can be that the chocolate when solidifies slip on the surface of the CC27 bob while the flights of the screw provides a better grip that helps to keep the chocolate attached to the screw surface.

The general conclusion from Figure 12 is that the screw-recirculation cup is capable to perform viscoelastic measurements in oscillatory tests and consequently is capable to detect phase changes through changes in G' and G''. Also the screw provides a better grip than the cylindrical surface of the CC27.

4 PRACTICAL APPLICATIONS

The results shown by the screw-recirculation cup provide the information needed to apply this calibration method into process monitoring of non-Newtonian and viscoelastic fluids. The use and installation of a screw type process rheometer was shown in Salas-Bringas et al. [13]. Previously [11-13] it was described how to measure the viscosity of fluids based in a calibration method using the slope formed between torque or downstream pressure versus the rotational speed. However, the usefulness of the previous method to measure changes in viscosity in a process was limited. The previous method was not able to provide the average shear stress and the mean shear rate which can lead to a new range of applications like the viscoelastic measurements shown in this article.

For process control, the changes in fluid viscosity can be monitored by running the screw-type process rheometer at constant speed while monitoring changes in either torque [11-13] or downstream pressure [13]. A simple measuring arrangement can be done by implementing the rheometer with a torque or a pressure sensor and a speed sensor to predict an average viscosity. For cases where fluid viscosity needs to be controlled at low cost, the information regarding torque and speed can be obtained through the electrical signal provided by a frequency converter and the screw can be mounted in a standard bearing. However, for cases where product quality is important for certification, the screw can be mounted in a more sensitive bearing system, providing this, the screw type process rheometer can be operated at continuous speed to monitor changes in viscosity or to repeat steps at different speeds to obtain the flow curve of a fluid. Furthermore, if a more complete rheological characterization of the fluid is required during process like the storage and loss modulus, the screw type process rheometer can be stopped to perform the oscillatory measurements, and after that rotated to bring new fluid into the system while at the same time performs the viscosity measurements or to provide the flow curve of a fluid.

The usefulness of the screw type process rheometer must be evaluated for each case that depends on the type of fluids and the accuracy of the expected measurements.

Future research can be done to show how this principle performs when measuring different sedimenting fluids, fluids having large particles and how the rheometer performs to evaluate the yield stress of fluids during processing.

5 CONCLUSIONS

The use of an analogue cylinder to determine shear stress from torque and shear rate from the rotational speed is appropriate to measure the flow characteristics of non-Newtonian fluids, both time independent and time dependent fluids. The flow curves obtained through the screw-recirculation cup resulted to be closer to the measurements of cone-plate, plate-plate and bob-cup when compared to the ST24 Paar Physica stirrer.

Similar shear stresses can be obtained using either torque or the normal force in the screw shaft, resulting in similar predictions of viscosity.

The screw-recirculation cup can measure satisfactorily the viscoelastic data of fluids and it can be used to detect phase changes in fluids. Its results are of similar magnitude to the measurements provided by standard measuring systems.

AKNOWLEDGEMENTS

The authors would like to thank Dr. Ulrike Böcker and Dr. Tom Tetzlaff for the translation of the abstract into German.

REFERENCES

[1] Barnes HA: On-Line or Process Viscometry - a Review, Applied Rheology 9 (1999) 102-107.
[2] Bourne M: Food Texture and Viscosity, Academic Press, London (2002).
[3] Chhabra RP, Richardson JF: Non-Newtonian Flow in the Process Industries, Butterworth-Heinemann, Oxford (1999).
[4] Dealy JM, Wissbrun KF: Melt Rheology and Its Role in Plastics Processing - Theory and Applications Kluwer Academic Publishers, The Netherlands (1999).
[5] Drozdek KD, Faller JF: Use of a Dual Orifice Die for on-Line Extruder Measurement of Flow Behavior Index in Starchy Foods, Journal of Food Engineering 55 (2002) 79-88.
[6] Heldman DR, Lund DB: Handbook of Food Engineering, CRC Press/Taylor & Francis, Boca Raton, Fla (2007).
[7] Kemblowski Z, Sęk J, Budzyński: The Concept of a Rotational Rheometer with Helical Screw Impeller, Rheologica Acta 27 (1988) 82-91.
[8] KIM CH, Lipták BG, Jamison JE: Viscometers-Industrial, In Process Measurements and Analysis, ed. Lipták BG, CRC Press, Boca Raton, FL (2003).
[9] McKenna BM, Lyng JG: Rheological Measurements of Foods, In Instrumentation and Sensors for the Food Industry, Eds. Kress-Rogers E, Brimelow CJB, CRC Press, Cambridge (2001).
[10] Roberts I: In-Line and on-Line Rheology Measurement, In Instrumentation and Sensors for the Food Industry, Eds. Kress-Rogers E, Brimelow CJB, CRC Press, Boca Raton, Fla (2001).
[11] Salas-Bringas C, Jeksrud WK, Lekang O-I, Schüller RB: A Calibration Method for a New Type of Rheometer, Annual Transactions of the Nordic Rheology Society 14 (2006) 197-201.
[12] Salas-Bringas C, Jeksrud WK, Schüller RB: A New on-Line Process Rheometer for Highly Viscous Food and Animal Feed Materials, Journal of Food Engineering 79 (2007) 383-391.
[13] Salas-Bringas C, Lekang OI, Schüller RB: Time Variations and Calibration of a Screw Type Process Rheometer, Applied Rheology 20 (2009) 34526-134526-11.
[14] Steffe JF: Rheological Methods in Food Process Engineering, Freeman Press, East Lansing, Mich. (1996).
[15] Metzner AB, Otto RE: Agitation of Non-Newtonian Fluids, AICHE Journal 3 (1957) 3-10.
[16] Rauwendaal C: Polymer Extrusion, Hanser Gardner Publications, Inc., Krugzell, Germany (2001).
[17] Colgate-Palmolive Co. Home Page Colgate Maxwhite. http://www.colgate.com.au/app/PDP/ColgateMaxWhite/AU/HomePage.cvsp

PAPER IV

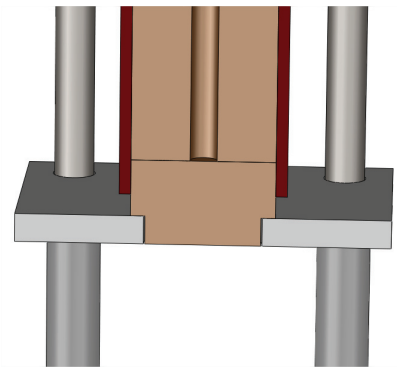

Compression rheology and physical quality of wood pellets pre-handled with four different conditions

Carlos Salas-Bringas[1], Tore Filbakk[2], Geir Skjevrak[3], Odd-Ivar Lekang[1], Olav Høibø[4] and Reidar Barfod Schüller[5]

[1]Dep. Of Mathematical Sciences and Technology, Norwegian University of Life Sciences, P.O. Box 5003, N-1432 Ås, Norway

[2]Norwegian Forest and Landscape Institute, P.O. Box 115, N-1431 Ås, Norway

[3]Dep. of Energy and Process engineering, Norwegian University of Science and Technology, N-7491 Trondheim, Norway.

[4]Dep. of Ecology and Natural Resource Management, Norwegian University of Life Sciences, P.O. Box 5003, N-1432 Ås, Norway

[5]Dep. Of Chemistry, Biotechnology and Food Science, Norwegian University of Life Sciences, P.O. Box 5003, N-1432 Ås, Norway

ABSTRACT

The effects of drying temperature and storage time on the compressibility and strength of Scots pine pellets were analysed in this article. Compressibility was not affected, whereas the highest pellet strength was obtained from the wood with longest storing and highest drying temperature.

INTRODUCTION

Traditionally, rest products from saw mills have been used as raw material for pellets. Increased demands have resulted in less available material from this resource. New raw materials are therefore needed to increase the wood pellet production. New raw materials most probably have different rheological properties like compressibility (i.e. compacting stress – density relationships[1]), compactibility (i.e. the ability of a material to form strong compacts) and resistance to flow, which influence the pelleting performance and product quality[2, 3].

It is a general statement[4-7] that the storing time of the raw material plays a major role on the durability and strength of the pellets. Storage of the raw material is necessary due to logistics, transport, etc. However, storage also increases the power demands of pelleting and reduces throughputs due to the loss of extractives that provides a lubrication effect in the die[5] (also called matrix).

For a feasible pellet production, the raw material has to be dried to a moisture content between 7 to 13% (w.b.), which only is achievable through artificial drying. One of the most common drying methods of today is drum drying using flu gas with temperatures around 450 ^{o}C. With such temperatures, part of the extractives will vaporize. Extractive content will be reduced even when drying the raw material below 100 ^{o}C.

Less extractives content, due to drying and storage of the raw material, will most likely influence the compressibility and compactibility of the raw materials, giving other pellet properties as a result.

Compressibility analysis can be performed through compression tests which have been used widely in pharmaceutics, ceramics, metallurgy, civil engineering, as

well as in the food powder field, because it is a simple and convenient technique to measure powder compressibility and flowability[8]. Compressibility indicates the stress level that is required to compact a material to a given density. This information is useful to select or design process equipments. Compressibility data are also important to describe the flowability of loose materials. Compressibility provides information for storage, transport and handling[1, 8, 9]. A stored powder having high compressibility can be highly compacted at the bottom, reducing its flowability. This can cause problems at the discharge of silos, bins and all transport ducts where the material is moved by gravity. Consequently, compressibility information is important in process design.

Compactibility is also important to determine the amount of stresses (i.e. consolidating stresses) required to form strong compacts or pellets. Compactibility provides information about durability of the pellet which is important for storage, transport and handling of pellets.

The main goal of this research is to characterize the changes in compressibility and compactibility of ground Scots pine materials treated by two different storage times and by two drying methods. Another goal is to analyze the capability of a new die pelleting rig to perform such studies. Scots pine was chosen because it is economically attractive for large scale production[10].

MATERIALS AND METHODS

Design features

Wood pellets were produced using a new customized die pelleting rig (see Fig. 1) as a fixture in a Lloyd LR 5K Plus texture analyzer. The die pelleting rig was connected to the texture analyzer using the same assembly that was described and used by Salas-Bringas et al.[11] and Rukke et al.[12]. The die pelleting rig (see Fig. 1) consists of a barrel made of brass having a compressing channel along the centre. The maximum load that can be produced in the texture analyzer is 5 kN. The compressing channel has a diameter of 9.5 mm and a 9.4 mm diameter rod is used to press the samples. The system can produce compacting stresses up to 72 MPa.

The barrel is connected to a closed or blank die made in brass. The barrel and die are covered with a jacket heater of 550 Watts. The temperature is measured by a thermocouple that is used by a PID controller to keep a steady temperature. The rod that is shown in Fig. 1 is made of iron to impose an adequate stiffness to avoid buckling at the maximum pressures.

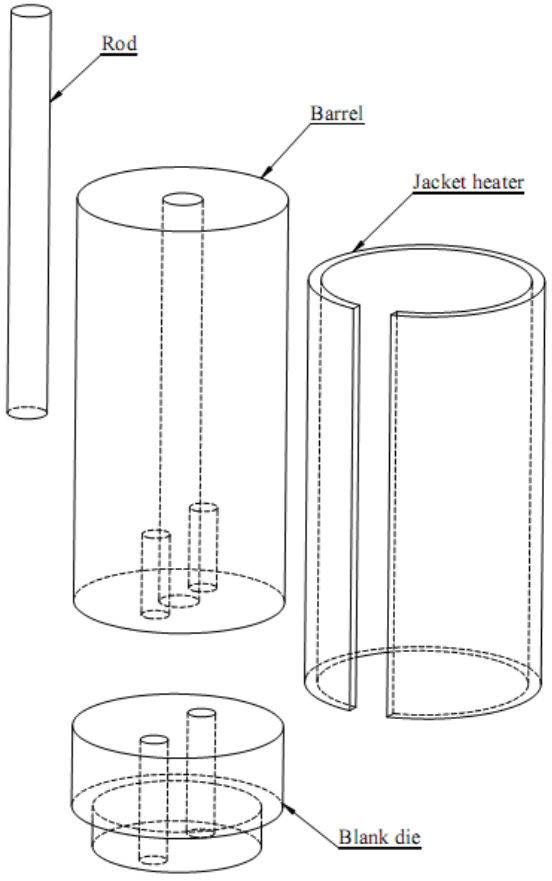

Figure 1. Exploded view of the barrel-blank die setup.

Preparation of the wood samples

The material used in the experiments was chipped from unbarked stemwood from a pine stand located in Bygland in Setesdal

in Southern Norway (EUREF N 6 533 862, E 82 480) at 220 m altitude. The stand was classified as F14 in the Norwegian site class system[13].

Parts of the chips were stored in a 6 meter high pile for 11 months (from May 2008 to April 2009). Samples from this pile is referred to as "Stored". The "fresh" material, stored for three months, was felled from a nearby and identical stand to the first.

The high temperature drying, referred as "HT", was performed in an industrial drum dryer using flue gas with an inlet temperature of 450 ^{o}C.

For the low temperature drying, referred as "LT", it was used a container with perforated bottom and air at 75 ^{o}C as drying medium.

The materials were dried to a moisture content between 7 to 13 % (w.b.) which is common when pelleting wood. However, a narrower range in moisture contents was sought, to avoid any moisture content effect on the rheological properties. As a consequence, the samples were further kept in a climatic chamber (Termarks, Type KBP6395 F, Bergen, Norway) during 48 h using a relative humidity of 50 % and 20 °C to even out the moisture content. The final range in moisture content from the climatic chamber was reduced to a range of 9 – 10% (w.b.).

Production of wood pellets

The ground and dried samples were added in the cylindrical compressing channel until the channel was fully covered. Wood pellets were produced using 20, 30, 40, 50, 60 and 70 MPa of normal stress. Three samples were produced for each normal stress.

There are disagreements in the indications of the production pressures in pellet presses. Some authors describe that the die pressures do not need to be higher than 50 MPa to produce pellets from Spruce sawdust[14]. Others give a general statement that die pressures are not higher than 70 MPa[15], while some estimate even higher pressures, around 300 MPa[5]. However, noticing the disagreements, it is important to keep in mind that the pressure drop through the die hole depends on the mass flow rate (throughputs), die diameter, die length, entry angle and the rheological properties of the materials related to resistance to flow, which also depend on particle size, moisture content, temperature, processing history, etc.

The pressing speed was set to 2 mm/s with a short retention time (1 s). Retention time under high pressure is very short in pellet presses due to the fast and intermittent pressure given by the rotating rollers inside the die ring in the nip area.

After the retention time period, the pressure was released and the blank die removed. The same compressing rod and texture analyzer were used to further move the pellet inside the channel until its gentle discharge from the barrel.

The source of error in this type of compression tests is that the friction between the material and the side walls of the channel reduces the stress from top to bottom[1]. This might result in a wood pellet having a density gradient, with its lowest density close to the blank die. However, the pellets that were produced, having a diameter of 9.5 mm, were relatively short (18 mm). Consequently, density gradients within the single pellets were neglected. The average density was calculated using the pellet weight and its volume, based on their well defined cylindrical shape.

The temperature was set to 110 °C for all tests. At this temperature the amorphous thermoplastic material lignin[16], acts as a binder since it is over its glass transition temperature[16, 17] and bellow its melting point[18]. Temperature in the range of glass transition is important to make durable particle-particle bonding in pellets[16].

The experiments were repeated three times and the results are presented in a compacting stress (MPa) versus density (kg m^{-3}) plot.

Measurement of pellet strength

The physical quality of the wood pellets were analyzed by measuring the maximum peak force registered during a diametrical compression, as similarly used by Rhén et al[14]. The first preliminary tests showed a plastic and ductile nature of the wood pellets. It was not possible to measure the tensile stresses based on the same criteria that have been used for brittle pellets[19, 20]. Instead maximum yield load producing a ductile failure (ref. Fig. 4) divided by the pellet length (kN mm^{-1}), which gives information about the shear strength per unit length, was used. This method has also been used by other authors characterizing wood pellets[14]. The results showing the normal force (kN), are plotted in Fig. 4. Maximum yield loads (kN mm^{-1}) are plotted in Fig. 5. The test speed was set to 1 mm/min and the test was ended when the probe reached 2.2 mm below the diameter of the pellet (strain ~ 0.23).

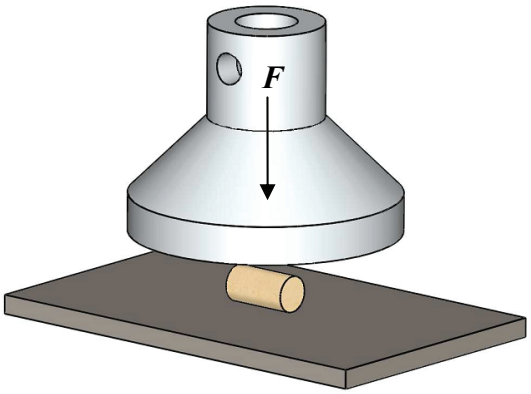

Figure 2. Representation of the diametrical compression of a wood pellet using a specially designed conical probe of 60 mm diameter. *F* is the normal force (kN).

RESULTS AND DISCUSSIONS

Production of wood pellets

The compressibility of all wood samples showed a clear ductile type of compression, similar to ductile powders[21] (see Fig. 3) following a power law trend. A power law curve fit resulted in high correlations ($R^2 > 0.94$), $n = 18$, where n is the number of samples, three samples for each of the six compacting stresses 20, 30, 40, 50, 60 and 70 MPa.

Following the power law curve, a large increase in density is expected at low compacting stresses followed by a smaller increase at higher stresses. Consequently, much larger changes in compacting stresses are required to increase the density of wood pellets at high stresses.

No significant differences ($p>0.05$) in compressibility was found between the regression curves for the four different raw materials (see Fig. 3).

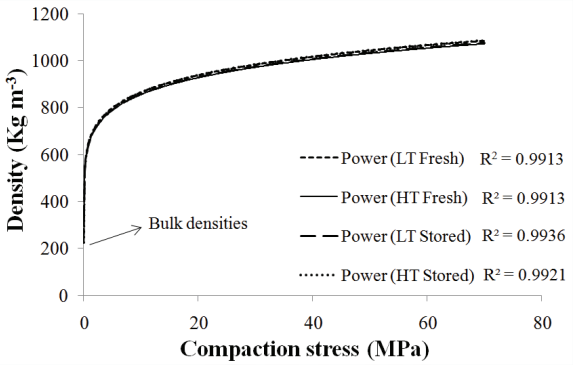

Figure 3. Compressibility data for pine under four pre-handling conditions. No significant differences were found between the four groups ($p>0.05$).

Measurement of pellet strength

A preliminary view of some of the results given by the texture analysis indicates the relationship between the ductile nature of wood pellets and Maximum Yield Load (Fig. 4).

Fig. 4 shows a long plastic region for the pellets having the lowest densities. This occurred to many of the pellets that were produced with low compacting stresses (20 MPa) and the least expected quantities of extractives (HT Stored and LT Stored). All pellets made from "HT Stored" raw material and one pellet from "LT Stored" having the lowest density (approximately 870 kg m^{-3}),

did not present any clear abrupt failure of its structure, but a continuous shear or frictional deformation in a long yield region, denoting a plastic nature. For these cases it was not possible to estimate a maximum yield load. This is why two of the linear regressions made in Fig. 5 were made with smaller number of samples. It is also possible to observe from Fig. 4 that the plastic pellet having 870 kg m^{-3} presents the smallest slope between 200-600 kN of normal force which indicates the smallest elastic modulus and thus the least stiffness.

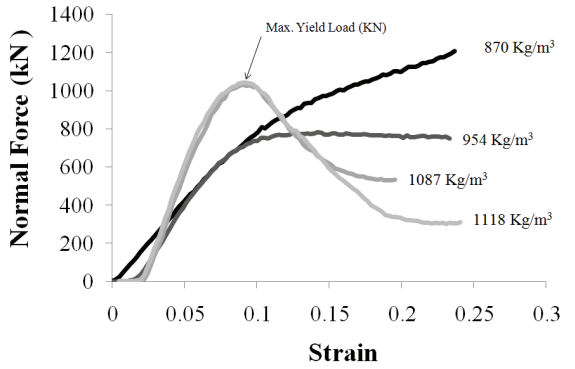

Figure 4. Examples of stress analysis for the wood pellets (HT Stored). The curves show the ductile nature of the wood pellets and how the ductility decreases as the density increases.

As the pellet density increases (>954 kg m^{-3}) the yield starts to show a maximum value (Fig 4), ductile failure appears in "HT Stored" pellets, allowing the determination of a maximum yield load which is used in Fig. 5.

It can be observed that as the density increases the slopes between 200-600 kN also increases, indicating that pellet stiffness increases with higher densification. The positive correlation between Maximum yield load and pellet density illustrated in Fig. 5 was significant ($p<0.05$).

Another observation is that as the density increases, the yield peak becomes sharper. This could indicate the loss of ductility as pellet density increases. Possibly at a much higher density, the wood pellets could become brittle in nature.

Fig. 5. indicates similar strength values (Max. Yield load · $length^{-1}$) for three of the samples (LT Fresh, HT Fresh and LT Stored) since these groups did not present any significant differences ($p>0.05$).

On the other hand the pellets based on stored and high temperature dried raw material (HT Stored), had significantly higher maximum yield load values ($p<0.05$) compared to the others. However, it was only possible to measure a maximum yield load to the pellets with densities above 950 kg m^{-3} for this kind of material, indicating that the linear relationship shown in Fig. 5 only is valid in the density range above 950 kg m^{-3}.

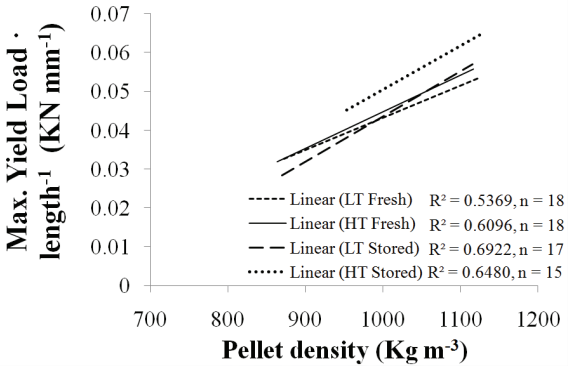

Figure 5. Strength of wood pellets produced with different densities. The word "Linear" indicates that a linear regression was applied to the data sets ($p<0.05$). *n* is the number of samples.

The significant higher maximum yield load values found for the "HT stored" material is in accordance with Nielsen et al.[5] saying that pellets produced from wood with lower extractive content have higher strength due to closer contact between the bonding sites of the lignocellulose particles. Still the basis for the found relationship is not clear. Samuelsson et al.[4] and Finell et al.[7] found that the reduction of fatty acids and resin acids after storage gave higher pellet durability. On the other hand, Arshadi

et al[6] could not find that the amount of fatty acids and resin in sawdust affected the pelleting process and pellet quality. They indicated that since no useful model was found in their data, there are other properties causing the difference between fresh and stored sawdust. During storage, in addition to loss of extractives, some degradation of cellulose, hemicellulose and lignin take place, depending on active fungi species present. This most probably also will affect the the pelleting process and pellet properties.

Despite the small density changes present at higher compacting stresses (~50-70 MPa), a significant ($p<0.05$) and a continuous increase in pellet strength occurred for all compacting stress levels (20-70 MPa).

CONCLUSIONS

Ground Scots pine (*Pinus sylvestris*) presented a ductile compression following a power law curve. The pellets produced in the die pelleting rig were plastic and ductile materials.

Drying temperatures and storing conditions did not change the compressibility of the wood materials significantly ($p>0.05$).

Ground Scots pine pre-handled by the highest drying temperature and longest storage time, produced pellets with the highest strength values under diametrical compression test.

A continuous increase in pellet strength occurred when increasing the compacting stresses from 20 to 70 MPa.

The die pelleting rig proved to be a useful device to perform compressibility tests and to create wood pellets under defined compacting stresses and temperatures.

REFERENCES

1. Schulze, D., (2007) "Powders and Bulk Solids: Behavior, Characterization, Storage and Flow". NY: Springer. 516, 3540737677

2. Salas-Bringas, C., T. Filbakk, G. Skjevrak, O.I. Lekang, and R.B. Schüller, (2010), "Assessment of a new die pelleting rig attached to a texture analyzer to prodict process-ability of wood pellets. Power consumption and pellet quality", *Annual Transactions of the Nordic Rheology Society*, **18**: p. Accepted.

3. Salas-Bringas, C., O.I. Lekang, and R.B. Schüller, (2008), "Rheology in Feed Production", *Annual Transactions of the Nordic Rheology Society*, **16**: p. 229-237.

4. Samuelsson, R., M. Thyrel, M. Sjöström, and T.A. Lestander, (2009), "Effect of biomaterial characteristics on pelletizing properties and biofuel pellet quality", *Fuel Processing Technology*, **90**(9): p. 1129.

5. Nielsen, N.P.K., D. Gardner, J., and C. Felby, (2010), "Effect of extractives and storage on the pelletizing process of sawdust", *Fuel*, **89**: p. 94-98.

6. Arshadi, M., R. Gref, P. Geladi, S.-A. Dahlqvist, and T. Lestander, (2008), "The influence of raw material characteristics on the industrial pelletizing process and pellet quality", *Fuel Processing Technology*, **89**(12): p. 1442.

7. Finell, M., M. Arshadi, R. Gref, T. Scherzer, W. Knolle, and T. Lestander, (2008), "Laboratory-scale production of buifuel pellets from electron beam treated Scots pine (Pinus silvestris L.) sawdust", *Radiation Physics and Chemistry*, **78**: p. 281-287.

8. Ortega-Rivas, E., P. Juliano, and H. Yan, (2005) "Food Powders", ed. G.V. Barbosa-Cánovas. NY: Springer. 372, 0306478064

9. Rauwendaal, C., (2001) "Polymer extrusion". Krugzell, Germany: Hanser Gardner Publications, Inc. XIV, 777., 1-56990-321-2

10. Stjørdal, S., *Feedstock situation for wood-pellets production in Southern Norway*, in *Østlandsforskning*. 2006.

11. Salas-Bringas, C., O.-I. Lekang, E.O. Rukke, and R.B. Schüller, (2009), "Development of a new capillary rheometer that uses direct pressure measurements in the capillary", *Annual Transactions of the Nordic Rheology Society*, **17**: p. 39-47.

12. Rukke, E.-O., C. Salas-Bringas, O.-I. Lekang, and R.B. Schüller, (2009), "Rheological characterization of liver paste with a new capillary rheometer that uses direct pressure measurements in the capillary", *Annual Transactions of the Nordic Rheology Society*, **17**: p. 243-248.

13. Braastad, H. *Tilvekstmodellprogram for furu (Growth model computer program for Pinus sylvestris)*. Reports of the Norwegian Forest Research Institute. Ås, Norway, 1980

14. Rhén, C., R. Gref, M. Sjöström, and I. Wästerlund, (2005), "Effects of raw material moisture content, densification pressure and temperature on some properties of Norway spruce pellets", *Fuel Processing Technology*, **87**: p. 11-16.

15. *Asian Biomass Handbook, Part 3. Physical conversion of biomass*, Y. Shinya and M. Yukihiko, Editors. 2008, The Japan Institute of Energy, 326 pp. http://shrinkify.com/1lul, Last Accessed. Jan. 2010.

16. Kaliyan, N. and R.V. Morey, (2010), "Natural binders and solid bridge type binding mechanisms in briquettes and pellets made from corn stover and switchgrass", *Bioresource Technology*, **101**: p. 1082-1090.

17. Irvine, G.M., (1984), "The glass transitions of lignin and hemicellulose and their measurement by differential thermal analysis.", *Tappi Journal.*, **67**(5): p. 118-121.

18. Mani, S., L.G. Tabil, and S. Sokhansanj, (2006), "Effects of compressive force, particle size and moisture content on mechanical properties of biomass pellets from grasses", *Biomass and Bioenergy*, **30**: p. 648-654.

19. Aarseth, K.A. and E. Prestlokken, (2003), "Mechanical Properties of Feed Pellets: Weibull Analysis", *Biosystems Engineering*, **84**(3): p. 349-361.

20. Li, Y., D. Wu, J. Zhang, L. Chang, D. Wu, Z. Fang, and Y. Shi, (2000), "Measurement and statistics of single pellet mechanical strength of differently shaped catalysts", *Powder Technology*, **113**(1-2): p. 176-184.

21. Doremus, P., *Model Input Data - Plastic Properties*, in *Modelling of Powder Die Compaction*, P.R. Brewin, et al., Editors. 2008, Springer: London. p. 77-93.

PAPER V

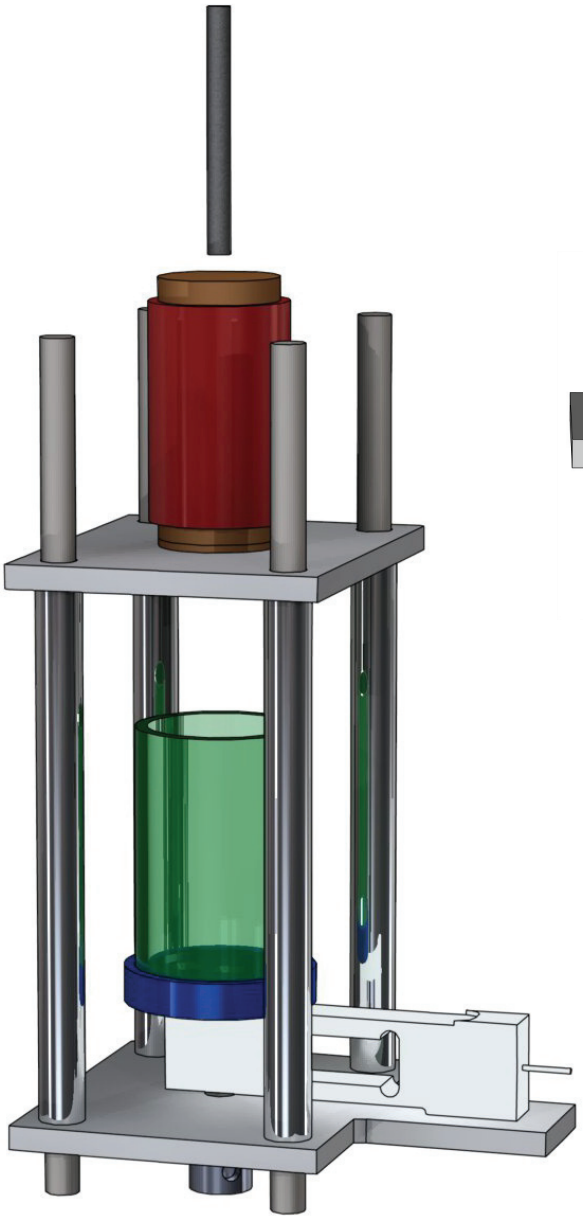

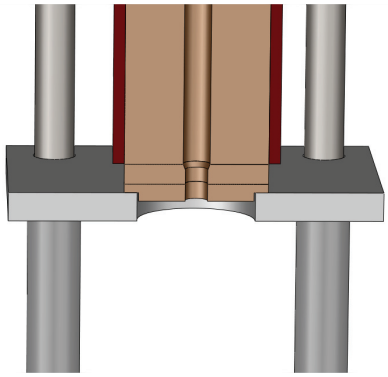

Assessment of a new laboratory die pelleting rig attached to a texture analyzer to predict process-ability of wood pellets. Energy consumption and pellet strength

Carlos Salas-Bringas[1], Tore Filbakk[2], Geir Skjevrak[3], Odd-Ivar Lekang[1], Olav Høibø[4] and Reidar Barfod Schüller[5]

[1]Dep. of Mathematical Sciences and Technology, Norwegian University of Life Sciences, P.O. Box 5003, N-1432 Ås, Norway

[2]Norwegian Forest and Landscape Institute, P.O.Box 115, N-1431 Ås, Norway

[3]Dep. of Energy and Process engineering, Norwegian University of Science and Technology, N-7491 Trondheim, Norway.

[4]Dep. of Ecology and Natural Resource Management, Norwegian University of Life Sciences, P.O. Box 5003, N-1432 Ås, Norway

[5]Dep. of Chemistry, Biotechnology and Food Science, Norwegian University of Life Sciences, P.O. Box 5003, N-1432 Ås, Norway

ABSTRACT

This article presents a laboratory die pelleting rig that was made to compare the pellet-ability of wood raw materials at low cost. It was found that the normal stresses at incipient flow and the yield stresses were correlated with the energy consumed by an industrial pellet press. It was not possible to calculate the stresses producing ductile failure in pellets from the diametrical compression tests.

INTRODUCTION

The use of biomass as energy supply has increased rapidly in the last years due to the increased prices of alternative fuels. Densification of biomass to pellets gives several advantages like easier combustion, transportation and standardisation. Wood pellets can be used as a substitute for oil based heating systems and can also be co-combusted in coal combustion plants. Therefore pellets are likely to have an important role in the increased biomass demands for energy.

The market for wood pellets is increasing rapidly. This has increased the interest for several new virgin - and residue feedstocks from forestry and agriculture. It is expected that using new raw materials which have different rheological characteristics, will change the process performance (e.g. energy consumption[1] and throughputs).

When considering new feedstocks for pelleting, different properties should be investigated, like the chemical and thermochemical properties.

Pelleting can be regarded as a kneading, compressing, heating and forming process where rheological transformations in the material take place[2]. For example, heated ground wood is able to deform plastically when stresses are applied towards a die hole as it softens in the range of the glass transition[3]. The pelleting process can be classified as a high pressure agglomeration process. Typically these products feature high strengths immediately after discharge, low product porosity and small voids[4, 5].

Rheological properties like compressibility (i.e. compacting stress – density relationships), compactibility (i.e. the ability of a material to form strong compacts) and resistance to flow, influence pelleting performance and product quality[2].

Rheological behaviour of compressible powders is more complex to deal with than that of incompressible solids. Therefore more sophisticated production planning and process controls are required. That includes knowledge about how the raw materials responds to the applied stresses during compaction and pellet release, keeping in mind crack prevention[2].

Quick laboratory tests at low costs, to characterize or to rank the pellet-ability of different mixtures of raw materials is of great interest, since manufacturing pellets in an industrial scale requires large volumes of raw materials which give high costs. Therefore a new laboratory die pelleting rig has been developed. The equipment is able to perform pelleting experiments under controlled settings like compressing stress, speed and temperature.

The main goal of this research is to find whether the information given by the die pelleting rig used to produce single pellets, can be used to estimate the pellet-ability of a sample. For this reason, raw materials with different characteristics are analyzed in both an industrial process and in the new laboratory die pelleting rig. It was used ground Scots pine (*Pinus sylvestris*) wood dried at two different temperatures and stored for two different periods of time.

MATERIALS AND METHODS

Preparation of the wood samples for pelleting

The effects of two different drying methods using low (LT) and high (HT) temperature were investigated on both newly felled material (Fresh, stored for 3 months) and material stored in a chip pile for 11 months (Stored). The chip pile was 6 m high and had a diameter of 10 m. All materials were harvested from identical neighbouring stands with a site index of F 14[6]. This resulted in four different assortments:

(i) Newly felled material dried at low temperature (75°C), LT Fresh.
(ii) Newly felled material dried at high temperature (450°C), HT Fresh.
(iii) Material stored for 11 months dried at low temperature (75°C), LT Stored.
(iv) Material stored for 11 months dried at high temperature (450°C), HT Stored.

For the industry scale experiments, all materials were dried to a moisture content between 7 and 13 % w.b., which is suitable for the Sprout Matador M30 industrial pellet press and the specific die ring (also called matrix) that was used in the plant. The raw materials used for the experiments in the laboratory die pelleting rig, were further conditioned in a climatic cabinet for about 5 days with a temperature of 20 °C and 50 % relative humidity, to make a smaller moisture contents range. After the conditioning process, a moisture content between 9-10% w.b. was achieved for all assortments.

To produce pellets in the laboratory die pelleting rig with a similar particle size distribution compared to the original pile of material, the samples were separated using sampler dividers. A 50 kg bag taken from the process stream was divided several times until obtaining approximately 7 ml of sample volume, which is the volume of the compressing channel (ref. Fig. 1) in the laboratory die pelleting rig.

Design Features. Industrial pellet press and die pelleting rig

The industrial pellets were produced in a Sprout Matador M30 pellet press with a nominal production capacity of 3.5 tonne h^{-1} of wood pellets. The pellet press had a common construction; a rotating die ring (or matrix) and pressing rollers. A die ring with

die holes of 8 mm in diameter and 60 mm pressure length was used (see Fig. 1). The pellet press, is an industrial equipment located at Møre Biovarme AS's which is a pellet factory in Sykkylven, western Norway (see Fig. 2). The material was fed into the production line immediately before the hammer mill, and was stored in a bin prior to the pelleting process.

The laboratory die pelleting rig used in this study is the same as the one used by Salas-Bringas et al.[7], except for the die (Fig 1). The laboratory die pelleting rig, have a barrel with a channel of 9.5 mm along the centre. The cylindrical channel has the same 9.5 mm diameter as the entry diameter to the die hole of the industry pellet press. Both die holes (industrial pellet press and laboratory die pelleting rig) have 8 mm in diameter (see Fig. 1), but the length of the die hole in the laboratory die pelleting rig was 48.7 mm shorter because it was not possible to produce flow using the 60 mm length with the maximum pressure of 72 MPa that can be achieved using a 9.4 mm diameter rod and 5 kN force. 5 kN is the maximum force given by the Lloyd LR 5K Plus texture analyzer which was used in this study.

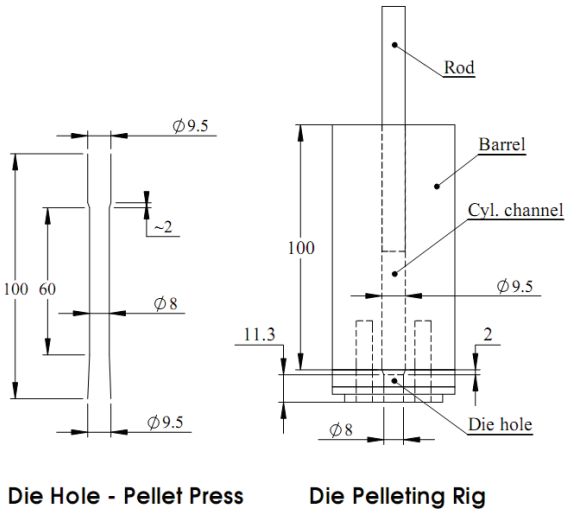

Figure 1. Die hole used in the Sprout matador M30 industrial pellet press (left), and laboratory die pelleting rig (right). Dimensions are in millimeters

Figure 2. Industrial pelleting line used for the experiments.
Source: Møre Biovarme AS

Grinding effect of the pellet press

To quantify the grinding given by the pellet press, pellets were added into water to be disintegrated. After that, the disintegrated pellets were dried to the moisture content recommended by the standard method for sieving[8]. The disintegrated pellets and raw materials taken from the pellet press inlet, were sieved to determine whether differences in particle size distribution existed or not. Standard methods were followed[8]. The procedure was repeated three times. The results are shown in Fig. 3.

Determination of energy consumption in the industrial pellet press

The experiments were performed using a pre-warmed die ring. For each test, the pelleting process was run for approximately four minutes until steady state was achieved. The duration of each test was about 20 minutes, corresponding to approximately 750 kg of pellets. The average electrical power recorded from the pellet press and the throughputs during steady state production were used to calculate the energy consumption (power/throughput). For each of the four materials, three replicates were made, resulting in 12 separate pelleting tests. The volumetric flow rate was kept constant through a screw conveyor during all tests.

The raw materials used in the laboratory die pelleting rig were collected from the product stream at the entry of the industrial pellet press during steady conditions. The samples were cooled at ambient room temperature and stored in a freezer in sealed plastic bags.

For the analysis of pellet strength, pellets were collected from the product stream at the pellet press outlet during steady state production. Only the pellets made from the raw materials having moisture contents in the range 9-10% w.b. were used for the strength analysis.

Laboratory die pelleting rig. Determination of the resistance to flow and yield stress

The resistance of the wood samples to flow through the laboratory die pelleting rig was performed by fully loading the compressing channel with wood (7 ml) and then pre-compressing the sample until 1.4 MPa was reached. A second full load was then performed to have sufficient material to fully cover the channel of the die hole and to produce flow for enough time. After the second load, the test started using a compressing speed of 2 mm s^{-1}. When the rod was almost completely inside the cylindrical channel, at 1.5 mm above the barrel, the test was stopped. This procedure was used in all stress-relaxation tests to quantify the viscous (fluid) and elastic (solid) nature of the wood samples. Temperature was set to 110 °C which is above the glass transition temperature of the lignin binder[3, 9] and below its melting point[10].

Changes in pressure during a relaxation time of 1.5 minutes were continuously recorded. The pressure at the end of the recording time was used as ΔP_{min} (ref. Fig. 5). Three tests were performed for each material to obtain an average ΔP_{min}.

The yield stress (τ_0) of a material in this system can be determined using the stress relaxation test. The yield stress is calculated from a force balance equation as follows[11, 12]:

$$\tau_0 = \frac{\Delta P_{min} R}{2L} \quad (1)$$

where R is the die radius, 4 mm, and L the die length, 11.3 mm (see Fig. 1).

The source of error for this type of tests is that the normal stress at the side walls of the channel reduces from top to bottom[5, 7]due to friction. It is possible to obtain small differences in normal stress from the rod to what is actually experienced by the wood material at the entry of the die hole (at 11.3 mm, from bottom to top). For this reason, in these tests at the moment of the relaxation time, the rod was set to stop at about 1.5 mm above the die entry.

Prediction of process-ability

The evaluation of the laboratory die pelleting rig as a method to estimate the industrial pellet-ability of wood materials was done by a comparative plot of the results given by the normal stress at incipient flow, versus the energy consumed by the pellet press in the industrial trial. It was also performed a comparison between the yield stress and the energy consumed by the industrial pellet press. It is hypothesized that the rheological properties (x-axis, Fig 9 and Fig. 10) affect the energy consumption in the industrial pellet press (y-axis).

Pellet strength

The mechanical strength of the wood pellets was analyzed by measuring the maximum peak force registered during a diametrical compression, as similarly used and described by Salas-Bringas et al[7].

It was planned to measure the mechanical strength of the pellets from the laboratory die pelleting rig after the stress relaxation test. However, as observed from Fig. 6, the bottom side of the pellet was irregular and less dense than the opposite side. Additionally, it was not possible to cut this end properly and make a cylindrical

pellet without damaging the sample. This shaping problem made it difficult to separate the samples and analyse and to compare their mechanical strength with the pellets produced in the industry. Consequently, the strength of the 9.5 mm pellets produced with a blank die[7] in the same laboratory die pelleting rig, using the same four raw materials and temperatures[7], are shown in this article together with the strength from the 8 mm diameter pellets produced in the industrial pelleting line.

Data analysis

To determine significant differences between different groups, it was used one-way ANOVA and Tukey's test.

RESULTS AND DISCUSSIONS

Preparation of the wood samples for pelleting

An important challenge when using the laboratory die pelleting rig, is to achieve a representative raw material sample, since the quantities of wood used is small. For example, the 7 ml of raw material used for one flow test, should have a particle size distribution, moisture content, etc., that represents the pile of the raw material used in the industrial pelleting process.

Grinding effect of the pellet press

It was found higher amounts of the fraction smaller than 0.5 mm from the disintegrated pellets than from the raw material taken from the pellet press inlet ($p<0.05$). This result demonstrates a grinding effect in the pellet press. The other fractions remained with no significant differences ($p>0.05$).

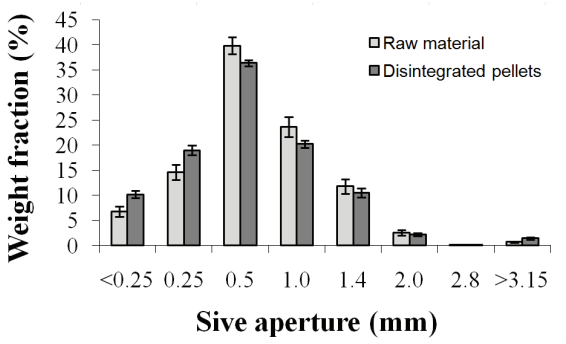

Figure 3. Particle size distribution of the raw materials and disintegrated pellets. Averages were calculated using all samples (LT Fresh, HT Fresh, LT Stored and HT Stored). The error bars represent ± standard error. Statistical differences ($p<0.05$) within a sieve aperture only occurred in the finer fractions (0.25 mm and <0.25 mm)

The grinding effect is probably a consequence of the shearing environment. In pellet presses the product in under stresses, strains and friction mostly in the gap rollers-die ring, in the nip area, as well as in the die hole[13]. In the Sprout Matador M30 pellet press used in the study, the gap between the rollers and the die ring was approximately 2 mm.

Determination of energy consumption in the industrial pellet press

The material expected to have the smallest amount of extractives required more energy (see Fig. 3). This might be due to less lubricant effect due to less extractives. The energy consumption was significantly higher when pelleting stored materials ($p<0.05$). However, drying methods did not produce significant differences ($p>0.05$).

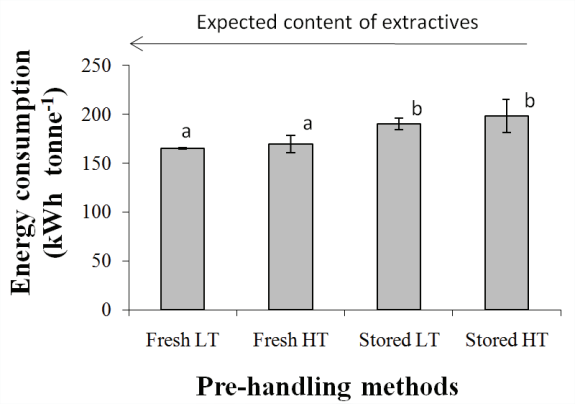

Figure 4. Average energy consumption obtained in the M30 Sprout matador pellet press for the four pre-handling conditions. The error bars represent ± standard error. Different letters indicate significant differences ($p<0.05$)

Laboratory die pelleting rig. Determination of the resistance to flow and yield stress

It was not possible to produce a continuous flow in the laboratory die pelleting rig during a long period due to the small quantity of sample used. Since the laboratory die pelleting rig had a limitation of 72 MPa, the material could not be pre-compressed more than two times. Compressibility information for the raw materials used in these experiments can be found in Salas-Bringas et al.[7]

Fig. 5 indicates the different regions and how the data was used. A first region of compression shows how the normal stress increases exponentially. A second region of plastic flow is initiated where the curve start to decrease the slope, the maximum normal stress was obtained in this region, where the incipient flow is produced. The curve then rapidly decays as the test is stopped to measure the minimum normal stress at the end of the relaxation part of the test.

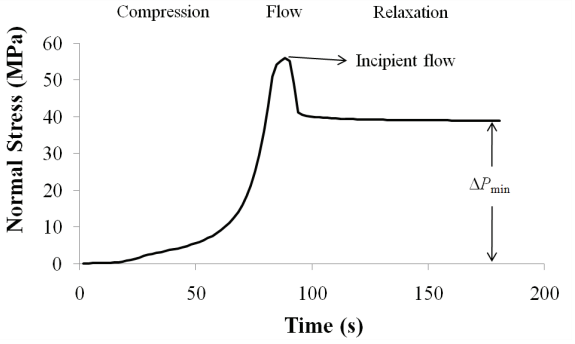

Figure 5. Example of a stress relaxation curve for one of the samples (HT Stored). The plot shows the viscoelastic behaviour of the wood materials

Fig. 5 shows that the wood samples when compressed present a viscoelastic solid nature since the curve decay to an equilibrium stress higher than zero (shown by a $\Delta P_{min} > 0$). Consequently, these materials exhibit a solid behaviour at stresses below τ_0, and the presence of a viscous behaviour can be noticed at higher stresses ($> \tau_0$).

Figure 6. Flow of Pine Scots through the laboratory die pelleting rig

No significant effects ($p>0.05$) on the stresses at incipient flow were present due to the different drying temperatures (ref. Fig. 7). However, significant higher ($p<0.05$) stresses at incipient flow were found for the stored material compared to the fresh material. This might be explained by the

viscous nature of the extractives. which evaporate during storage [14].

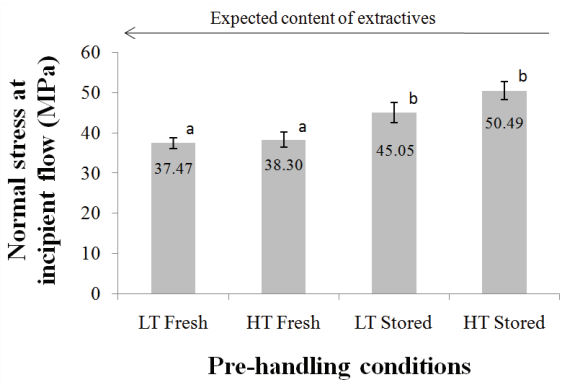

Figure 7. Average (n = 3) normal stresses at incipient flow (MPa) for the materials pre-handled by the four conditions. Different letters indicate significant differences ($p<0.05$). The error bars represents ± the standard error

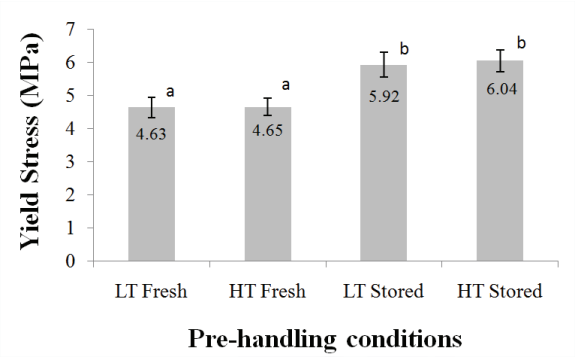

Figure 8. Average (n = 3) yield stresses (MPa) for the four pre-handling conditions. Different letters indicate significant differences ($p<0.05$). The error bars represents ± the standard error

Significantly larger yield stresses were found for the stored raw material ($p>0.05$). This might be due to less extractives. However no differences were found between the different drying methods. This is in accordance with the results given by the normal stresses at incipient flow and by the energy consumption used by the industrial pellet press.

Prediction of process-ability

The data used in Fig. 9 and Fig. 10 are the raw data of Fig. 3, Fig. 7 and Fig. 8.

A significant positive correlation was found between normal stress at incipient flow and the energy consumption used in the industrial trial (Fig 9). It also was a significant positive correlation between yield stress and energy consumption used (Fig 10).

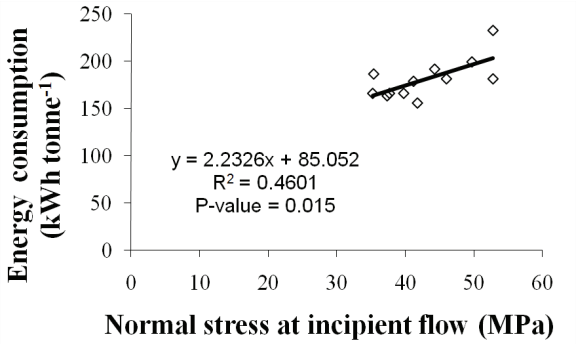

Figure 9. Correlations between energy consumption in the pellet press and the normal stresses at incipient flow in the laboratory die pelleting rig

The above commented relationships indicate that it is possible to predict energy consumption in an industrial pellet press from measurements done with the laboratory die pelleting rig. The R^2 values were 46 and 61 % respectively (Fig. 9 and Fig. 10). Still new studies have to be done in order to validate the models. However, comparisons of process-ability among raw materials can be made by comparing the different resistances to flow, when no energy predictions are required.

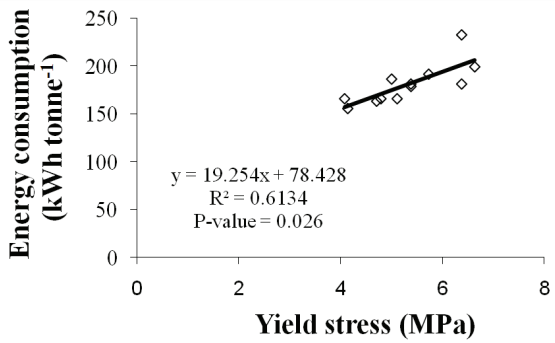

Figure 10. Correlations between energy consumption in the pellet press and yield stress determined in the laboratory die pelleting rig.

Pellet strength

It was not possible to compare strength values for the 8 mm (industrial pellet) and 9.5 mm (laboratory pellets with blank die) directly[7] since the industry pellet geometry was not possible to describe exactly, which gives errors into stress calculations. The 8 mm pellets produced in the industrial pelleting line did not have defined ends that could allow a reliable measurement of an area of stress. More research should be done to find methods to calculate pellet strength considering different diameters.

Since large plastic deformations (approximately 10% strain) occurred at the moment of ductile failure in all pellets, leaving different and random thresholds such as cracks. This implicates that the failure mechanisms (compressive stresses and tensile stresses) and stress distribution could not be well represented analytically. Additionally, the strength of these pellets is possibly anisotropic.

Pellet density affected the pellet strength, made in the laboratory die pelleting rig, significantly ($p<0.05$). Significant differences between the four raw materials were found. Detailed information about these differences can be found in Salas-Bringas et al[7]. Still, pellet density did not reduce the residual variance for the strength of the pellet made in the industrial line. The reason for this is the small range in density for this pellet and the large variance for maximum yield load for a specific density (Fig. 11).

Both types of pellets are plotted in Fig. 11. However, the plot does not consider the effect of diameter.

The pellets produced by the laboratory die pelleting rig had lower densities than the pellets produced in the industrial pelleting line. However, differences in densities cannot be directly associated to the compacting stresses without considering the changes in particle size distribution produced in the industrial pellet press. As a consequence, strength differences can be caused by different compacting stresses or by the changes in the compressibility given by the changes in particle size distributions.

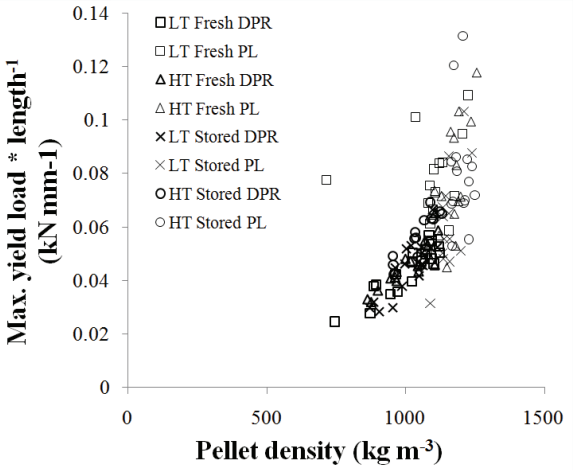

Figure 11. Physical strength of the pellets made in the laboratory die pelleting rig (DPR) and the pellets made in the pelleting line (PL).

CONCLUSIONS

Care should be taken when preparing small samples like the 7 ml samples used in the laboratory die pelleting rig, since it represents a much larger amount of material processed in the industry.

The grinding effect given by the pellet press should be considered when performing direct comparisons or predictions. However, this effect should not affect studies ranking the process-ability of raw materials.

Long storage time of the raw material produced higher normal stresses at incipient flow and higher yield stresses in the materials. Most probably this is important for the higher energy consumption when making pellets from stored wood. Drying temperatures did not change incipient flow and normal stress significantly.

Normal stresses at incipient flow, and yield stresses correlated with the energy consumed by the industrial pellet press.

Higher pellet strength was present at higher densifications.

REFERENCES

1. Samuelsson, R., M. Thyrel, M. Sjöström, and T.A. Lestander, (2009), "Effect of biomaterial characteristics on pelletizing properties and biofuel pellet quality", *Fuel Processing Technology*, **90**(9): p. 1129.

2. Salas-Bringas, C., O.I. Lekang, and R.B. Schüller, (2008), "Rheology in Feed Production", *Annual Transactions of the Nordic Rheology Society*, **16**: p. 229-237.

3. Kaliyan, N. and R.V. Morey, (2010), "Natural binders and solid bridge type binding mechanisms in briquettes and pellets made from corn stover and switchgrass", *Bioresource Technology*, **101**: p. 1082-1090.

4. Ortega-Rivas, E., P. Juliano, and H. Yan, (2005) "Food Powders", ed. G.V. Barbosa-Cánovas. NY: Springer. 372, 0306478064

5. Schulze, D., (2007) "Powders and Bulk Solids: Behavior, Characterization, Storage and Flow". NY: Springer. 516, 3540737677

6. Braastad, H. *Tilvekstmodellprogram for furu (Growth model computer program for Pinus sylvestris).* Reports of the Norwegian Forest Research Institute. Ås, Norway, 1980

7. Salas-Bringas, C., T. Filbakk, G. Skjevrak, O.I. Lekang, and R.B. Schüller, (2010), "Compression rheology and physical quality of wood pellets pre-handled with four different conditions", *Annual Transactions of the Nordic Rheology Society*, **18**: p. Accepted.

8. *CEN/TS 15149-2: Solid biofuels - Methods for determination of particle size distribution* in *Part 2: Vibrating screen method using sieve apertures of 3.15 mm and below*. 2006.

9. Irvine, G.M., (1984), "The glass transitions of lignin and hemicellulose and their measurement by differential thermal analysis.", *Tappi Journal.*, **67**(5): p. 118-121.

10. Mani, S., L.G. Tabil, and S. Sokhansanj, (2006), "Effects of compressive force, particle size and moisture content on mechanical properties of biomass pellets from grasses", *Biomass and Bioenergy*, **30**: p. 648-654.

11. Salas-Bringas, C., O.-I. Lekang, E.O. Rukke, and R.B. Schüller, (2009), "Development of a new capillary rheometer that uses direct pressure measurements in the capillary", *Annual Transactions of the Nordic Rheology Society*, **17**: p. 39-47.

12. Steffe, J.F., (1996) "Rheological methods in food process engineering". East Lansing, Mich.: Freeman Press. XIII, 418., 0-9632036-1-4

13. Salas-Bringas, C., W.K. Jeksrud, O.I. Lekang, and R.B. Schüller, (2007), "Noncontact Temperature Monitoring of a Pelleting Process Using Infrared Thermography ", *Journal of Food Process Engineering*, **30**(1): p. 24-37.

14. Jirjis, R., (1995), "Storage and drying of wood fuel", *Biomass and Bioenergy*, **9**: p. 191-190.